SAND91-7038
Unlimited Release
Printed September 1992

Distribution
Category UC-814

SAND--91-7038

DE93 002513

PERFORMANCE PREDICTION OF MECHANICAL EXCAVATORS FROM LINEAR CUTTER TESTS ON YUCCA MOUNTAIN WELDED TUFFS

by

Richard Gertsch
Levent Ozdemir

Earth Mechanics Institute
Colorado School of Mines
Golden, CO 80401

for

Sandia National Laboratories
P.O. Box 5800
Albuquerque, NM 87185

Under Sandia Contract No. 35-0039
Sandia Contract Monitor
Frank Hansen

ABSTRACT

The performances of mechanical excavators are predicted for excavations in welded tuff. Emphasis is given to tunnel boring machine evaluations based on linear cutting machine test data obtained on samples of Topopah Spring welded tuff. The tests involve measurement of forces as cutters are applied to the rock surface at certain spacings and penetrations. Two disc and two point-attack cutters representing currently available technology are thus evaluated. The performance predictions based on these direct experimental measurements are believed to be more accurate than any previous values for mechanical excavation of welded tuff.

The calculations of performance are predicated on minimizing the amount of energy required to excavate the welded tuff. Specific energy decreases with increasing spacing and penetration, and reaches its lowest at the widest spacing and deepest penetration used in this test program. Using the force, spacing, and penetration data from this experimental program, the thrust, torque, power, and rate of penetration are calculated for several types of mechanical excavators. The results of this study show that the candidate excavators will require higher torque and power than heretofore estimated.

WORK BREAKDOWN STRUCTURE INFORMATION

The work discussed in this report was conducted under the aegis of Work Breakdown Structure (WBS) element 1.2.4.2.1.3, entitled "Rock Mechanics Field Testing."

This report is the second of a series describing the work performed by the Earth Mechanics Institute of the Colorado School of Mines for Sandia National Laboratories under contract number 35-0039. The data collected are placed in the Data Records Management System (DRMS) file number 51/L02 - 07/11/90.

ACKNOWLEDGMENTS

This report represents the combined efforts of a number of people, from both Sandia National Laboratories (SNL) and the Colorado School of Mines (CSM). Special thanks are extended to Dr. Frank Hansen of SNL who served as the technical project officer, and to CSM students B. Asbury, B. Blair, J. Rostami, and S. Daniels who performed the majority of the laboratory test work.

James Friant and David Neil brought many years of experience to the test program. Their input and ideas directly contributed to the quality of the test program and the interpretation of the results.

CONTENTS

FIGURES

TABLES

1.0 INTRODUCTION

The work described herein was performed for Sandia National Laboratories (SNL) as part of the Yucca Mountain Site Characterization Project (YMP). SNL is one of the principal organizations participating in the project, which is managed by the U.S. Department of Energy's (DOE) Office of Civilian Radioactive Waste Management. The project is part of the DOE's Terminal Storage program to safely dispose of the radioactive waste from nuclear power plants.

The DOE has determined that the safest and most feasible method currently known to dispose of such wastes is to place them in a mined geologic repository. The YMP is conducting detailed studies to determine the suitability of siting a potential repository at depth in the welded tuffs at Yucca Mountain, Nevada. The rock mass will be characterized by excavation of an Exploratory Studies Facility (ESF) prior to potential repository construction. Various means of excavating the ESF and the repository are being examined, including mechanical excavators. Current design features of the ESF emphasize the use of various mechanical excavators and can take advantage of the significant benefits offered by mechanized excavation techniques, including faster project completion times, lower construction costs, improved ground stability, reduced support requirements, and enhanced operational safety.

This report describes the results of laboratory rock cutting tests performed as part of SNL contract #35-0039. Actual cutter force data were used to predict the performance of mechanical excavators operating in the potential repository horizon material and to increase the efficiency of the excavator design. Excavator operation at optimal performance provides for high rates of advance and reduced cutter costs. The primary emphasis is on tunnel boring machines (TBM), but the recommendations for system optimization and performance estimation include roadheaders and Mobile Miners, as well as shaft and raise borers.

This report is the second of a series evaluating the performance of various types of mechanical excavators for use in planned site characterization studies as well as the construction of the potential repository. The first report (Ozdemir et al., 1992) describes the initial performance predictions developed from the physical and geologic properties of the welded tuffs at the site. It consists of three parts: performance estimates derived from previously published geologic and physical property data, measurement of additional physical properties related to boreability, and subsequent revision of the estimated performance based on the additional data. The present report continues the process of refining the performance predictions; in this case, directly measured cutter force data have been included.

1.1 Background

Mechanical excavators fragment and remove rock with an array of cutting tools mounted on a rotating cutterhead. The energy consumed and the power required by mechanical rock excavation are influenced primarily by the type and geometry of the cutters, the cutter penetration at each pass, the cutter spacing and layout, the cutterhead shape, and the physical and

geologic properties of the rock. Testing representative cutters at full scale in the candidate rock provides accurate information from which excavator performance can be evaluated.

It has been shown that the specific energy, which is the energy required to break a unit volume of rock, reaches a minimum at a certain ratio of cutter spacing to penetration (SP ratio). The optimum SP ratio varies from 10 to 20 for disc cutters and from 2 to 4 for point-attack cutters. The optimum SP ratio depends on rock hardness, matrix characteristics, brittleness, and internal weaknesses such as foliation, microfractures, bedding, and grain alignment. Thus, for a given lithology, machine performance can be optimized through the design of the cutters and the cutterhead, and through the selection of the muck removal and backup systems.

1.2 Excavators Considered

The ESF may have combinations of shafts, raises, drifts, ramps, alcoves, and chambers or rooms. To construct these diverse openings, several types of mechanical excavation systems are evaluated in this study: TBMs, roadheaders, the Mobile Miner, the blind shaft borer (BSB), the vertical wheel shaft boring machine (SBM), raise borers, and the V-Mole. Each machine type is better suited to excavating certain types of underground openings than others. Complete discussions and illustrations of these machines are found in Ozdemir et al. (1992).

The TBM is best suited for relatively long, straight drivages, where it achieves its highest advance rates. The TBM is a high production machine that is effective in a wide variety of rock types and ground conditions. TBMs are capable of spectacular rates of advance at costs much below conventional drill-and-blast techniques. Recent improvements in TBM technology include more efficient cutters, enhanced maneuverability, more effective ground control systems, significantly improved machine reliability, and conveyor muck haulage. New TBM designs make turns much tighter than were previously feasible. For ESF construction, the TBM is most suitable for excavating the ramps and the long drifts where high production rates can be achieved.

The roadheader is a highly versatile mobile excavator with the capability to excavate openings of various shapes and sizes. It is a very common machine in mining and underground construction, although its use is usually limited to rock with less than 15,000 psi (103 MPa) compressive strength. Higher strength rocks can be excavated successfully if the rock is extensively jointed. This machine's mobility allows easy relocation from site to site. For the ESF, the roadheader can be used to excavate crosscuts, short ramps, and drifts, as well as small side rooms off of the main drifts excavated by TBM. It also is useful for finishing the shaping of complex openings.

The Mobile Miner, a relatively new machine design, excavates rectangular openings in rocks ranging from soft to very hard. It is more flexible and mobile than the TBM, but is less suitable for large openings, either in length or cross section, because it is not a full-face machine and cannot match TBM production rates. For ESF construction, the Mobile Miner appears most suitable for excavating side rooms off of the main tunnels excavated by TBM or for driving shorter drifts or crosscuts.

The BSB closely resembles a double-shielded TBM. The cutterhead design allows muck pickup from the shaft bottom. The BSB is a dry shaft boring device, using a mechanical muck pickup system rather than water flushing. As with other mechanical shaft excavation systems, its performance is governed primarily by the limitation of the muck removal and the shaft lining systems.

The SBM is an adaptation of the Mobile Miner for vertical downward excavation. The rock is excavated by a thin rotating cutterwheel equipped with a series of peripherally mounted disc roller cutters. The cutterwheel assembly rotates about the shaft axis, while being thrust downward, in addition to the cutterwheel rotating about its own horizontal axis. A bulldozer-type blade follows the cutterwheel and scrapes the cuttings into a pile. A clamshell bucket picks up the pile at intervals and loads it into a hoist for transport to the surface.

Raise boring is a relatively fast and highly efficient technique for construction of raises and small shafts. Raise boring uses a pilot hole and therefore requires underground access. Access to the face for science investigations during excavation is poor, because the bit must be completely withdrawn from the bore before personnel can reach the face. Raise boring is the most widely used method of raise construction. With current technology, it is limited to a 20-ft (6.1-m) diameter and to a depth of about 3000 ft (914 m). This is controlled primarily by hole deviation considerations.

The V-Mole is a mechanical shaft reamer. Requiring existing underground access, it reams a drilled pilot hole downward to the final shaft diameter. The pilot hole, which usually is created by a raise borer, serves to remove the rock cuttings generated during the reaming operation. Numerous mine shafts already have been constructed with V-Moles. Overall, the V-Mole has achieved advance rates much higher than those feasible with conventional drill-and-blast shaft excavation. Shaft lining can be installed directly above the machine as it reams downward.

1.3 Rationale

To determine the economic feasibility of applying any mechanical excavation techniques to any underground construction project, a reliable and accurate estimate of the rate at which the rock can be excavated is required. Further, the machine design and, more importantly, the cutter layout, geometry, and mode of operation need to be optimized for the particular rock and ground conditions to achieve high production rates at the lowest cost possible.

Full-scale laboratory testing of candidate cutters is a reliable means of determining these operating parameters at the actual spacings and penetrations to be used in the field. The linear cutting machine (LCM) is a full-scale test apparatus designed to measure the forces acting on a single cutter during excavation. The results from the linear cutter tests are the basis for assessing the performance of a mechanical excavator operating in the repository horizon material and for optimizing the excavator design. Operating an excavator at optimal performance allows

high rates of advance, shorter project completion times, and reduced costs. Over the last 20 years, the Earth Mechanics Institute has performed extensive LCM tests and has found the LCM to be a very reliable tool for predicting rock boreability in the field. Past performance predictions using LCM results have generally been within 10 percent of the actual field performance.

Two main types of cutters are used for mechanical rock excavation: disc cutters and drag bits. Both are mounted in multiples on cutterheads. Figures 1-1 and 1-2 illustrate the basic features of both types. Disc cutters consist of a hardened steel ring mounted on a heavy-duty bearing which allows the cutter to turn freely. They are used on TBMs, drills, shaft borers, and Mobile Miners for excavating nearly all types of rock ranging from soft to very hard, abrasive formations.

Drag bits, which can be plow or point-attack types, consist of a hardened steel or tungsten carbide tip inserted into the end of a robust steel shank. Instead of being rolled through the rock, like disc cutters, point-attack cutters are dragged through the rock. Accordingly, they cannot withstand the high loads that disc cutters can. In general, point-attack bits can excavate harder rock than plow bits because they are free to rotate in their holders. This allows for self-sharpening during cutting which prolongs bit life. They can also sustain higher cutting loads without premature structural failure. Point-attack cutters are, generally, limited to rock strength below 15,000 psi (103 MPa), although new technology is under development.

1.4 Objectives

Laboratory linear cutting tests provide a reliable means for predicting and optimizing the field performance of mechanical excavators. In this effort, an extensive series of linear cutting tests was undertaken in order to develop cutting data to

- Provide an understanding of how the forces on the cutters respond to changes in cut spacing, penetration, and cutter geometry in welded tuffs representative of the repository horizon;
- Determine which combination of cutting parameters consumes the least amount of specific energy to allow optimum machine design;
- Improve the accuracy of previously developed machine performance and cutter wear predictions in the excavation of welded tuff;
- Develop guidelines for the optimum design and performance of various types of mechanical excavators for the construction of the ESF and the potential repository; and
- Identify the areas and opportunities for further research and development with respect to improving the performance of mechanical excavators at the potential repository site.

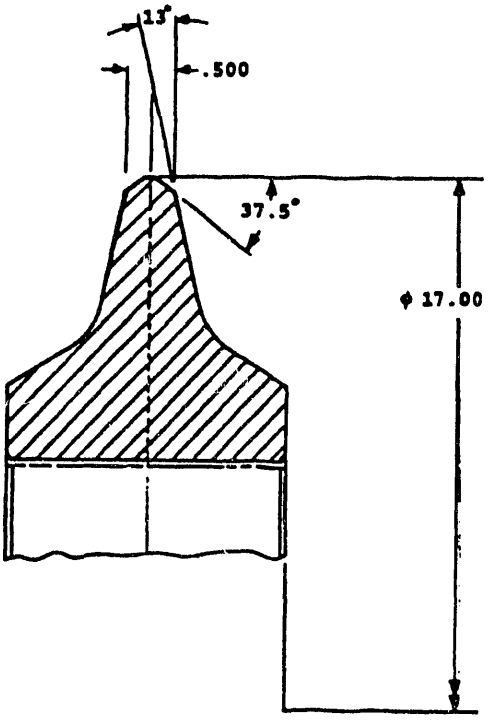

Figure 1-1. A30581 Constant Cross-Section Disc Cutter

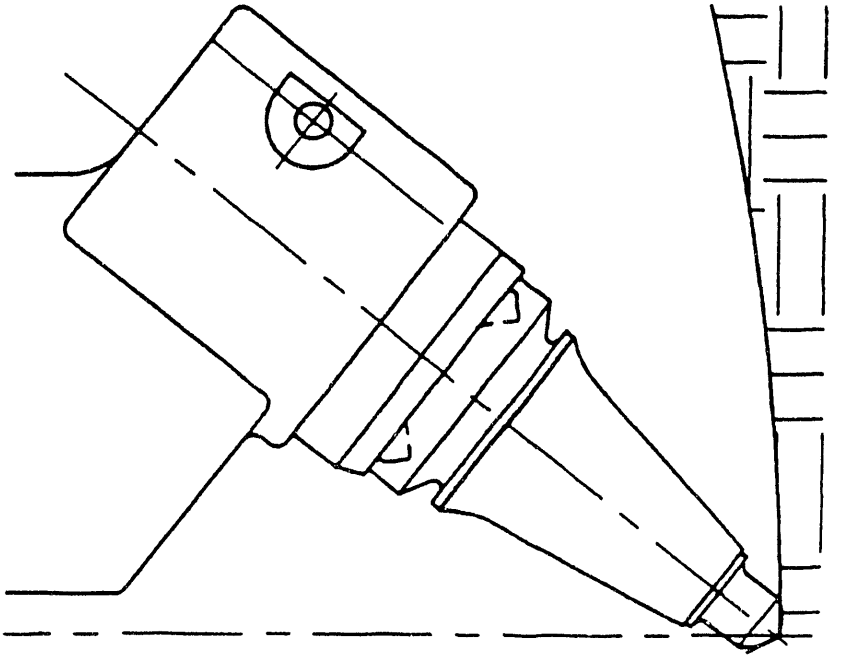

Figure 1-2. System 35 Point-Attack Cutter

1.5 Scope

The work reported here includes a series of LCM tests designed to generate cutter performance data in the repository horizon welded tuffs. It also includes a set of physical property measurements for the rock samples used in the LCM tests. The purpose was to improve the accuracy of the machine performance predictions that were based originally on rock physical property and geologic considerations (Ozdemir et al., 1992). All samples tested were from the Topopah Spring welded tuff unit #2 (TSw2).

Rock samples representative of the welded tuffs at the potential repository horizon were tested on the LCM with state-of-the-art, commercially available rock cutters (two disc cutters and two point-attack cutters). The resulting forces on each single cutter were measured in three dimensions at different combinations of spacing and penetration while cutting the welded tuff. This procedure simulates the action of multiple cutters found on a mechanical excavator. By varying cutter spacing and penetration, cutter forces were obtained as a function of these two important variables. The force data also were used to identify those combinations of cut spacing and penetration that provided the lowest specific energy for rock excavation. The recorded information also included observations regarding the rock chipping and failure process. The cuttings generated from each test were collected and analyzed for size distribution.

Physical properties that have been shown to influence the mechanical cuttability of rock also were measured. These included density, uniaxial compressive strength (UCS), splitting (Brazilian or indirect) tensile strength, acoustic velocities, dynamic elastic constants, and Cerchar abrasivity.

Section 2.0 of this report describes the experimental program. Section 3.0 presents and discusses the results from the LCM tests. The data output from the LCM tests include the cutter forces in response to the variables of spacing, penetration, and rock type and calculated results such as specific energy. Section 4.0 presents and discusses the performance predictions that were calculated from the LCM test results. Recommended thrusts, torques, power, and the estimated rates of penetration for candidate mechanical excavators were generated from the LCM data. Conclusions are presented in Section 5.0 and recommendations in Section 6.0.

2.0 EXPERIMENTAL PROGRAM

2.1 Background

The principal objective of conducting LCM testing is to determine the three-dimensional forces that act on a cutter during the excavation process. This information relates directly to machine operating parameters such as thrust, torque, and power.

Figure 2-1 illustrates the three-dimensional forces measured in the LCM tests. The normal force is the component that acts on the cutter perpendicular to the rock surface. The rolling force acts tangentially on the cutter edge, opposing the direction of travel; on a point-attack cutter this is referred to as the drag force. The side force acts perpendicular to the plane of the cutter.

2.2 Sample Acquisition

Samples of welded tuff were obtained from the Nevada Test Site. These included 43 large rock pieces from the East Lower Test Pit at Fran Ridge. The rock samples from Fran Ridge represent the TSw2 thermomechanical unit of the Paintbrush Tuff (Ortiz et al., 1985). This unit is being proposed for construction of the potential repository.

2.3 Cutter Types Tested

Four commercially available cutters were tested in order to obtain data representative of standard industry practice. Two representative disc cutters and two representative point-attack cutters were included in the test program. In the following discussion, manufacturers' names are listed. No recommendation of these particular cutters or the manufacturers is implied. The cutters were selected for their availability and because they were appropriate for the test program.

Both disc cutters had a 17-in. (432-mm) diameter and a constant cross-section profile. Both were manufactured by the Robbins Company. One cutter, the A30581, had a sharp edge and the other, the AM1723, a blunt edge. The two disc cutters (Robbins type A30581 and AM1723) selected for LCM testing are among the most commonly used cutters designed for hard, abrasive rock. They feature a constant cross-section edge profile so that the cutter performance is not severely degraded as edge wear develops. The A30581 cutter has an edge that is approximately 0.45 in. thick while the AM1723 cutter has an edge that is approximately 0.54 in. thick.

In general, narrow cutter profiles are employed on TBMs in the face and center positions to maximize the rate of penetration. The wider-edge cutters are primarily intended for gage positions where cutter wear occurs faster due to longer traverse distances and the cutters running through the muck accumulated in the invert. The wider profile provides more cutter material, increasing its wear resistance and thus extending the useful cutter life before replacement becomes necessary. The blunt profile of the

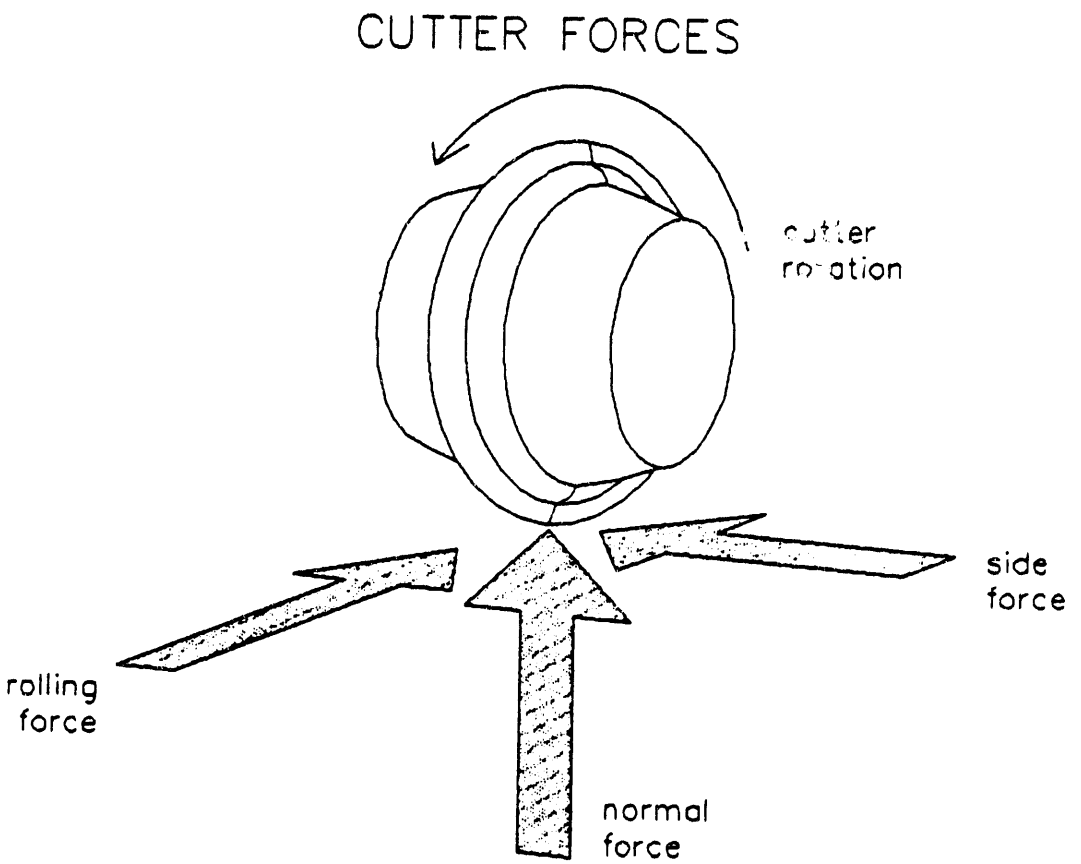

Figure 2-1. Forces on a Cutter in Three Dimensions

AM1723 is less efficient for cutting rock, but it gives better wear resistance because it has more metal at the cutting edge, which lowers the surface fatigue stresses on the blade.

The two point-attack cutters are also commonly used in the industry. Both cutters, the 84HCT and the System 35, have large, robust bodies and tungsten carbide inserts on the working tip. Both are manufactured by Sandvik. The 84HCT is longer and narrower than the System 35. It is designed for lower strength rock than the System 35, but has higher advance rates in softer rock. The System 35 has a higher strength carbide tip than the 84 HCT, which is the result of new carbide technology. The System 35 has a heavier, more robust body and bearing surface than the 84HCT.

2.4 Test Equipment Operation

This section describes the LCM and its operating procedures. A more detailed account of the equipment and the procedures is included in Appendix B.

The LCM features a large, stiff reaction frame on which the cutter is mounted (Figure 2-2). A triaxial load cell between the cutter and the frame monitors forces, and a linear variable displacement transducer (LVDT) monitors travel. The rock sample is cast in concrete within a heavy steel box to provide the necessary confinement during testing. Tests are conducted after the concrete has cured.

A servo-controlled hydraulic actuator forces the sample past the cutter at a preset depth of penetration, width of spacing, and constant velocity. After each cut the rock box is moved sideways by a preset spacing to duplicate the action of the multiple cutters on a mechanical excavator. A triaxial load cell between the cutter saddle and the reaction frame continuously monitors the normal, rolling, and side force components acting on the cutter.

2.5 Test Procedures

In field excavation, the individual cutters on the machine always operate on a rock surface damaged from the previous cutting action. This is referred to as the steady-state cutting condition. The steady-state cutting condition was duplicated in the laboratory by thoroughly conditioning the rock surface before testing began. This was accomplished by making several passes before data were collected.

Testing consisted of making several passes over the rock surface. A pass is defined as a group of cuts at the preset spacing and penetration across the width of the sample. Figure 2-3 illustrates the LCM test nomenclature. For each cut, the rock was forced into the cutter for the length of the sample, then was retracted. Following retraction, the rock box was displaced sideways at the predetermined spacing distance before the next cut was begun. The data reduction program calculated the mean, maximum, and minimum forces for each cut and for each test. Each test consisted of several cuts at one spacing and penetration.

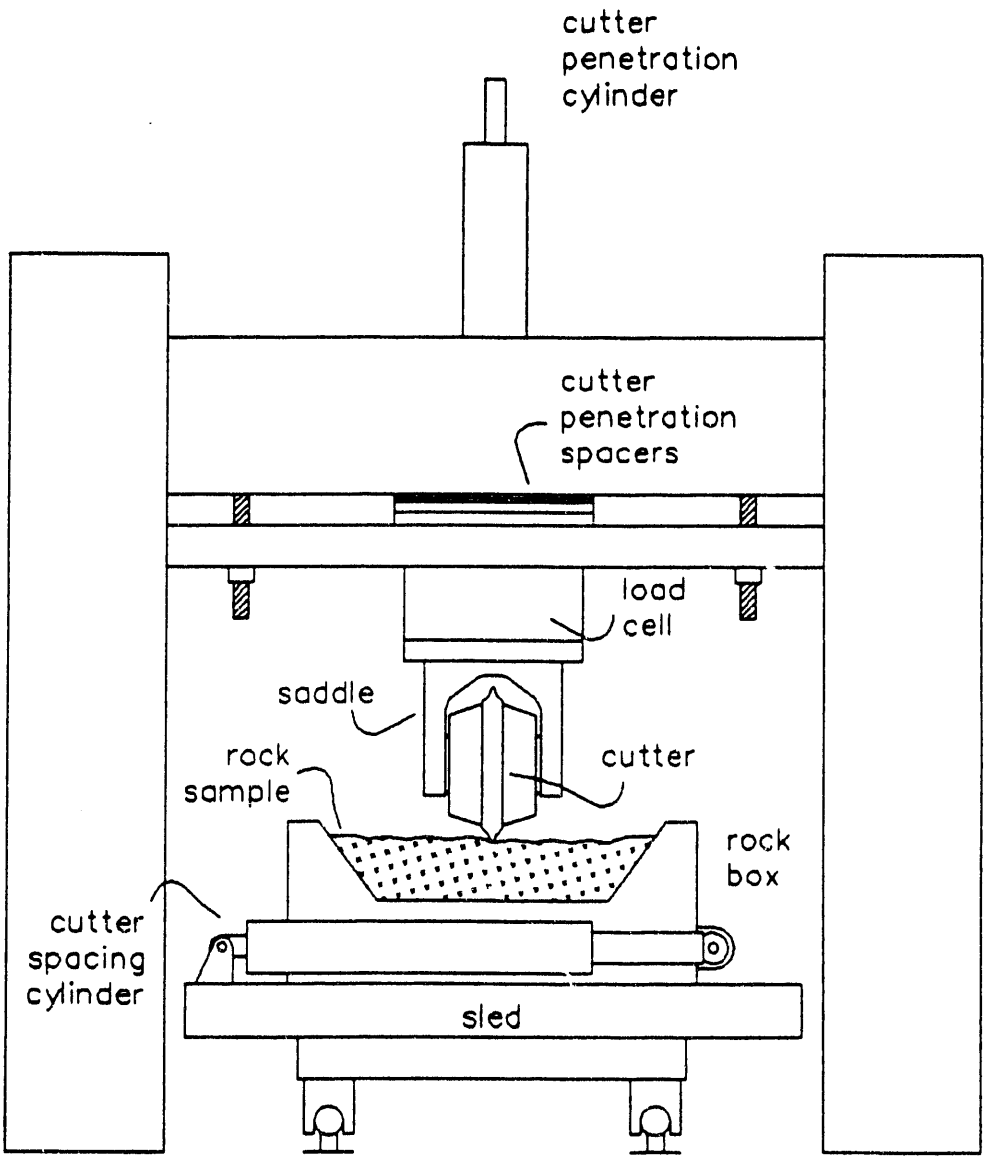

Figure 2-2. The Linear Cutting Machine (LCM)

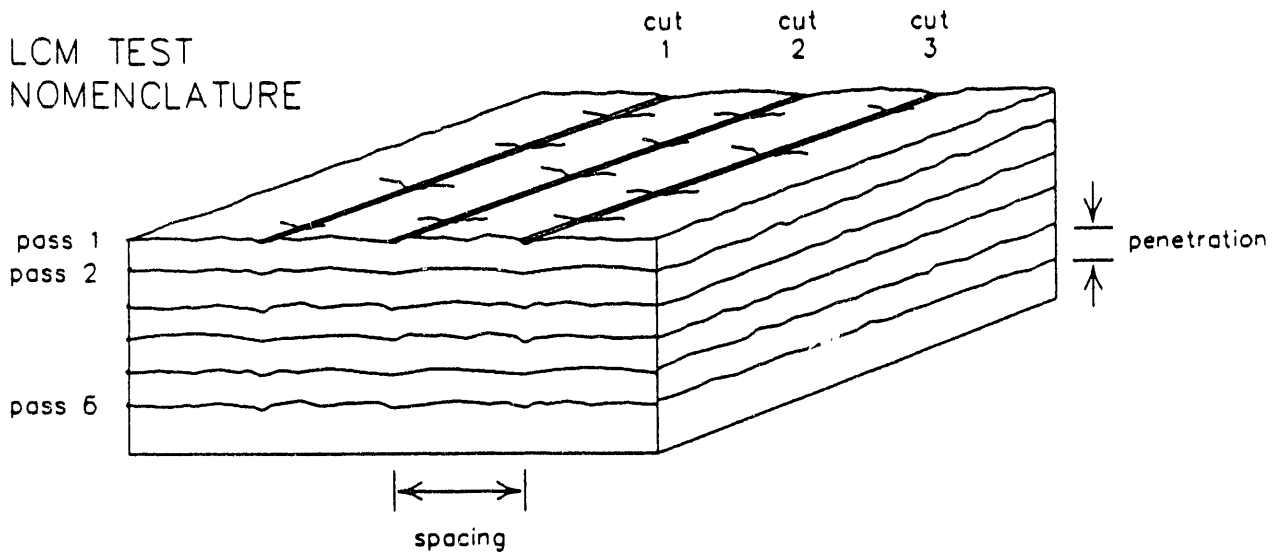

Figure 2-3. LCM Test Nomenclature

To vary the penetration, spacers were inserted above the cutter to ensure that the desired penetration was maintained throughout the entire cut. A new spacer was inserted after each pass. Data were acquired only from the center region of the sample, eliminating edge effects. For each test, the cutter made several passes over the rock surface; each pass consisting of several regularly spaced cuts. A computer-based data acquisition system recorded data from the load cell at 1000 points per channel per second. After test completion, the software provided summaries of all force data together with averages, standard deviations, maximums, and minimums.

When spacing was changed, a new rock sample was used. Changing spacings within a single rock sample causes spurious chipping effects, due to interactions with the damaged zone caused by the previous spacing. Changing samples with spacing also simulates more accurately the behavior of TBM disc cutters, which travel over the same paths.

2.6 Test Matrix

For both disc and point-attack cutters, the test method was the same. Only the spacing values in the testing matrices were different. The cutter spacings and penetrations used in this study are shown in Table 2-1. Nine separate tests, i.e., three penetrations at three spacings, were performed for each of the four cutters. In addition, one disc cutter (A30581) was tested at an additional penetration.

These spacings and penetrations were selected because they represent current industry practice. Spacings and penetrations outside this test matrix are rarely found on operating TBMs.

2.7 Physical Properties

The physical properties of the LCM test samples were determined using standard industry procedures, either ASTM-specified or otherwise published in the technical literature. The properties determined included density, uniaxial compressive strength, splitting tensile strength, compressive-to-tensile strength ratio, ultrasonic pulse velocities, dynamic elastic constants, and Cerchar abrasivity. Details of the testing procedures are described by Ozdemir et al. (1992).

Table 2-1

Linear Cutting Machine Test
Program in Welded Tuff

Series 1: A30581 Disc Cutter 17-in. Constant Cross Section

Penetration (in.)	Spacings (in.)		
	3	4	5
0.2	8[a]	12	16
0.3	9	13	17
0.4	10	14	18
0.5	11	15	

Series 2: AM1723 Disc Cutter 17-in. Constant Cross Section

Penetration (in.)	Spacings (in.)		
	3	4	5
0.2	19	25	22
0.3	20	26	23
0.4	21	27	24

Series 3: 84HCT Point-Attack Cutter, Conical Body, Carbide Tip

Penetration (in.)	Spacings (in.)		
	1.5	2	2.5
0.2	33	28	30
0.3	34	29	31
0.4	35	42	32

Series 4: System 35 Point-Attack Cutter, Conical Body, Carbide Tip

Penetration (in.)	Spacings (in.)		
	1.5	2	2.5
0.2	39	36	43
0.3	40	37	44
0.4	41	38	45

[a]The number for each penetration and spacing combination is the test number.

Totals: 38 Tests; 4 Cutters.

3.0 LCM TEST RESULTS AND DISCUSSION

This section presents the results from the LCM test program. The LCM results are the three-dimensional forces experienced by the cutter and other parameters calculated from the force data.

Four sets of data are presented in the following tables and figures--two sets for the disc cutters, and two for the point-attack cutters. The tables include cutter spacing and penetration, the measured average normal, rolling, and side forces, and the peak forces. They also include the calculated cutting coefficient, specific energy of cutting, and the peak-to-mean force ratios. The figures present the data in graphical form as a function of cutter spacing. Additional graphical results are included in the DRMS (file number 51/L02 - 07/11/90).

3.1 Disc Cutters

As noted previously, a series of linear cutting tests was performed with two constant cross-section 17-in.-diameter disc cutters, Robbins types A30581 and AM1723. The disc cutter data are shown in Table 3-1 and in the following ten figures.

3.1.1 Cutter Forces

Figures 3-1 and 3-2 show the normal cutter forces as a function of spacing for different depths of penetration. In general, normal force increases with spacing and penetration for both cutters. The effect is much more pronounced for penetration than for spacing. An increase in penetration makes a definite increase in normal force, but an increase in spacing does not consistently have the same effect. For the sharp cutter (A30581), an increase in spacing causes small increases in normal force. For the blunt cutter (AM1723), an increase in spacing appears to have a mixed effect on normal force. These values fall within the experimental error, however, and are interpreted to mean that cut spacing has a small effect on normal cutter force requirements for welded tuff.

The rolling forces (Figures 3-3 and 3-4) tend to mirror the normal forces, but at smaller magnitudes. For both the sharp and blunt cutters, the rolling force increases with increases in penetration. Spacing again has a mixed effect on the magnitude of the rolling forces.

Contrary to the trends observed for the normal and rolling forces, the side forces, in general, are seen to decrease as cut spacing becomes larger, but to increase as the cutter penetrates deeper (Figures 3-5 and 3-6). Side forces can act in either direction, depending on which side of the cutter the major chipping occurs. But the majority of the side force acts in the direction of chipping, due to unbalanced forces imposed on the cutter edge following chip formation.

Table 3-1

Linear Cutting Machine Test Results for Two Disc Cutters

17-in. Constant Cross-Section Disk Cutter - A30581

Test Number	Spacing (in.)	Penetration (in.)	S/P	Average Forces (lb)			Peak Forces (lb)			Cutting Coefficient	Specific Energy ($hp\text{-}hr/yd^3$)	Peak/Mean Ratio		
				Normal	Rolling	Side	Normal	Rolling	Side			Normal	Rolling	Side
8	3	0.2	15.0	22,489	2,012	934	49,078	4,792	6,432	0.09	6.6	2.2	2.4	6.9
9	3	0.3	10.0	29,857	3,729	2,811	63,384	8,440	10,153	0.12	8.1	2.1	2.3	3.6
10	3	0.4	7.5	31,239	4,496	2,769	66,537	10,354	12,132	0.14	7.4	2.1	2.3	4.4
11	3	0.5	6.0	35,179	5,441	3,873	84,490	15,789	12,877	0.15	7.1	2.4	2.9	3.3
12	4	0.2	20.0	25,469	2,405	765	51,437	5,790	6,619	0.09	5.9	2.0	2.4	8.7
13	4	0.3	13.3	25,565	3,690	2,027	57,041	8,292	9,156	0.14	6.0	2.2	2.2	4.5
14	4	0.4	10.0	32,087	5,312	2,602	67,618	11,216	12,002	0.17	6.5	2.1	2.1	4.6
15	4	0.5	8.0	40,001	6,430	3,448	93,582	16,805	14,421	0.16	6.3	2.3	2.6	4.2
16	5	0.2	25.0	26,193	2,758	1,279	57,415	6,873	7,676	0.11	5.4	2.2	2.5	6.0
17	5	0.3	16.7	30,408	3,774	1,141	64,357	8,709	10,584	0.12	4.9	2.1	2.3	9.3
18	5	0.4	12.5	32,472	4,316	1,298	78,675	11,357	10,680	0.13	4.2	2.4	2.6	8.2
17-in. Constant Cross-Section Disk Cutter - AM1723														
33	3	0.2	15.0	25,211	3,519	1,023	52,729	7,635	4,799	0.14	11.5	2.1	2.2	4.7
34	3	0.3	10.0	28,574	4,632	1,438	63,462	10,776	6,666	0.16	10.1	2.2	2.3	4.6
35	3	0.4	7.5	34,388	6,609	1,919	88,598	19,233	12,866	0.19	10.8	2.6	2.9	6.7
28	4	0.2	20.0	25,860	3,328	1,019	59,755	8,023	5,827	0.13	8.2	2.3	2.4	5.7
29	4	0.3	13.3	30,290	4,441	1,460	75,209	11,793	7,512	0.15	7.3	2.5	2.7	5.1
42	4	0.4	10.0	36,823	5,139	1,420	84,213	12,293	8,036	0.14	6.3	2.3	2.4	5.7
30	5	0.2	25.0	27,449	3,319	19	62,704	8,046	1,288	0.12	6.5	2.3	2.4	67.8
31	5	0.3	16.7	28,978	4,142	653	67,804	9,798	7,156	0.14	5.4	2.3	2.4	11.0
32	5	0.4	12.5	31,023	4,801	781	58,527	9,769	5,757	0.15	4.7	1.9	2.0	7.4

NOTE: Data are considered accurate to 3 significant figures.

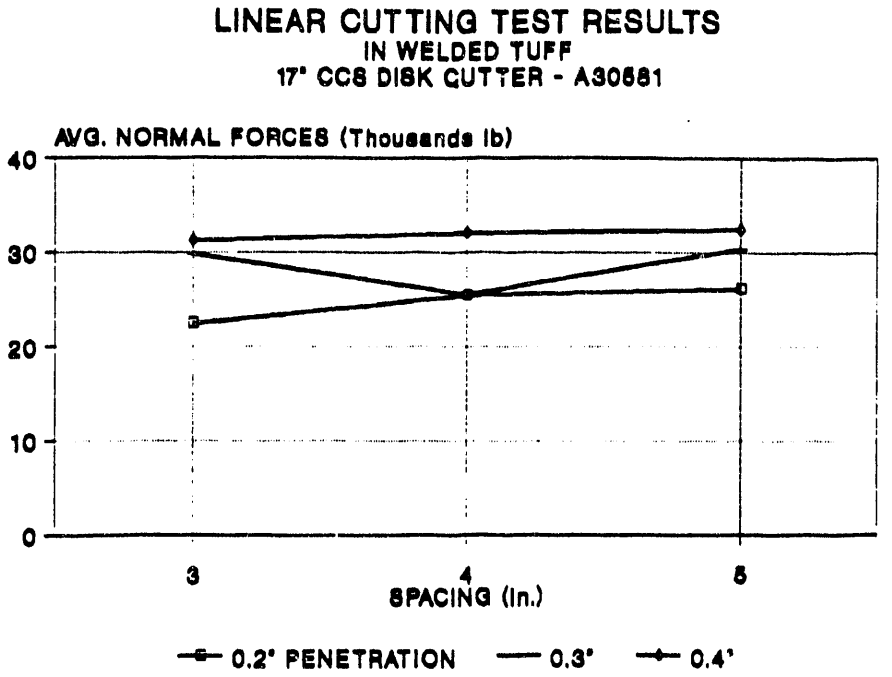

Figure 3-1. Normal Forces on the A30581 Disc Cutter

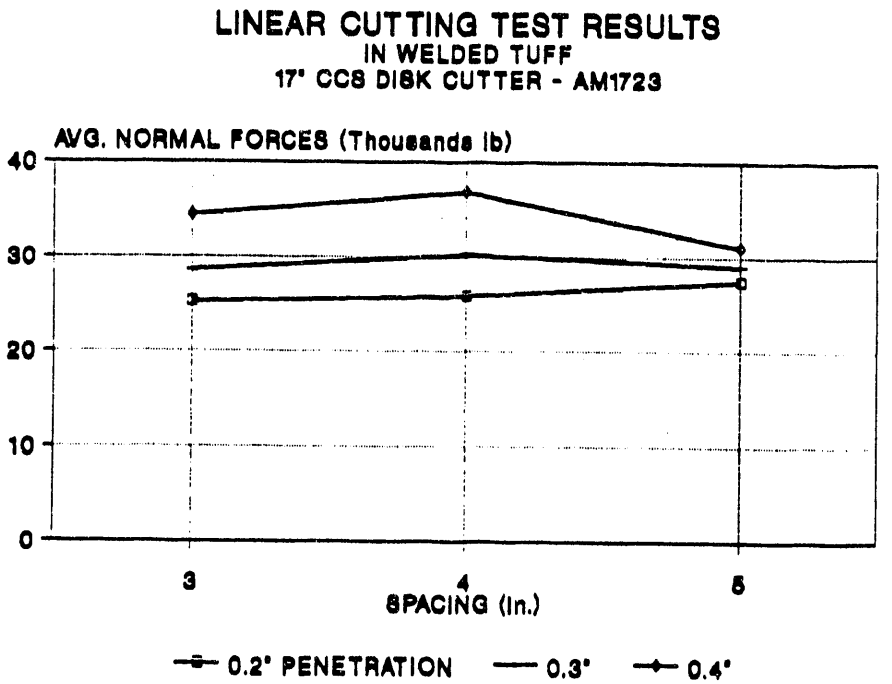

Figure 3-2. Normal Forces on the AM1723 Disc Cutter

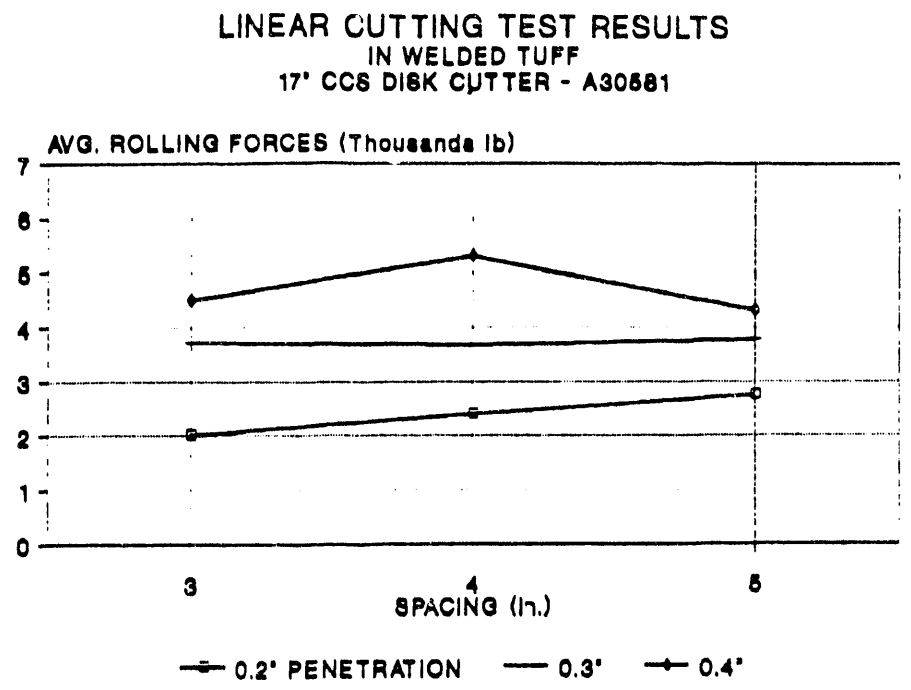

Figure 3-3. Rolling Forces on the A30581 Disc Cutter

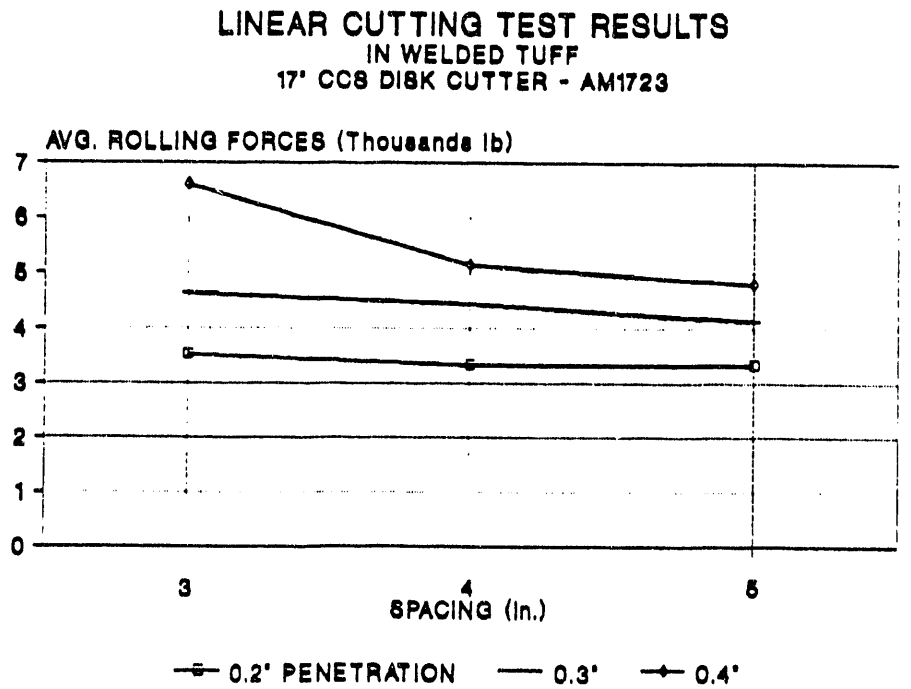

Figure 3-4. Rolling Forces on the AM1723 Disc Cutter

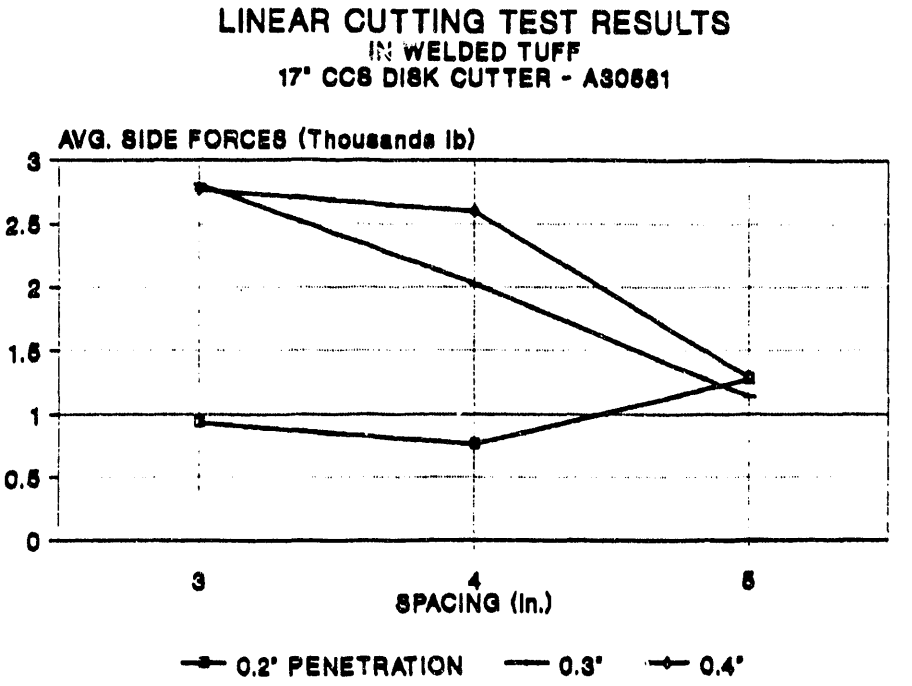

Figure 3-5. Side Forces on the A30581 Disc Cutter

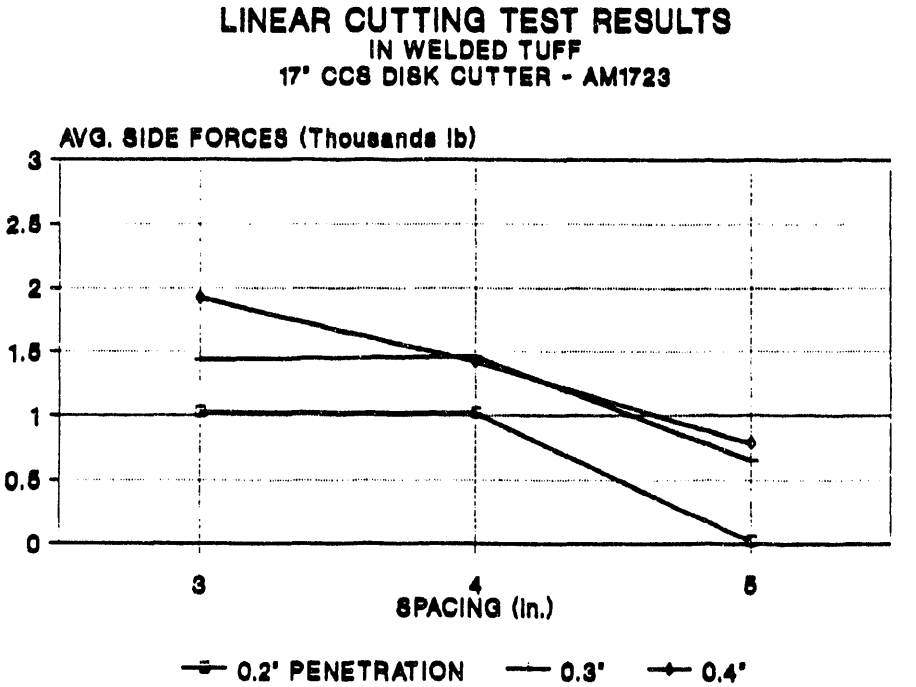

Figure 3-6. Side Forces on the AM1723 Disc Cutter

3.1.2 Cutting Coefficient

The cutting coefficient is the ratio of rolling to normal forces. It is used to determine the torque requirements for mechanical excavators. A high cutting coefficient means high torque requirements for a given machine thrust, which may lead to an excavation system being power-limited, as will be discussed later. Usually, machines excavating soft formations tend to be torque- or power-limited before ever reaching their thrust capacity.

For both disc cutters, the cutting coefficient is higher than expected due to the high rolling force requirements of the cutter operating in welded tuff. Cutting coefficients are typically in the range of 0.10 to 0.12 for rock formations similar to welded tuff. At the higher penetrations, values of 0.15 and 0.16 are seen for the tuff (Figures 3-7 and 3-8).

A high cutting coefficient indicates that the torque requirements for an excavator using disc cutters will be relatively high. This means that for welded tuff, a TBM may be torque-limited during operation, rather than thrust-limited. The relationship of machine torque and thrust will be explored in more detail in the section on performance prediction.

3.1.3 Specific Energy

Specific energy is defined as the energy required to excavate a unit volume of rock. The spacing and penetration values where specific energy reaches its lowest point define the most efficient cutter geometry. For both cutters, the lowest specific energy occurs at a spacing of 5 in. and a penetration of 0.4 in. (Figures 3-9 and 3-10).

In general, for both disc cutters, the specific energy decreases as both spacing and penetration increase. However, the effect of spacing is more pronounced than the effect of penetration. An increase in spacing significantly lowers the specific energy, while the effect of penetration is mixed.

The results indicate a continual decrease in specific energy at wider spacings. Since the test matrix only extends to 5-in. (13-cm) spacing, it is possible that a further decrease in specific energy may be gained by increasing cut spacing beyond 5 in.

A decrease of specific energy as a function of increasing penetration is not entirely clear. At 3-in. (7.6-cm) spacing, specific energy actually increases with increasing penetration. However, at higher spacings, particularly 5 in. (13 cm), specific energy decreases with increased penetration.

For both cutters, the specific energy is seen to reach its minimum at a penetration of 0.4 in. (1.0 cm) and at a spacing of 5 in. (13 cm). These were the highest penetrations and spacings tested in the laboratory. As expected, the blunt cutter required a higher specific energy of cutting.

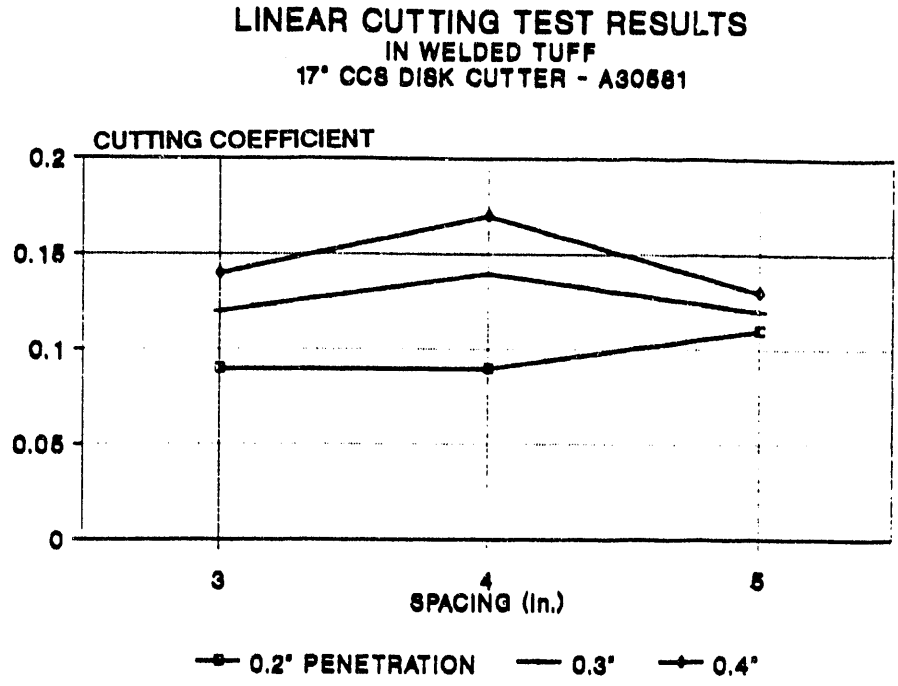

Figure 3-7. Cutting Coefficient for the A30581 Disc Cutter

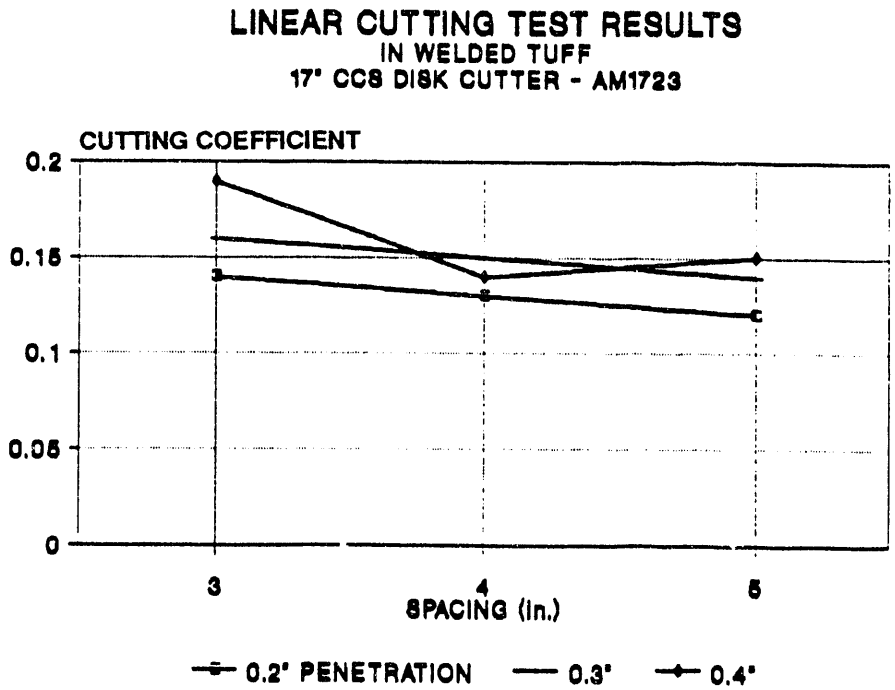

Figure 3-8. Cutting Coefficient for the AM1723 Disc Cutter

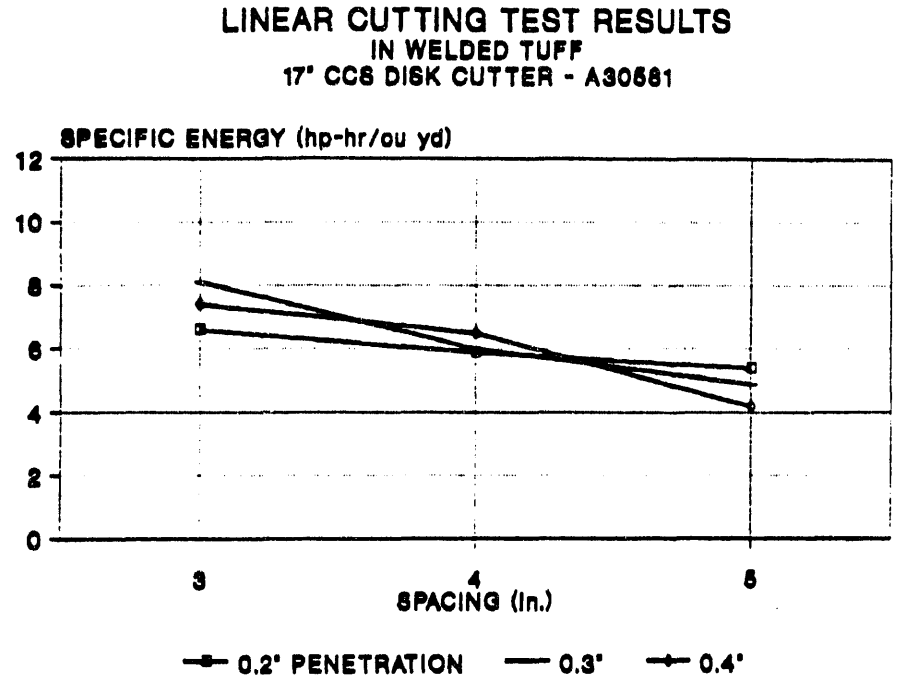

Figure 3-9. Specific Energy for the A30581 Disc Cutter

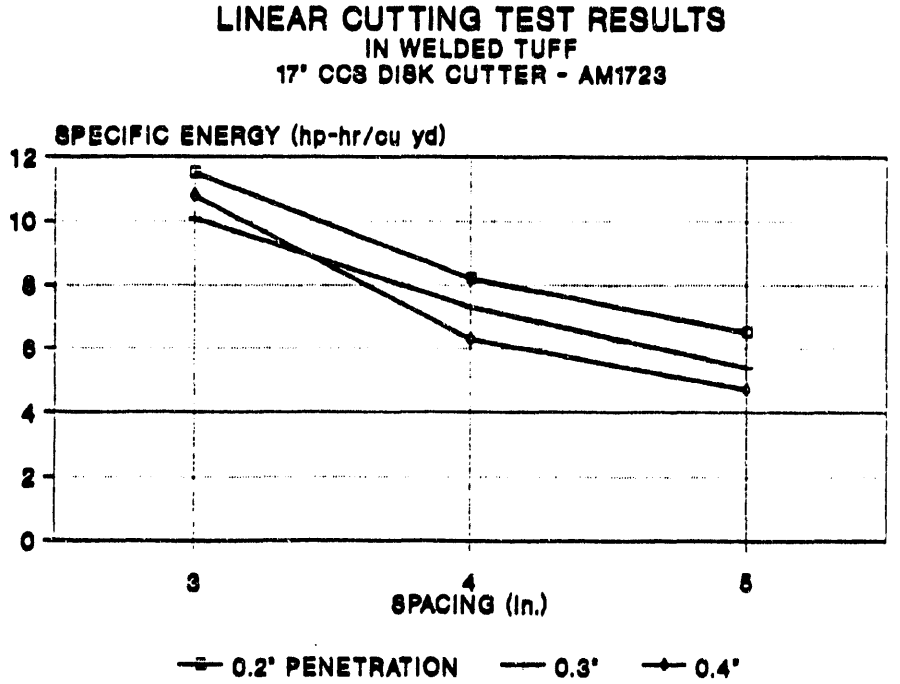

Figure 3-10. Specific Energy for the AM1723 Disc Cutter

3.2 Point-Attack Cutters

Two point-attack cutters designed for use on heavy-duty roadheaders were employed in the test program (Sandvik System 35 and System 84HCT). Both consist of robust bodies tipped with tungsten carbide inserts. The System 35 has a larger body and is designed for higher loads than the 84HCT. Both cutters were tested at an attack angle of 56°, a common setting for hard rock. Table 3-2 summarizes the test results, which also are presented in graphical form in Figures 3-11 through 3-20 as a function of cutter spacing.

3.2.1 Cutter Forces

As expected, the normal and drag forces increase with wider spacing and deeper penetration (Figures 3-11 and 3-12). Increases in spacing and penetration on a TBM means that the machine is excavating more rock. Rock cutting theory (e.g., Ozdemir et al., 1977) predicts higher forces in response to increased spacing and penetration. The force response pattern of the two point-attack cutters is the same, with the System 35 exhibiting higher forces.

Drag forces acting on the point-attack bits have trends similar to the disc cutters and remain smaller than the normal forces. Both spacing and penetration affect the drag force significantly (Figures 3-13 and 3-14).

Cut spacing appears to have a mixed effect on the side forces. Side forces are seen to increase with deeper penetration, due to creation of larger cuttings and a higher degree of force imbalance on the cutter tip (Figures 3-15 and 3-16).

3.2.2 Cutting Coefficient

The cutting coefficient is the dimensionless ratio of drag to normal forces. It is an indicator of the torque requirements for the candidate excavator; the higher the cutting coefficient, the higher the torque requirement.

As expected, cutting coefficient increases with penetration (Figures 3-17 and 3-18) because cutter drag forces increase at a higher rate than the normal forces as penetration increases. Also, deeper penetrations cause increased friction on the cutter edge, again translating into higher drag forces.

3.2.3 Specific Energy

The specific energy decreases with penetration, but tends to be unaffected by increases in spacing (Figures 3-19 and 3-20). The results show the System 35 bit to be less efficient than the 84HCT bit, requiring higher specific energies at all spacings and penetrations tested. However, the System 35 cutter is more robust and is designed to withstand higher cutting loads and provide longer wear life.

The results indicate that, from the viewpoint of energy efficiency, the point-attack cutters should be operated at the largest spacings and

Table 3-2

Linear Cutting Machine Test Results for Two Point-Attack Cutters

Test Number	Spacing (in.)	Penetration (in.)	S/P	Average Forces (lb)			Peak Forces (lb)			Cutting Coefficient	Specific Energy (hp-hr/yd^3)	Peak/Mean Ratio		
				Normal	Rolling	Side	Normal	Rolling	Side			Normal	Rolling	Side
Point-Attack Pick Cutter - 84HCT														
19	1.5	0.2	7.5	2,574	1,221	282	11,881	7,625	3,217	0.47	8.0	4.6	6.2	11.4
20	1.5	0.3	5.0	2,757	1,331	359	12,799	8,055	3,172	0.48	5.8	4.6	6.1	8.8
21	1.5	0.4	3.8	3,103	1,710	534	16,097	11,527	4,623	0.55	5.6	5.2	6.7	8.7
25	2	0.2	10.0	2,178	1,095	67	12,374	7,647	2,715	0.50	5.4	5.7	7.0	40.5
26	2	0.3	6.7	2,661	2,692	262	13,040	16,969	3,268	1.01	8.8	4.9	6.3	12.5
27	2	0.4	5.0	4,029	2,149	615	16,394	11,244	4,450	0.53	5.3	4.1	5.2	7.2
22	2.5	0.2	12.5	6,142	2,947	(599)	20,843	12,059	4,215	0.48	11.6	3.4	4.1	-7.0
23	2.5	0.3	8.3	5,436	2,793	459	18,374	12,594	4,431	0.51	7.3	3.4	4.5	9.7
24	2.5	0.4	6.3	4,964	2,838	381	20,382	14,092	4,762	0.57	5.6	4.1	5.0	12.5
Point-Attack Pick Cutter - System 35														
39	1.5	0.2	7.5	3,395	1,562	458	12,800	8,096	3,582	0.46	10.2	3.8	5.2	7.8
40	1.5	0.3	5.0	3,723	1,918	834	13,928	9,675	4,759	0.52	8.4	3.7	5.0	5.7
41	1.5	0.4	3.8	3,507	1,784	814	15,591	10,623	4,990	0.51	5.8	4.4	6.0	6.1
36	2	0.2	10.0	4,352	2,089	607	16,188	10,221	4,309	0.48	10.3	3.7	4.9	7.1
37	2	0.3	6.7	4,135	2,161	526	16,929	10,812	4,374	0.52	7.1	4.1	5.0	8.3
38	2	0.4	5.0	4,624	2,574	869	17,519	12,035	5,183	0.56	6.3	3.8	4.7	6.0
43	2.5	0.2	12.5	5,240	2,576	167	16,798	10,778	3,395	0.49	10.1	3.2	4.2	20.3
44	2.5	0.3	8.3	6,078	3,230	729	19,307	13,124	4,438	0.53	8.5	3.2	4.1	6.1
45	2.5	0.4	6.3	6,152	3,609	1,126	19,732	14,177	4,718	0.59	7.1	3.2	3.9	4.2

NOTE: Data are considered accurate to 3 significant figures.

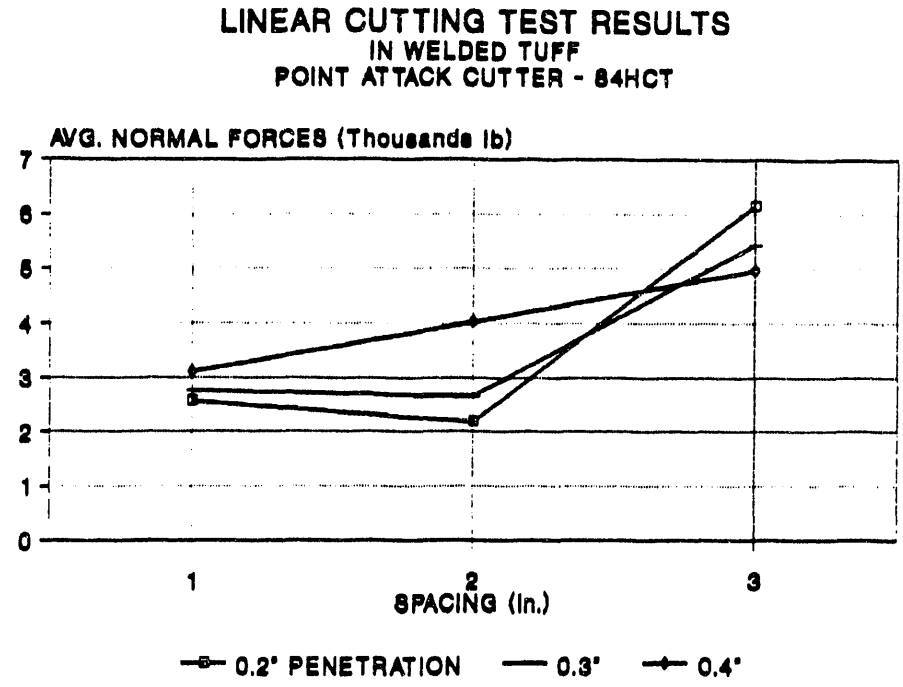

Figure 3-11. Normal Forces on the 84HCT Point-Attack Cutter

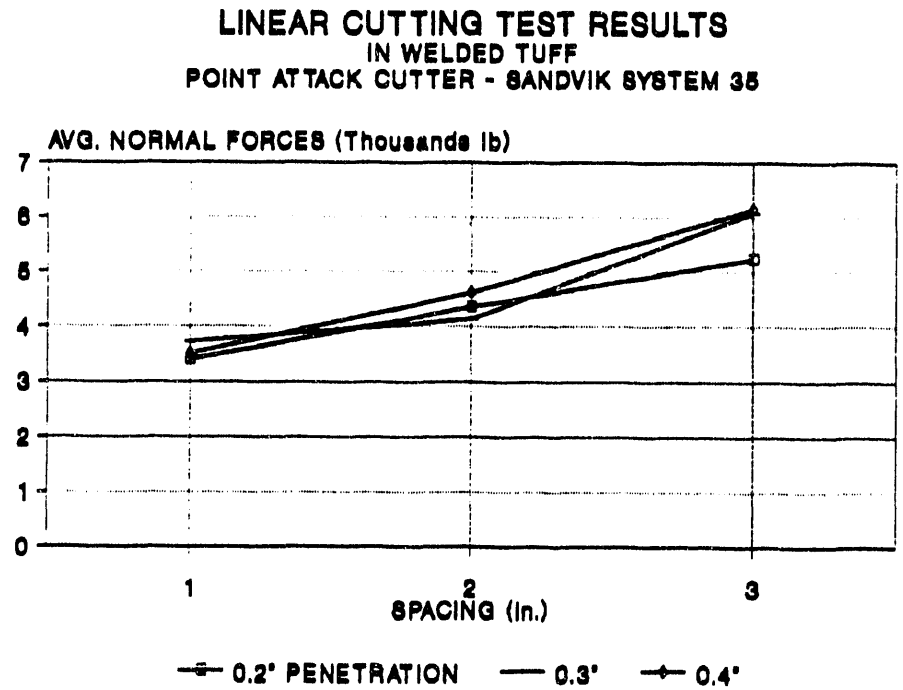

Figure 3-12. Normal Forces on the System 35 Point-Attack Cutter

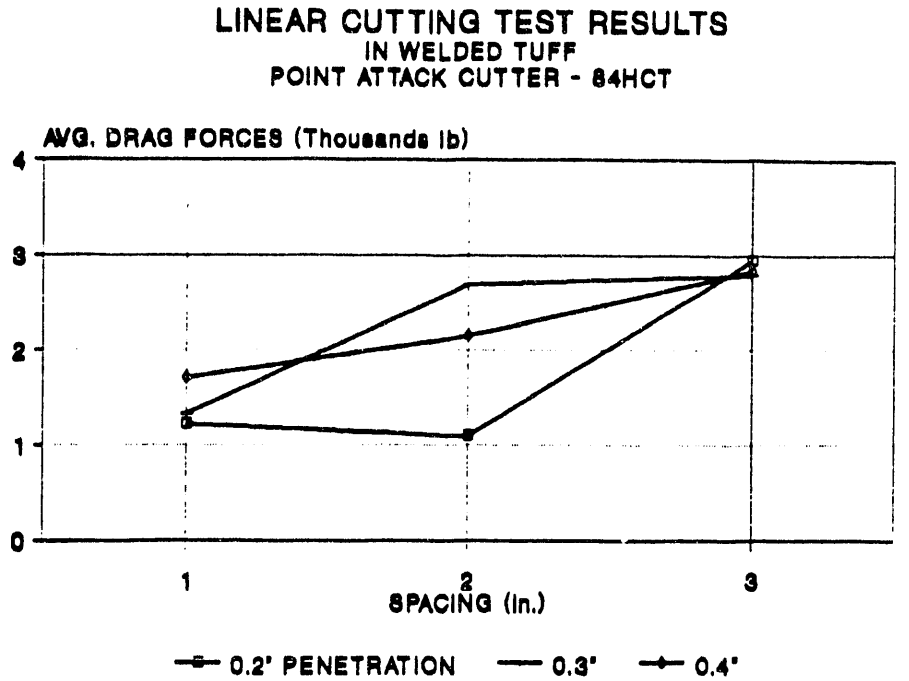

Figure 3-13. Rolling Forces on the 84HCT Point-Attack Cutter

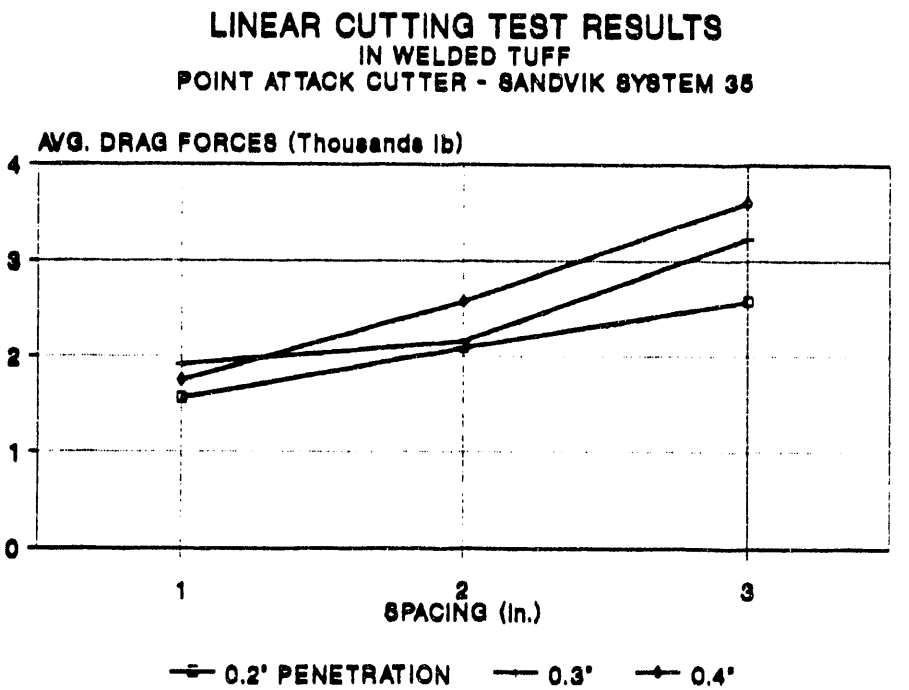

Figure 3-14. Rolling Forces on the System 35 Point-Attack Cutter

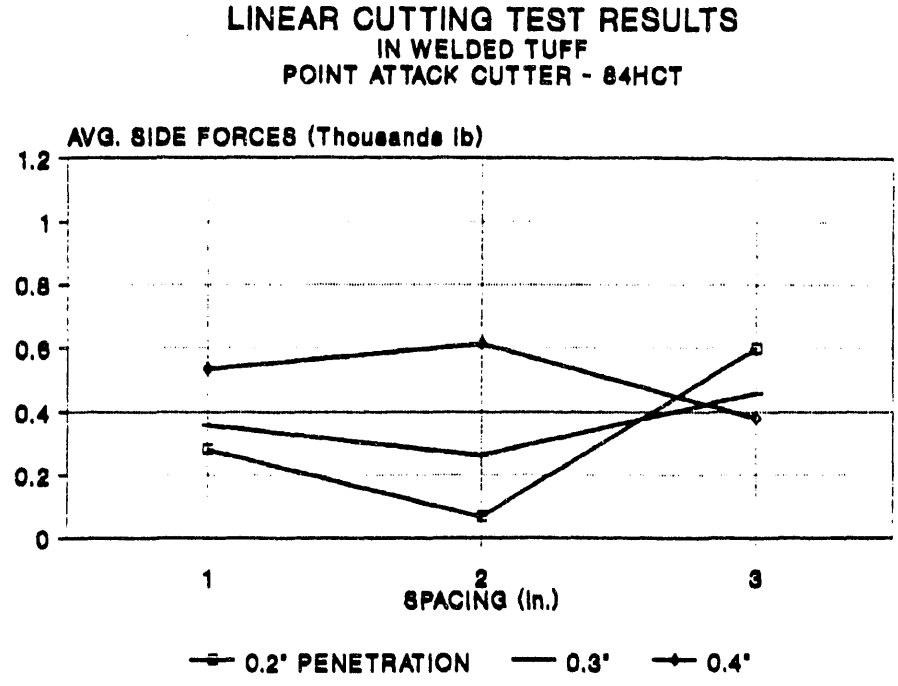

Figure 3-15. Side Forces on the 84HCT Point-Attack Cutter

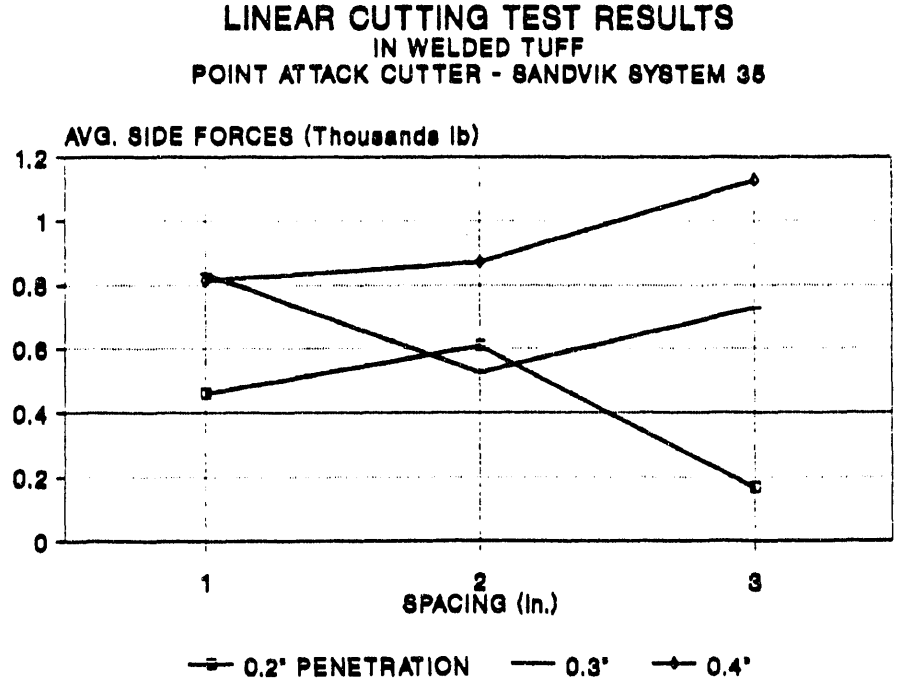

Figure 3-16. Side Forces on the System 35 Point-Attack Cutter

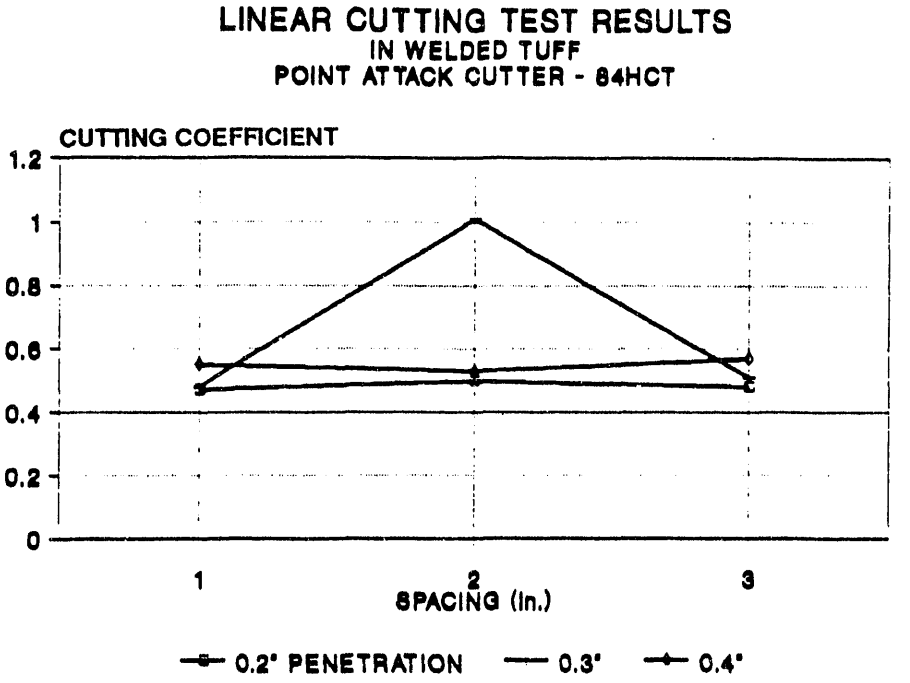

Figure 3-17. Cutting Coefficient for the 84HCT Point-Attack Cutter

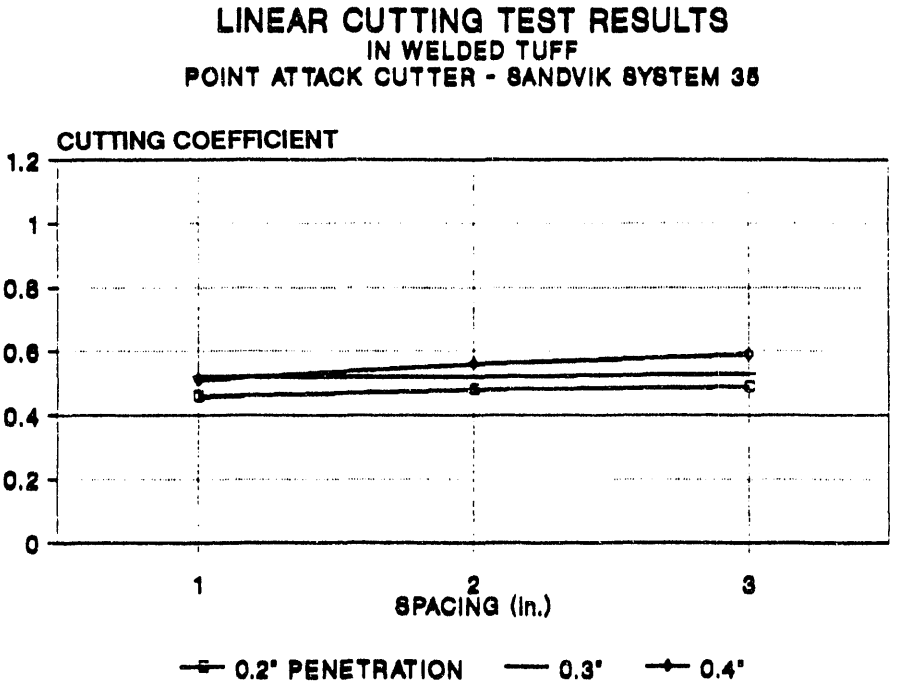

Figure 3-18. Cutting Coefficient for the System 35 Point-Attack Cutter

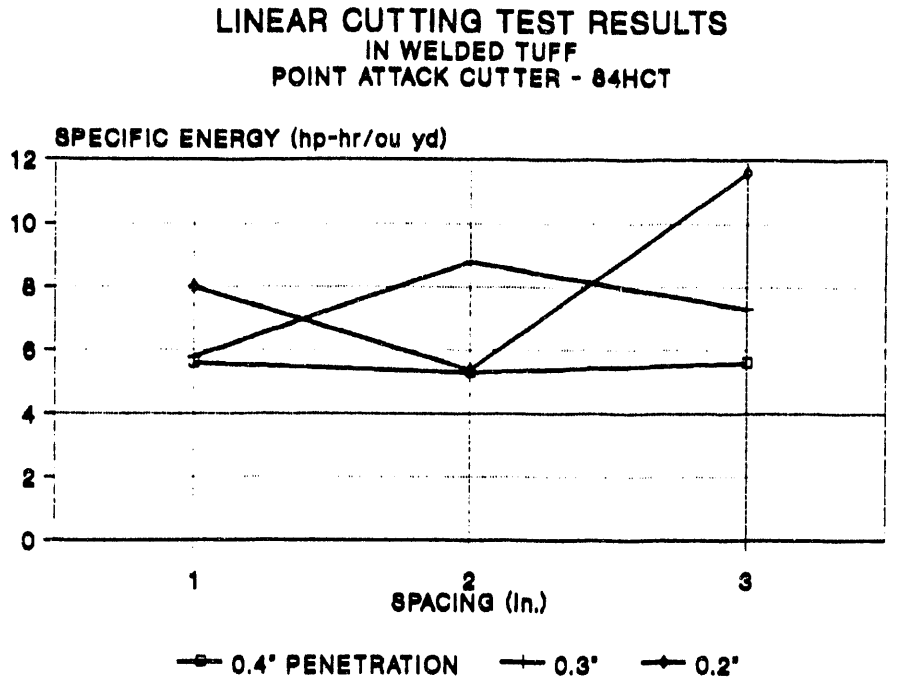

Figure 3-19. Specific Energy for the 84HCT Point-Attack Cutter

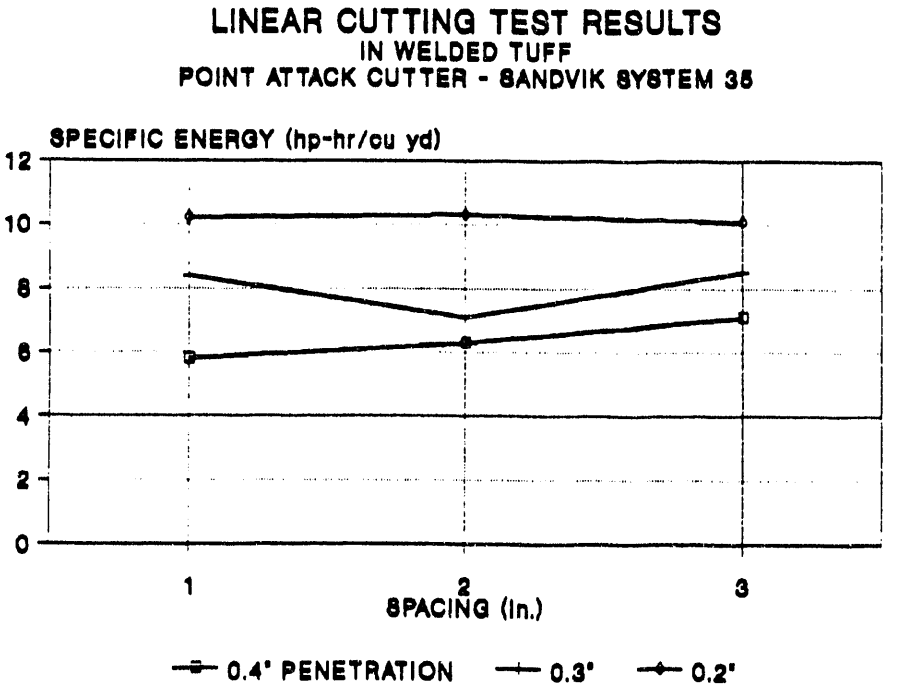

Figure 3-20. Specific Energy for the System 35 Point-Attack Cutter

penetrations investigated in this test program. This provides for the lowest specific energy requirement and a higher rate of production. For a roadheader operating in harder rock formations, such as welded tuff, a larger spacing means fewer cutters on the cutterhead and, therefore, lower torque requirements. Also, individual cutter loads will be higher, meaning deeper penetrations and higher production rates.

3.3 Sieve Analysis

For each linear cutting test, a representative sample of the rock cuttings was obtained and analyzed for particle size distribution. Tables in Appendix C summarize the results from sieve analysis of the rock chips.

Since water spray dust suppression may not be allowed during site characterization studies, a rock-cutting geometry that reduces dust generation is desirable. This section will address the amount of fine rock material produced by each spacing and penetration combination. Fine rock material (called fines) is defined as the fraction passing through sieve openings less than 0.023 in. (0.589 mm). Other fractions may be of interest and are included in the results (Appendix C).

Some general trends in the size of the material from the sieve analysis are noted. In all tests, the bulk of the chips is retained in the plus-one-inch (2.54 cm) sieve. The point-attack cutters produce less plus-one-inch material and more fines than the disc cutters. The plus-one-inch fraction increases as spacing increases, a trend which is more pronounced for the point-attack cutters than for the disc cutters.

For the disc cutters, the amount of fines in the chips generally decreases as spacing and penetration increase. Fines result from crushing of the rock under or alongside the cutter. As spacing and penetration increase, the chip sizes become larger, but the crushing remains relatively constant. Thus the relative amount of fines is reduced as cut spacing and penetration are increased. The lowest fines production coincides with low specific energy values, an expected result.

As with the disc cutters, chips collected from the point-attack cutter tests also contain a decreasing percentage of fines as spacing and penetration increase. Thus the cutting geometries with the low specific energy produce the lowest amount of fines. The amount of fines usually decreases as the attack angle for a point-attack bit increases, but this effect was not investigated in this effort.

3.4 Physical Property Test Results

The test results described in this section were performed to support the interpretation of the LCM tests. Each rock sample selected for testing in the LCM was subjected to physical and mechanical property tests. These included both standard strength tests and other measurements known to influence cuttability. The results are listed in Table 3-3. Each test was performed three times for each LCM rock sample.

Table 3-3

Summary of Physical Property Test Results

Sample Number (short)	Specific Gravity	Compressive[1] Strength (psi)	Splitting Tensile Strength (psi)	Dynamic Young's Modulus (E6 psi)	Compression-to-Tension Ratio	CAI	Cutter Life (linear ft of travel)	Cutters Tested	LCM Test Numbers
YMP3	2.304	18,829	2,073	6.19	9.1	3.93	1,590,000	A30581,AM1723	12,13,14,28,29
YMP4	2.310	13,497	2,350	6.43	5.7	4.13	1,510,000	84HCT	25,26,27
YMP5	2.298	18,615	2,142	6.29	8.7	4.50	1,390,000	84HCT	22,23,24
YMP10	2.308	20,393	2,611	5.82	7.8	4.63	1,350,000	System 35	43,44,45
YMP11	2.302	13,530	999	5.90	13.5	4.15	1,500,000	System 35	36,37,38,42
YMP12	2.267	12,806	1,094	5.74	11.7	4.25	1,470,000	AM1723	31,32
YMP13	2.241	10,187	1,644	3.87	6.2	4.26	1,470,000	AM1723	32
YMP17	2.291	11,010	2,049	5.72	5.4	4.47	1,400,000	A30581	16,17,18
YMP21	2.259	9,874	1,858	6.01	5.3	4.43	1,410,000	AM1723	8,9,10,33,34,35
YMP24	2.276	7,736	2,276	4.97	3.4	4.28	1,460,000	A30581	8,9,10,11
YMP27	2.294	16,181	2,313	6.50	7.0	3.79	1,650,000	84HCT	19,20,21
YMP32	2.308	15,754	1,265	6.13	12.4	4.29	1,450,000	A30581	12,13,14,15
YMP33	2.303	10,028	2,268	5.90	4.4	4.63	1,350,000	A30581,AM1723	16,17,18,30,31
YMP34	2.251	8,064	1,717	5.48	4.7	4.39	1,420,000	System 35	19,20,21,39,40,41
Average:	2.287	13,322	1,904	5.78	7.53	4.30	1,460,000		
± σ:	0.022	3,960	480	0.65	3.06	0.23	82,015		
Maximum:	2.310	20,393	2,611	6.50	13.54	4.63	1,650,000		
Minimum:	2.241	7,736	999	3.87	3.40	3.79	1,350,000		

[1]Length-to-diameter ratio (L/D) equals 2.0.

3.4.1 Compressive Strength

The disc cutter tests at the wider spacings (especially the 5-in. spacing) were conducted in samples of relatively lower uniaxial compressive strength (UCS). This may account for some of the reduction in specific energy for the disc cutters at wider spacings; however, the trend is somewhat mixed.

The point-attack cutter tests at larger spacings were conducted in samples of relatively higher UCS. This may account for the minimal effect of spacing on specific energy. It requires more energy to cut higher strength rock. Thus, the tendency for the specific energy to decrease with increasing spacing for the point-attack cutters may be offset by the higher strength rock.

UCS variability in the TSw2 may be attributable to the vugs and small-scale cracks in the rock. The scale of these features could influence the UCS results, but would have a much lesser effect on rock cutting. A vug on the order of an inch in size is a large feature in a 2-in. core, but is a minor feature in a tunnel face or LCM sample.

3.4.2 Cerchar Abrasivity

The Cerchar Abrasivity Index (CAI) provides an estimate of cutter life in terms of distance traveled. The test used to develop the CAI is described by Ozdemir et al. (1992). Essentially, it involves scratching the surface of a freshly broken piece of rock with a metal pin made of the same material as the cutter. The wear flat which develops on the pin tip then gives an indirect measure of the abrasivity and the expected cutter life in rolling feet. This value in turn is used to calculate cutter costs per unit volume of material excavated by the machine. The CAI has been shown to provide accurate estimates of field cutter wear in a wide range of rock formations.

Three Cerchar Abrasivity tests were performed on each LCM rock sample (listed in Table 3-3). From the CAI, the projected cutter life in terms of rolling distance is calculated by

$$CL = 6.24(10^6)/CAI \qquad (1)$$

where

CL = cutter life (ft)
CAI = Cerchar Abrasivity Index.

The cutter life results are also listed in Table 3-3. As can be seen, the average estimated cutter life for the welded tuff is 1.45 million ft.

3.4.3 Density

Rock density allows the projected production tonnages to be calculated from the volume production rate. An average value of 2.3 g/cm^3 was used in the calculations.

3.4.4 Compression-to-Tension (C/T) Ratio

The C/T ratio refers to the ratio of the UCS to the tensile strength and is a measure of the toughness of the rock fabric. The ratio is used in predicting roadheader performance. The higher the tensile strength (i.e., the lower the ratio), the tougher the rock fabric, as seen in Table 3-4.

Table 3-4

Compression-to-Tension (C/T) Ratios
for Rock Toughness and Cuttability Estimates

C/T Ratio	Qualitative Toughness	Efficiency Factor (e)
>20	Weak	1.00
>15	Moderate	0.75
>10	Moderately tough	0.50
<5	Tough	0.25

With an average C/T value of 7.4, TSw2 has a relatively tough fabric for an igneous rock. This contributes to the relatively high rolling forces seen in Section 3.1.1. The efficiency factor (e) (Section 4.2) will be used to predict roadheader performance.

4.0 PERFORMANCE PREDICTIONS

The machine performance predictions were derived directly from the force data from the LCM test results. Performance prediction requires a determination of the force response on the cutter (either disc or point-attack) as a function of spacing and penetration. With this information, the machine performance can be directly calculated from the measured normal and rolling forces.

In the LCM tests, the penetration and spacing are set, becoming the independent variables. The force response is measured for each spacing and penetration combination; the force response is the dependent variable. For a TBM, machine thrust and rotation rate are set and become the independent variables. The resulting penetration is the dependent variable. Whether LCM or TBM, the interaction of the independent and dependent variables is controlled by the force response on the cutter to changes in penetration and spacing.

The cut spacing cannot be changed on an operating TBM unless cutters are repositioned or a new cutterhead featuring a different cutter layout pattern is installed. Either change requires a fairly long machine-shutdown time and is generally not considered practical.

Earlier work in this program developed machine performance predictions from the physical and geologic properties of the rock (Ozdemir et al., 1992). This involved the prediction of cutter normal and rolling forces from the rock properties and the tool cutting geometry. In the LCM prediction method, cutter forces as a function of spacing and penetration are measured directly, eliminating the need for force prediction. Therefore, the LCM tests allow more accurate predictions of excavator performance than those based solely on physical and geologic properties of the rock.

4.1 Methodology for Predicting Tunnel Boring Machine Performance

The TBM performance characteristics that are of interest include thrust, torque, power, number of cutters, the rate of penetration, and the cutterhead rotation rate. Except for cutterhead rotation rate, each is calculated directly from the LCM force measurements and the cutting geometry. For each spacing and penetration combination, the machine performance characteristics (thrust, torque, etc.) are determined.

In order to provide more representative results and to allow extrapolation of the existing data, regression analyses were performed on cutter forces measured during the LCM tests. The resultant regression equations were then used as a basis to evaluate the TBM performance and to establish guidelines for design optimization. The performance results in Tables 4-1 and 4-2 include both measured and regressed data.

4.1.1 Number of Cutters

The number of cutters on a TBM is a function of machine diameter and cutter spacing. In the simplest case, the number of cutters is determined by dividing the cutterhead radius by the cutter spacing; however, the center

Table 4-1

Performance Predictions for A30581 Disk Cutter

Measured Data and Resulting Performance Predictions

Spacing (in.)	Penetration (in.)	#C	Average Forces (lb) Normal	Rolling	Side	Performance Predictions Thrust (lb)	Torque (ft-#)	Power (hp)	Cutting Coefficient	Specific Energy (hp-hr/yd^3)	S/P Ratio	Peak/Mean Ratio Normal	Rolling	Side
3	0.2	56	22,489	2,012	934	1,680,000	1,310,000	1,700	0.09	6.59	15.0	2.2	2.4	6.9
3	0.3	56	29,857	3,729	2,811	2,230,000	2,440,000	3,300	0.12	8.14	10.0	2.1	2.3	3.6
3	0.4	56	31,239	4,496	2,769	2,330,000	2,940,000	3,900	0.14	7.36	7.4	2.1	2.3	4.4
3	0.5	56	35,179	5,441	3,873	2,630,000	3,550,000	4,700	0.15	7.13	6.0	2.4	2.9	3.3
4	0.2	47	25,469	2,405	765	1,600,000	1,320,000	1,800	0.09	5.91	20.0	2.0	2.4	8.7
4	0.3	47	25,565	3,690	2,027	1,600,000	2,020,000	2,700	0.14	6.04	13.3	2.2	2.2	4.5
4	0.4	47	32,087	5,312	2,602	2,010,000	2,910,000	3,900	0.17	6.52	10.0	2.1	2.1	4.6
4	0.5	47	40,001	6,430	3,448	2,510,000	3,530,000	4,700	0.16	6.32	8.0	2.3	2.6	4.2
5	0.2	41	26,193	2,758	1,279	1,430,000	1,320,000	1,800	0.11	5.42	25.0	2.2	2.5	6.0
5	0.3	41	30,408	3,774	1,141	1,660,000	1,800,000	2,400	0.12	4.94	16.7	2.1	2.3	9.3
5	0.4	41	32,472	4,316	1,298	1,780,000	2,060,000	2,700	0.13	4.24	12.5	2.4	2.6	8.2

Regressed Data and Resulting Performance Predictions

Spacing (in.)	Penetration (in.)	#C	Average Forces (lb) Normal	Rolling	Performance Predictions Thrust (lb)	Torque (ft-#)	Power (hp)	Cutting Coefficient	Specific Energy (hp-hr/yd^3)	S/P Ratio	Rate of Penetration (ft/hr)	UCS (ksi)
3	0.14	56	23,300	2,270	1,740,000	1,480,000	2,000	0.10	10.6	21.4	4.9	5.3
3	0.21	56	27,600	3,460	2,060,000	2,260,000	3,000	0.13	10.8	14.3	7.4	5.7
3	0.28	56	31,800	4,640	2,370,000	3,030,000	4,000	0.15	10.9	10.7	9.8	5.7
3	0.35	56	36,100	5,820	2,700,000	3,800,000	5,100	0.16	10.9	8.6	12.3	3.4
4	0.14	47	24,400	2,440	1,530,000	1,340,000	1,800	0.10	8.56	28.6	4.9	16.5
4	0.21	47	28,600	3,620	1,790,000	1,980,000	2,600	0.13	8.47	19.0	7.4	16.6
4	0.28	47	32,900	4,800	2,060,000	2,630,000	3,500	0.15	8.42	14.3	9.8	16.7
4	0.35	47	37,100	5,990	2,320,000	3,280,000	4,400	0.16	8.41	11.4	12.3	15.7
5	0.14	41	25,400	2,600	1,390,000	1,240,000	1,700	0.10	7.30	35.7	4.9	10.8
5	0.21	41	29,700	3,780	1,620,000	1,810,000	2,400	0.13	7.07	23.8	7.4	10.7
5	0.28	41	34,000	4,970	1,860,000	2,380,000	3,200	0.15	6.97	17.9	9.8	10.5

Tunnel Diameter = 25 ft. Machine Efficiency = 0.75%
Cutterhead rpm = 7 rpm. Cutter Wear Factor = 0.70

Table 4-2

Performance Predictions for AM1723 Disc Cutter

Measured Data and Resulting Performance Predictions

Spacing (in.)	Penetration (in.)	#C	Average Forces (lb) Normal	Rolling	Side	Performance Predictions Thrust (lb)	Torque (ft-#)	Power (hp)	Cutting Coefficient	Specific Energy (hp-hr/yd^3)	S/P Ratio	Peak/Mean Ratio Normal	Rolling	Side
3	0.2	56	25,211	3,518	1,023	1,880,000	2,300,000	3,100	0.14	11.5	15.0	2.1	2.2	4.7
3	0.3	56	28,574	4,632	1,438	2,130,000	3,030,000	4,000	0.16	10.1	10.0	2.2	2.3	4.6
3	0.4	56	34,388	6,609	1,919	2,570,000	4,320,000	5,800	0.19	10.8	7.5	2.6	2.9	6.7
4	0.2	47	25,860	3,328	1,019	1,620,000	1,820,000	2,400	0.13	8.2	20.0	2.3	2.4	5.7
4	0.3	47	30,290	4,441	1,460	1,900,000	2,430,000	3,200	0.15	7.3	13.3	2.5	2.7	5.1
4	0.4	47	36,823	5,139	1,420	2,310,000	2,820,000	3,800	0.14	6.3	10.0	2.3	2.4	5.7
5	0.2	41	27,449	3,319	19	1,500,000	1,590,000	2,100	0.12	6.5	25.0	2.3	2.4	67.8
5	0.3	41	28,978	4,142	653	1,580,000	1,980,000	2,600	0.14	5.4	16.7	2.3	2.4	11.0
5	0.4	41	31,023	4,801	781	1,700,000	2,300,000	3,100	0.15	4.7	12.5	1.9	2.0	7.4

Regressed Data and Resulting Performance Predictions

Spacing (in.)	Penetration (in.)	#C	Average Forces (lb) Normal	Rolling	Performance Predictions Thrust (lb)	Torque (ft-#)	Power (hp)	Cutting Coefficient	Specific Energy (hp-hr/yd^3)	S/P Ratio	Rate of Penetration (ft/hr)	UCS (ksi)
3	0.14	56	25,770	3,790	1,920,000	2,480,000	3,300	0.15	17.7	21.4	4.9	9.9
3	0.21	56	29,585	4,854	2,210,000	3,170,000	4,200	0.16	15.1	14.3	7.4	9.9
3	0.28	56	33,400	5,918	2,490,000	3,870,000	5,200	0.18	13.8	10.7	9.8	9.9
4	0.14	47	25,650	3,374	1,610,000	1,850,000	2,500	0.13	11.8	28.6	4.9	18.8
4	0.21	47	29,465	4,438	1,850,000	2,430,000	3,200	0.15	10.4	19.0	7.4	18.8
4	0.28	47	33,280	5,502	2,090,000	3,020,000	4,000	0.17	9.7	14.3	9.8	18.8
5	0.14	41	25,530	2,958	1,400,000	1,410,000	1,900	0.12	8.3	35.7	4.9	10.0
5	0.21	41	29,345	4,022	1,600,000	1,920,000	2,600	0.14	7.5	23.8	7.4	11.5
5	0.28	41	33,160	5,086	1,810,000	2,430,000	3,200	0.15	7.1	17.9	9.8	10.0

Tunnel Diameter = 25 ft. Machine Efficiency = 0.75%
Cutterhead rpm = 7 rpm. Cutter Wear Factor = 0.70

and gage cutters are rarely set at the optimal spacing. They operate at smaller spacings to compensate for the difficult cutting conditions to which these cutters are subjected during boring. The center cutters exhibit high wear because the small radius at which they operate causes them to skid. The gage cutters exhibit high wear because they operate at the outermost radius of the cutterhead, where they experience high velocities and experience off-center side forces.

For this effort, standard center and gage arrays commonly used by TBM manufacturers were adopted. For the center cutters, an array of six cutters that covered a radius of 9.8 in. from the center of the cutterhead was used. For the gage cutters, an array of 13 cutters cutting the last 18.5 in. of radius was used. Thus, the space occupied by the standard arrays was subtracted from the cutterhead radius. Cutters were evenly spaced across the remaining radius according to the LCM spacing and their numbers were calculated. Finally, the cutters in the standard arrays were added to the number of cutters. Combining these measurements yields the following equation for calculating the number of cutters as a function of cutter spacing and tunnel diameter:

$$\#C = (6D - 38)/S + 19 \qquad (2)$$

where

#C = number of cutters (rounded to the nearest integer)
D = diameter of cutterhead (ft)
S = spacing (in.).

4.1.2 Rotation Rate

The limiting factor on the rotation rate of the cutterhead is the allowable linear velocity of the muck-pickup buckets, located at the outermost gage cutters. Above this limiting velocity, the muck buckets may not discharge the rock cuttings into the muck chute due to the centrifugal forces. At present, the maximum linear velocity at the gage cutters is restricted to 550 ft/min. Further, above this velocity, the bearing life of the outermost gage cutters may be adversely affected. Using the relationship of linear-to-rotational velocity, the following expression is derived for maximum rotations per minute (rpm):

$$rpm = V_l/(D)(pi) = 7.0 \text{ rpm} \qquad (3)$$

where

V_l = linear velocity limit (550 ft/min)
D = cutterhead diameter (ft).

Solving this expression for a diameter of 25 ft gives a maximum rotation rate of 7 rpm, which was used for machine power and penetration rate calculations. The 550-ft/min limit is not an absolute rule. For the preliminary predictions based on rock properties by Ozdemir et al. (1992)

500 ft/min was used, giving 6.36 rpm as the cutterhead rotation rate. Performance predictions were made using the LCM results and compared to the preliminary predictions of Ozdemir et al. (1992) (see Tables 4-3 and 4-4).

Table 4-3

Comparison of Performance Predictions
of Two Standard Power TBM Configurations

Parameter	Standard TBM From Preliminary[1]	Standard TBM From LCM Results
Cutterhead diameter (ft)	25	25
Rotational speed (rpm)	6.36	6.36
Cutters (# @ diameter [in.])	50 @ 17	50 @ 17
Maximum design cutter load (lbf)	50,000	50,000
Cutter spacing (in.)	3	3
Cutterhead power (hp)	2,400	2,400
Maximum operating torque (ft-lbf)	1,982,000	2,020,000
Operating thrust (lbf)	2,500,000	1,840,000
Penetration per revolution (in.)	0.24	0.21
Penetration rate (ft/hr)	7.63	6.68
Cutter life (hr)	74	68
Tunnel length per cutter (ft)	421	386
Approximate cutter cost ($/yd^3)	4.83	5.75

[1]Ozdemir et al. (1992)

4.1.3 Thrust

Total cutterhead thrust is the sum of the normal forces acting on each cutter for a given spacing and penetration.

$$Th = \#C(F_n) \tag{4}$$

where

Th = total cutterhead thrust (lbf)
#C = number of cutters on the cutterhead
F_n = normal force from the LCM tests (lbf).

Table 4-4

Comparison of Performance Predictions
of Two High-Power TBM Configurations

Parameter	High-Power TBM From Preliminary[1]	High-Power TBM From LCM Results
Cutterhead diameter (ft)	25	25
Rotational speed (rpm)	7.0	7.0
Cutters (# @ diameter [in.])	47 @ 19	47 @ 19
Maximum design cutter load (lbf)	60,000	60,000
Cutter spacing (in.)	3.2	3.2
Power (hp)	3,150	3,150
Maximum operating torque (ft-lbf)	2,026,000	2,360,000
Operating thrust (lbf)	2,820,000	1,920,000
Penetration per revolution (in.)	0.35	0.258
Penetration rate (ft/hr)	12.3	9.03
Cutter life (hr)	86	75
Tunnel length per cutter (ft)	750	660
Approximate cutter cost ($/yd^3)	4.37	4.65

[1]Ozdemir et al. (1992)

4.1.4 Torque

Cutterhead torque is a function of the rolling force on the cutter and its position. During cutting, each cutter experiences a rolling force. Each rolling force acts at a moment arm that is the distance of the cutter from the center of the cutterhead. The individual cutter torque is rolling force times the distance of each cutter from the center of the cutterhead. The total torque on the cutterhead is the sum of the torques generated by the individual cutters.

To simplify the analysis, machine torque was calculated using an average torque center, the rolling force, and the number of cutters. It is known that the center of torque shifts out past one-half the radius during field operation. One-half the radius is the center of torque when all cutters are equally loaded with the same spacing. The exact position of the center of torque is a function of the cutters' layout pattern in the cutterhead, variations in rolling force on the cutters, and other factors such as bucket loading and tunnel wall friction. Experience has shown the center of torque commonly varies from 0.56 to 0.66 from the center of the cutterhead, and can reach 0.7. A conservative value of 0.7 was used, which gives the following formula for calculating total torque:

$$Tq = (D)(\#C)(F_R)(0.35) \quad (5)$$

where

Tq = total cutterhead torque (ft-lbs)
D = diameter of the cutterhead (ft)
#C = number of cutters
F_R = Rolling force from the LCM tests (lbf).

4.1.5 Power

The power required for the cutterhead is a function of the torque and the rotation rate. It is calculated with the following formula:

$$P = (Tq)(N)/5252 \quad (6)$$

where

P = power (hp)
Tq = torque (ft-lbf)
N = cutterhead rotation rate (rpm).

4.1.6 Instantaneous Penetration Rate

The instantaneous penetration rate is a function of the LCM penetration and the rotation rate. The excavator is designed to penetrate the rock at the LCM penetration per one revolution of the cutterhead. Thus the instantaneous penetration rate is

$$IP = (N)(P)(5) \quad (7)$$

where

IP = instantaneous penetration rate (ft/hr)
N = cutterhead rotation rate (rpm)
P = the LCM penetration (in.).

4.1.7 Machine Efficiency

Two factors influence machine efficiency, the mechanical losses in the excavator and the effect of cutter wear. These factors are introduced into the performance predictions as follows.

Mechanical losses account for the inefficiencies in transferring the power from the power source to the excavation action at the rock face. The LCM measures the power needed to excavate the rock at the rock face. This is the cutterhead power. The cutterhead power determined from the LCM tests then must be translated into machine power by taking into account the drive system losses. The exact value of efficiency depends on the specific

machine design. When the design is unspecified, common industry practice assumes a 75-percent efficiency for the machine thrust and torque systems:

$$Th_m = Th_c/0.75 \quad (8)$$

and

$$Tq_m = Tq_c/0.75 \quad (9)$$

where

Th_m = machine thrust (lbf)
Th_c = cutterhead thrust (lbf)
Tq_m = machine torque (ft-lbs)
Tq_c = cutterhead torque (ft-lbs).

Note that by adjusting the torque for mechanical losses and using the adjusted torque value in the power calculation, the power is also adjusted for machine losses by Equation 5.

The effect of cutter dulling is considered by reducing the cutter penetration for a given cutter load. During field operation, cutters on a mechanical excavator are continually replaced as they wear out. Thus, the excavator may have a set of cutters that range from new to almost completely worn. From extensive field projects in hard rock, cutter wear was assumed to cause a 30-percent reduction in machine performance. Penetration, then, becomes:

$$P_m = 0.7(P_c) \quad (10)$$

where

P_m = actual penetration (ft/hr)
P_c = LCM penetration (ft/hr).

Note that when LCM-derived forces are adjusted for cutter wear effects, the values for rate of penetration are also reduced according to the relationship given by Equation 7 for a given machine thrust, torque, and power. This means the original penetration rate that would be achieved with completely new cutters can only be maintained with an increase in machine thrust and power.

All results presented in this report, therefore, compensate for machine efficiency and cutter wear.

4.2 Methodology for Predicting Roadheader Performance

While the LCM tests provide the same type of information for TBMs and roadheaders, the performance prediction methodology is different. In addition to cutter spacings and penetrations, LCM tests for a point-attack cutter add another cutting variable, the bit angle of attack. Changing the angle of attack can significantly change the force response of the cutter to spacing and penetration. Only one angle of attack, 56°, was used in the tests.

Unlike the TBM, the performance prediction for a roadheader is calculated from specific energy. The difference in methodology is due to the differences in cutting action of the two machine types.

The TBM is a full-face machine, requiring only one motion (rotation) in addition to the thrust to cut the entire tunnel face. A full-face machine operates at a fixed cutter spacing and, therefore, allows straightforward use of the forces measured in the laboratory to develop performance predictions.

The roadheader is a partial-face machine, requiring several motions (e.g., lifting and arcing) in addition to the thrust to cut the entire face. These cutterhead motions have an effect on machine performance as the machine must cut the entire face with arcing and lifting motions before it can advance. The roadheader has more design variables because the cutting action creates variable cut spacing depending on bit layout, cutterhead motion, and cutterhead rotational speed.

In addition to cutterhead motions, the engagement of the cutterhead with the rock is a design factor. A TBM cutterhead always fully engages the face, while the roadheader cutterhead may lose contact with the rock due to vibrations generated during cutting. A tougher rock will cause more vibrations unless the cutterhead sumping distance into the rock is reduced, meaning less production. The fewer the number of cutters in contact with the rock, the lower the machine performance and rate of penetration.

One major roadheader design factor is the difference between transverse (ripper) and axial (milling) cutterheads; each has fundamentally different cutting actions. The ripper head thrusts two cylindrical-shaped heads into the rock with their cutting axis perpendicular to the boom. The milling head thrusts a cone-shaped head into the rock with its cutting axis parallel to the boom. The milling cutterhead operates at a lower speed than the ripper, and requires more machine mass or stelling to give the necessary stiffness required to efficiently transfer the machine power into cutting action.

The shape and size of the cutterhead determines many design details for a roadheader. For a given thrust, a smaller cutterhead will develop higher forces on each cutter due to fewer cutters in contact with the rock. Conversely, a larger cutterhead will develop lower cutter forces, but, in general, will require more torque. Hence, there are many trade-offs which enter into the design and bit layout of a roadheader cutterhead.

To ensure that the most appropriate roadheader is specified for a project, a complete analysis of the many candidate machines is performed. The analysis uses the LCM data to determine in detail the suitability of each machine for the job. Each roadheader is examined to ensure that the necessary power can be transferred into rock cutting. This requires an analysis of cutter forces, torque requirements, number of cutters, sumping forces, cutterhead rotational velocity, cutterhead motions and size, and other factors.

For this study, it was impractical to consider the necessary variety of roadheaders and to analyze the unique capabilities of each. The roadheader performance was calculated directly from the specific energy response to changes in spacing and penetration. Specific energy is the energy required to excavate a unit volume of rock. When the machine power is divided by the specific energy, the result is the instantaneous production rate,

$$IPR = (.75)(P)/(SE) \qquad (11)$$

where

IPR = instantaneous production rate (yd^3/hr)
P = machine power (hp)
SE = specific energy ($hp\text{-}hr/yd^3$).

Note that the efficiency of the power transfer to the rock is assumed to be 75 percent, as was the case for the TBM (Section 4.1.7).

Equation 11 predicts the production rate if the value of specific energy is known. The LCM tests have been shown to provide accurate estimates of specific energy. Further, the minimum specific energy values can be determined from the LCM tests. By using the minimum value determined by the test program, the most efficient cutting action and the highest production rate are achieved for the available machine output power.

As noted before, the roadheader cannot match the stiffness of a full-face machine such as a TBM. The lack of stiffness causes a reduction in the amount of power that is effectively transferred to the rock. Equation 11, then, is always reduced by some amount that is dependent on rock conditions, cutter wear, machine stiffness, and other factors. These factors can also vary from one manufacturer to another. Accounting for these factors, Equation 11 becomes

$$IPR = (e)(.75)(P)/(SE) \qquad (12)$$

where

IPR = instantaneous production rate (yd^3/hr)
e = efficiency factor
P = machine power (hp)
SE = specific energy ($hp\text{-}hr/yd^3$).

An efficiency factor of 0.5 was used for the performance predictions for the roadheader presented below. This is a nominal number for the conditions found in the mechanical excavation of rocks similar to TSw2. The factor comes from Table 3-4 for a rock with a C/T ratio of 7.4.

The roadheader penetration rate is calculated from the LCM penetration.

$$IP = (27)IPR/A \tag{13}$$

where

IP = penetration rate (ft/hr)
A = tunnel cross-sectional area (ft^2).

Note that the IPR has already been adjusted for machine efficiency and rock conditions; therefore, the IP is also adjusted.

Similarly, the production rate in tons per hour can be calculated from the density of the rock and the instantaneous penetration rate.

$$ITR = IPR(sg)(0.8424) \tag{14}$$

where

ITR = instantaneous production rate (t/hr)
sg = specific gravity.

Note that the specific gravity used for this analysis was 2.3.

4.2.1 Specifying the Roadheader

Unlike a TBM, where cutting geometry remains the same (each cutter travels in its respective kerf), a roadheader produces a complex cutting pattern where both bit penetration and spacing continually vary as the cutterhead sumps into the rock and commences its slewing action. Also the cutting action is different depending on whether a milling or ripper head is used.

The complexity of the roadheader cutting action means that the cutterhead is designed for the specific rock conditions, but the rest of the machine is generally an existing off-the-shelf design. The cutterhead is given the best available spacing and penetration to attack the rock, as determined by the LCM test program. The off-the-shelf machine that supports the cutterhead is then analyzed to ensure that it has enough power, mass, and stiffness to efficiently transfer the necessary power to the cutterhead.

In practice, the potential roadheader user will analyze machines from several manufacturers and different machines from the same manufacturer. During the analysis, the cutter force data measured by the LCM tests are

used to determine if the allowable loads on the machine will be exceeded. The machine's productivity is calculated from the measured specific energy using Equation 11. The details of the cutterhead design and its supporting machinery determine how that productivity is reached.

Each cutter type has an allowable load recommended by the manufacturer. When those loads are exceeded, the cutters may undergo premature structural failure or experience excessive wear, resulting in high bit costs and uneconomical operation. The force data measured from the LCM tests allow determination of the cutter loads required to achieve the desired production rate for a given machine and geology.

In addition to allowable cutter loads, the other design features of the roadheader discussed in Section 4.2 are analyzed using the LCM data. The effect of machine stiffness and mass, cutterhead motions, cutterhead size, cutting action, etc. are all addressed.

For this effort, specific machines and, hence, the cutter forces, will not be considered. The cutter forces are included to allow designers and potential users to analyze candidate roadheaders once the desired production rates and excavation sizes are established.

4.3 Tunnel Boring Machine Performance Predictions

As described in the methodology (Section 4.1), the results in this section are based on the cutter force responses determined by the LCM test program. For each spacing and penetration combination, the predicted thrust, torque, power, and rate of advance were calculated. The calculated machine thrust, torque, and power (i.e., performance) predictions for each spacing and penetration are given in Tables 4-1 and 4-2, along with the LCM test data. Also included are the results of the regression analysis performed on the test data.

In the LCM tests, spacing and penetration were independent variables, and the measured force response was the dependent variable. Then, the predicted operating parameters--thrust torque, power, and rate of penetration--were calculated from the measured force response. For a TBM operating in the field, thrust and rotation rate are set as the independent variables and torque, power, and penetration rate become the dependent variables. For either approach, the basic relationship is the power needed to excavate the rock for a set of cutting parameters and geologic conditions.

The trends depicted in Tables 4-1 and 4-2 and Figures 4-1 through 4-18 are as expected for both the A30581 and the AM1723 constant cross-section cutters. The machine thrust, torque, and power requirements decrease with greater spacing and increase with deeper penetration.

Two sets of performance data are given in Tables 4-1 and 4-2, measured data and regressed data. The measured data are included to show the performance in terms of the observed LCM results. In addition, the regressed data are useful for interpolating machine performance.

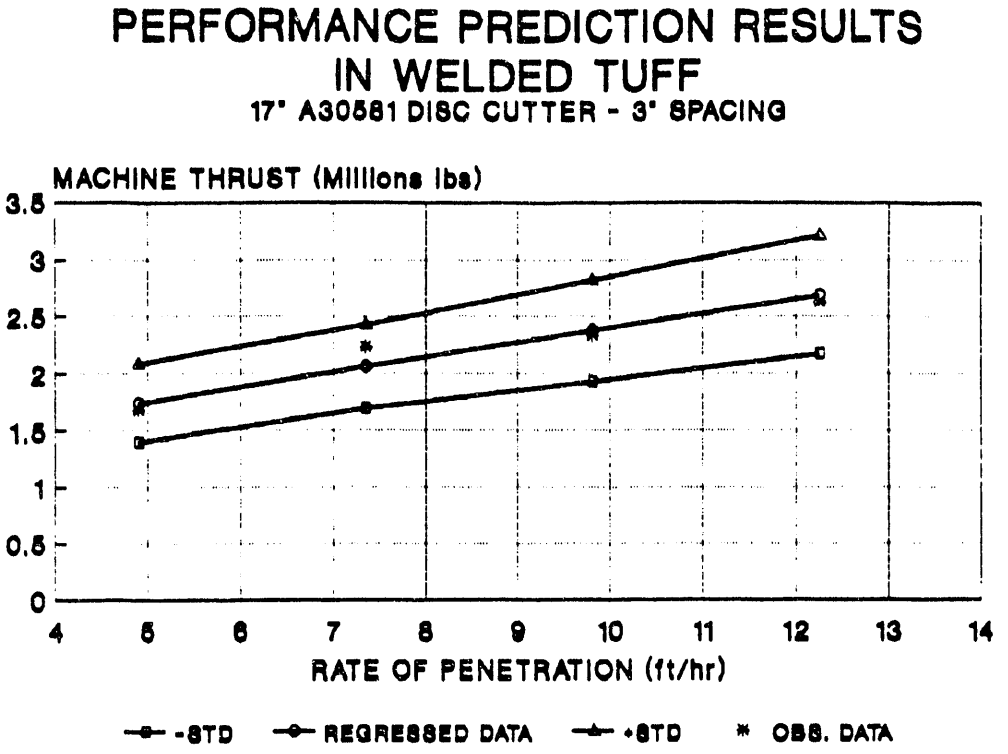

Figure 4-1. Thrust Prediction at 3-in. Spacing for the A30581 Disc Cutter

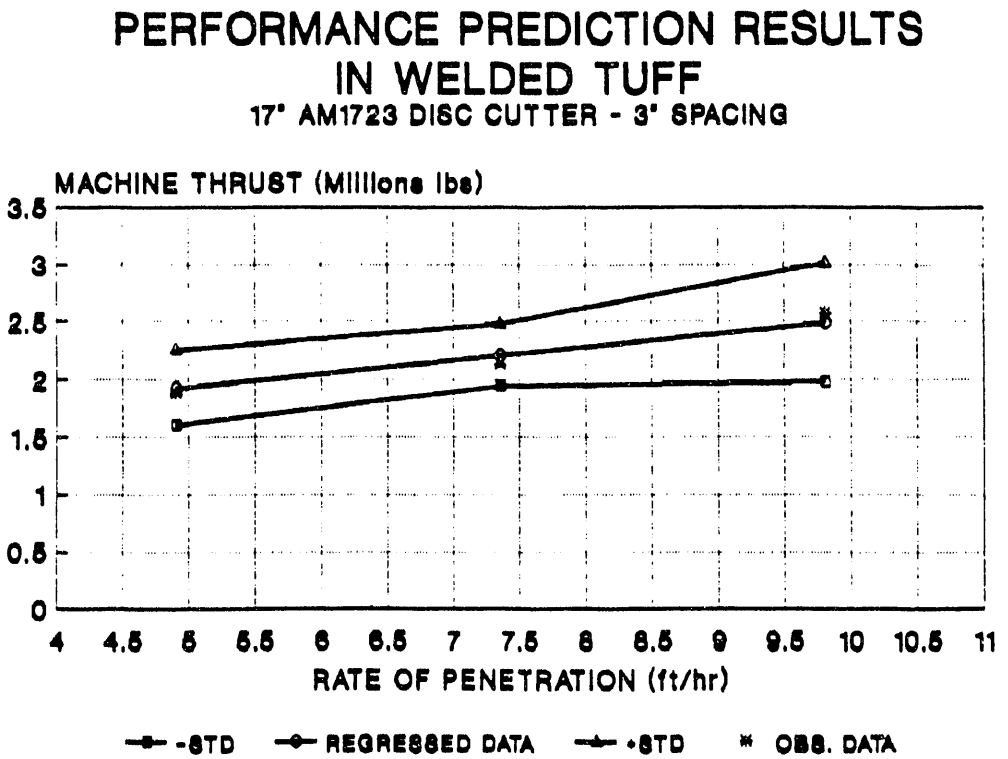

Figure 4-2. Thrust Prediction at 3-in. Spacing for the AM1723 Disc Cutter

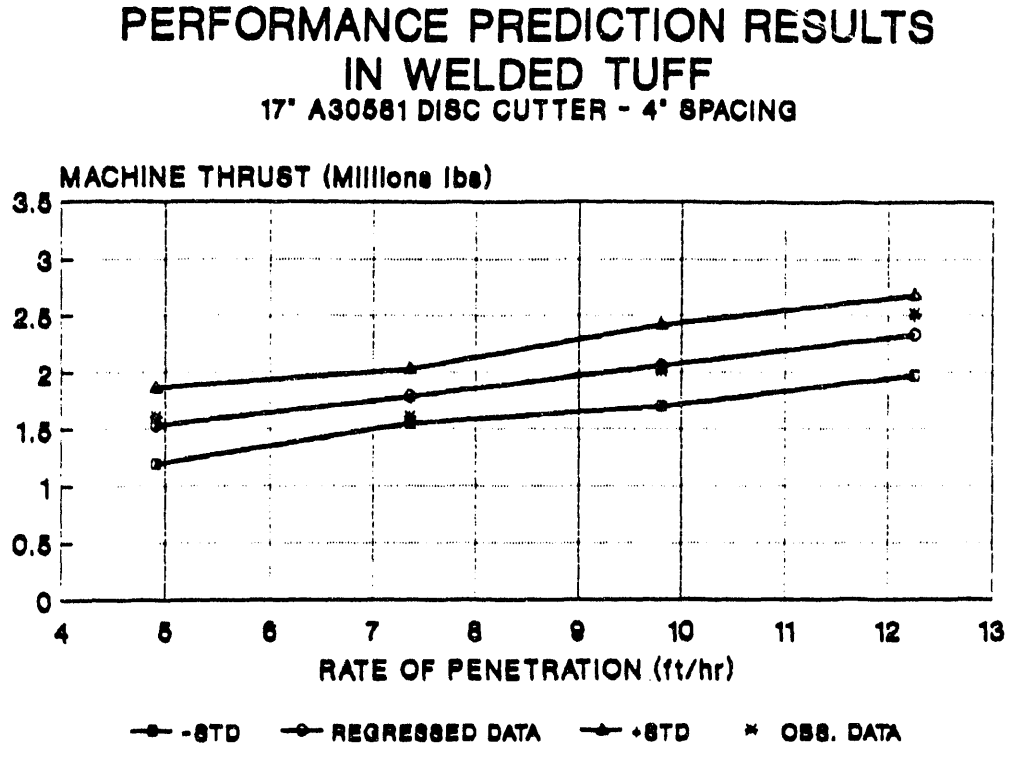

Figure 4-3. Thrust Prediction at 4-in. Spacing for the A30581 Disc Cutter

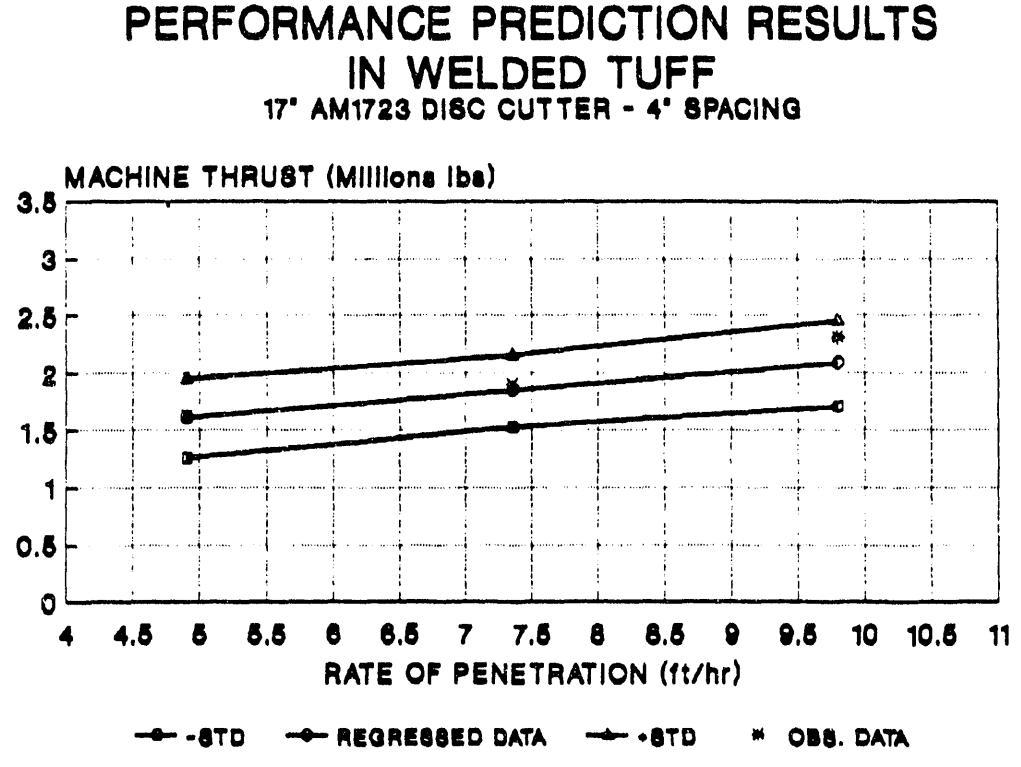

Figure 4-4. Thrust Prediction at 4-in. Spacing for the AM1723 Disc Cutter

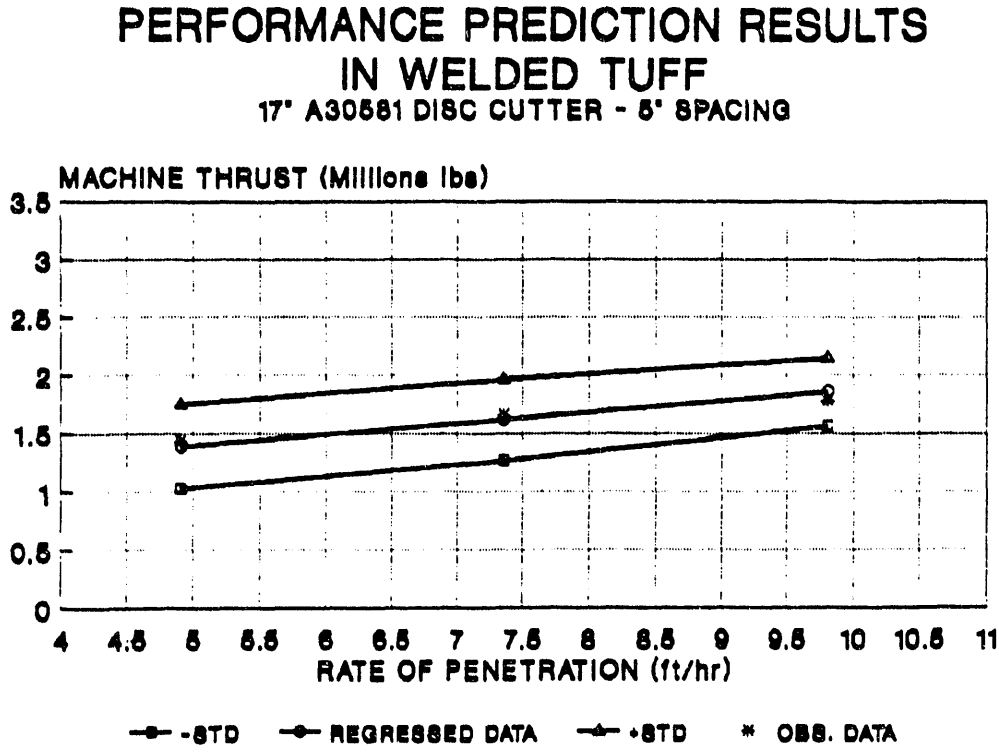

Figure 4-5. Thrust Prediction at 5-in. Spacing for the A30581 Disc Cutter

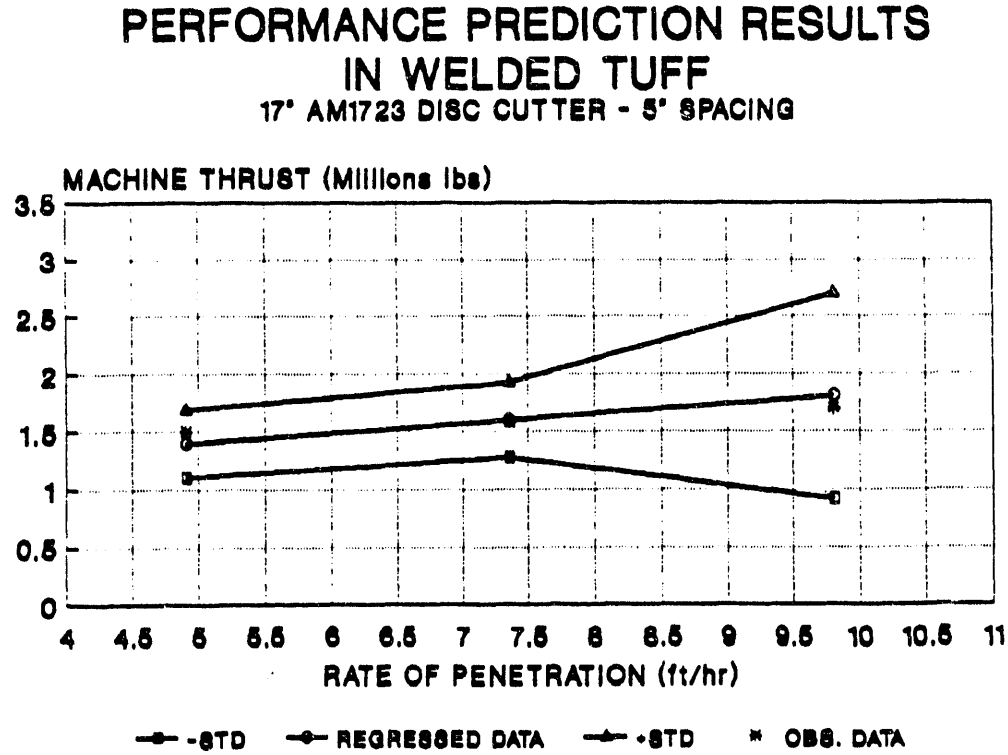

Figure 4-6. Thrust Prediction at 5-in. Spacing for the AM1723 Disc Cutter

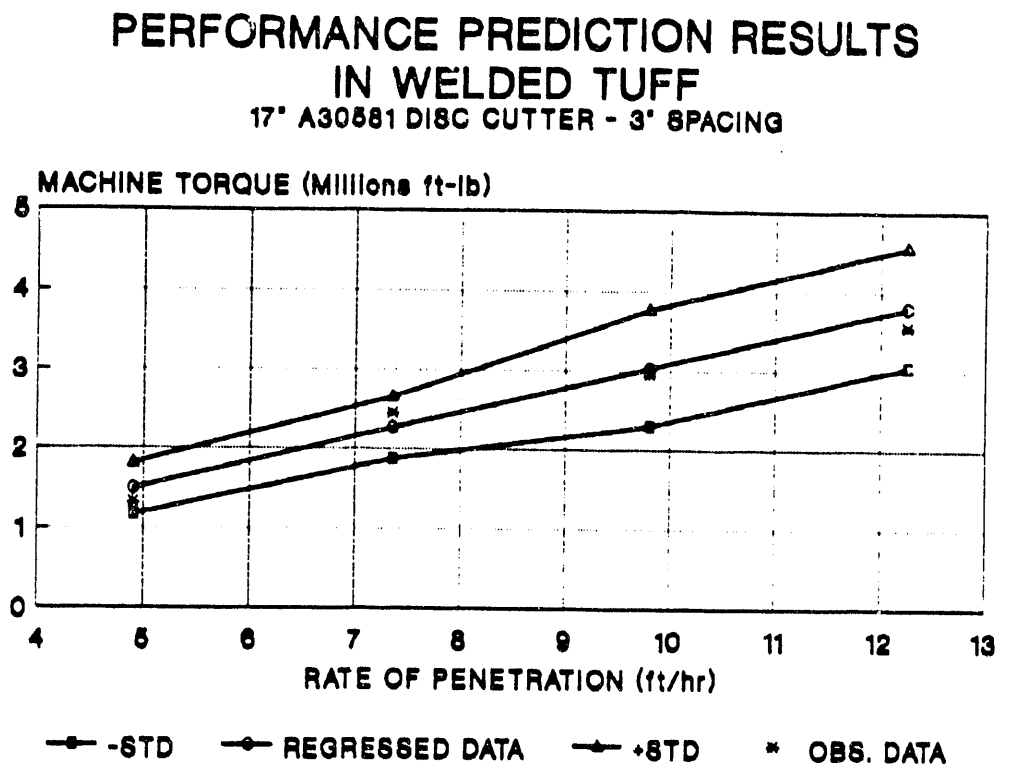

Figure 4-7. Torque Prediction at 3-in. Spacing for the A30581 Disc Cutter

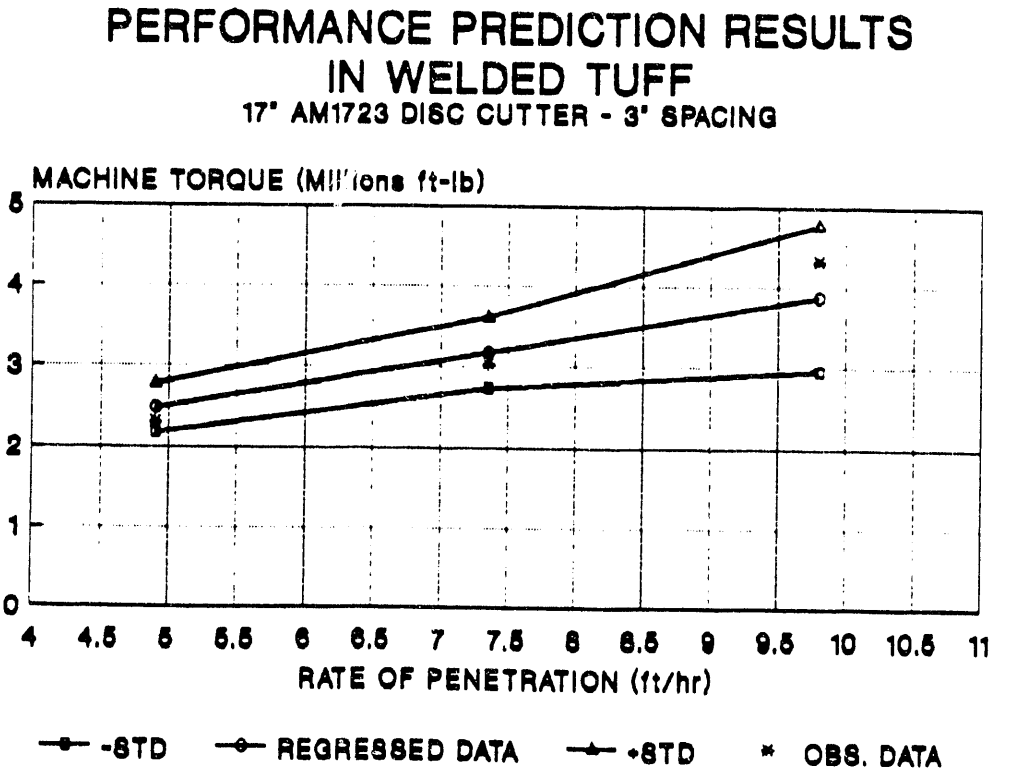

Figure 4-8. Torque Prediction at 3-in. Spacing for the AM1723 Disc Cutter

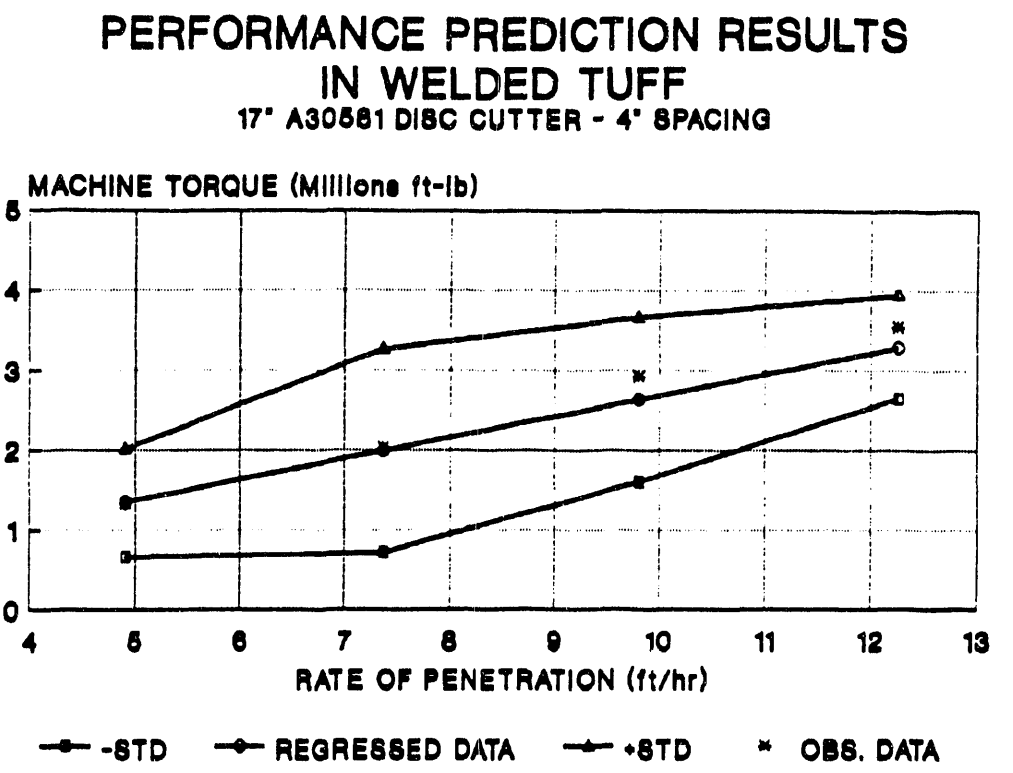

Figure 4-9. Torque Prediction at 4-in. Spacing for the A30581 Disc Cutter

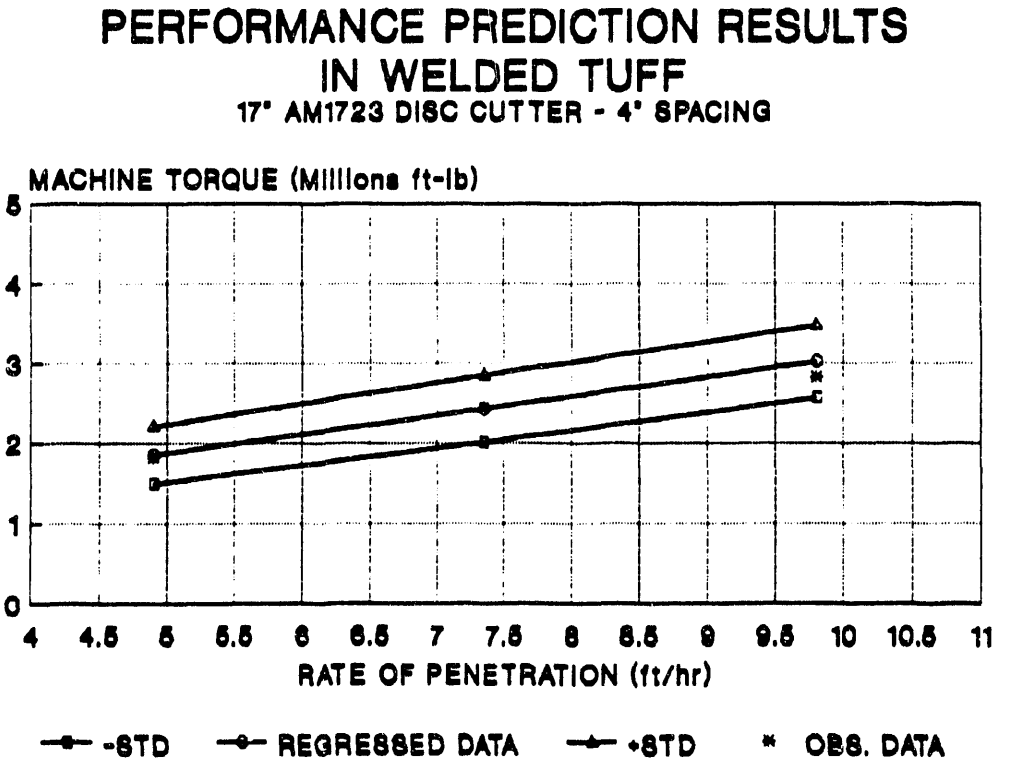

Figure 4-10. Torque Prediction at 4-in. Spacing for the AM1723 Disc Cutter

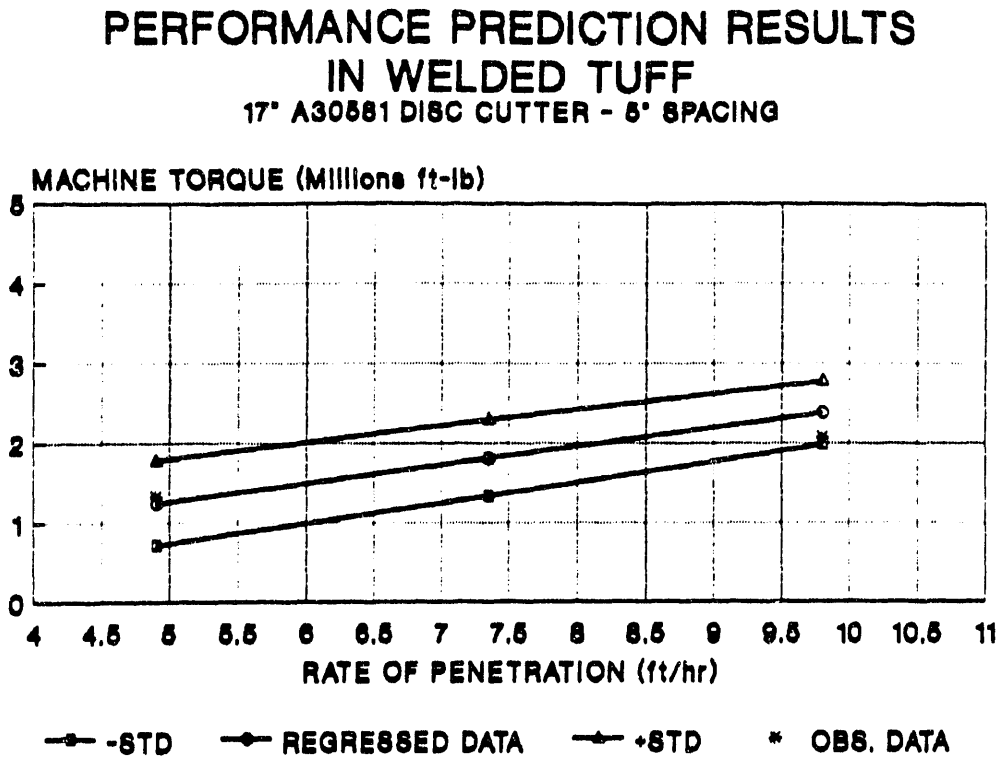

Figure 4-11. Torque Prediction at 5-in. Spacing for the A30581 Disc Cutter

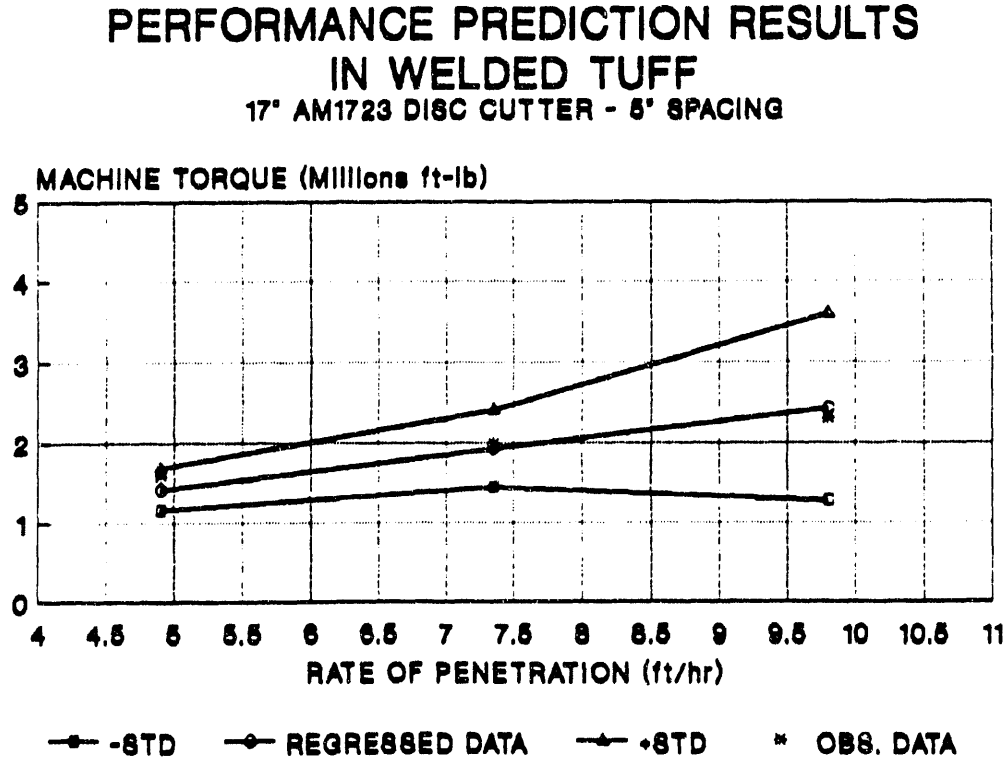

Figure 4-12. Torque Prediction at 5-in. Spacing for the AM1723 Disc Cutter

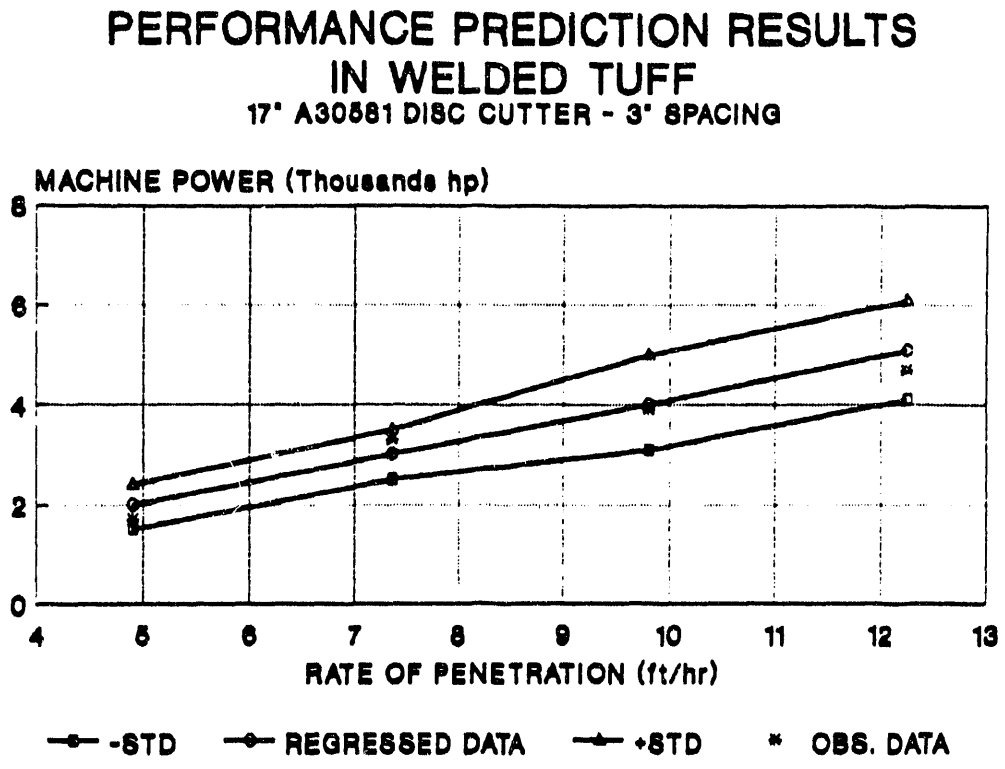

Figure 4-13. Power Prediction at 3-in. Spacing for the A30581 Disc Cutter

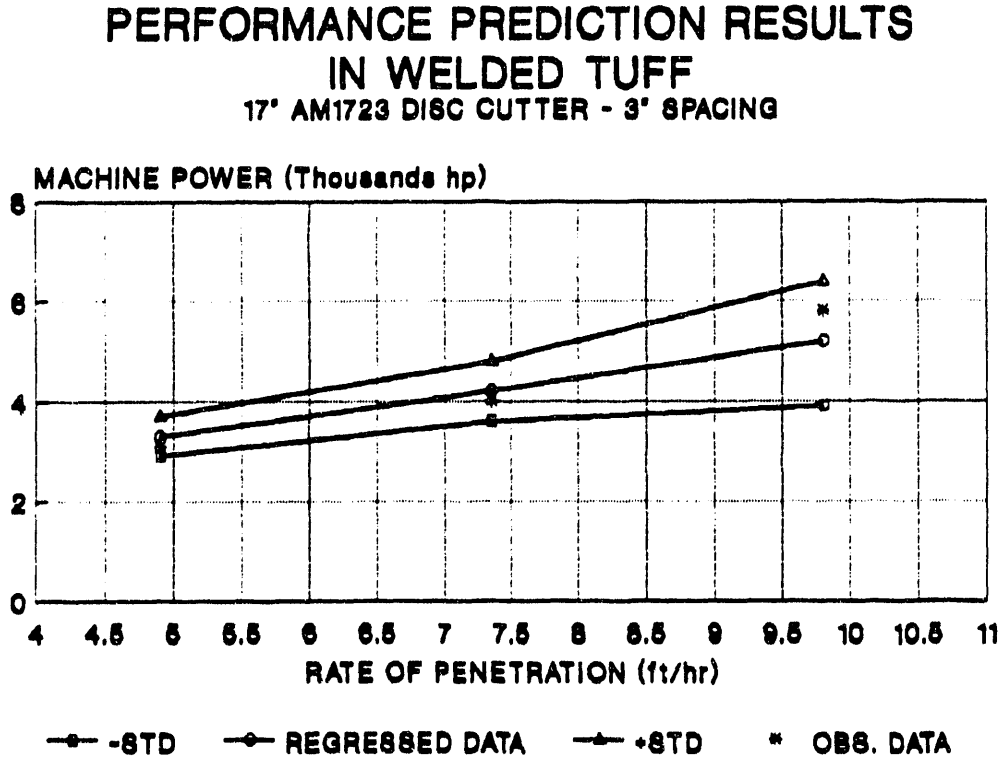

Figure 4-14. Power Prediction at 3-in. Spacing for the AM1723 Disc Cutter

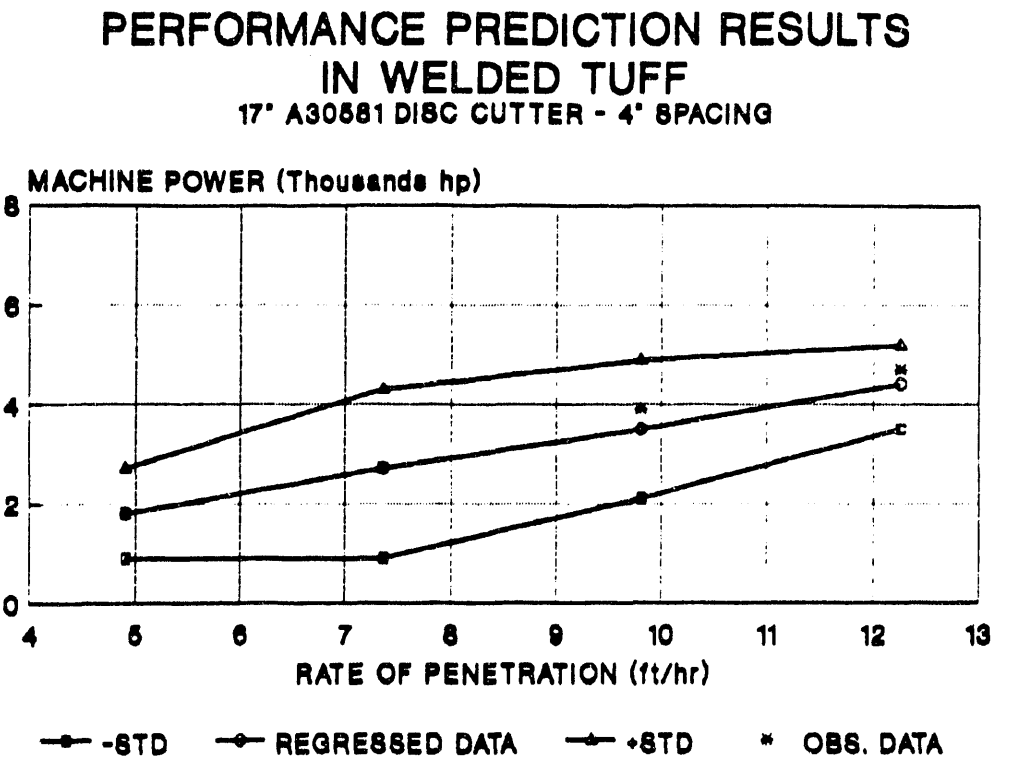

Figure 4-15. Power Prediction at 4-in. Spacing for the A30581 Disc Cutter

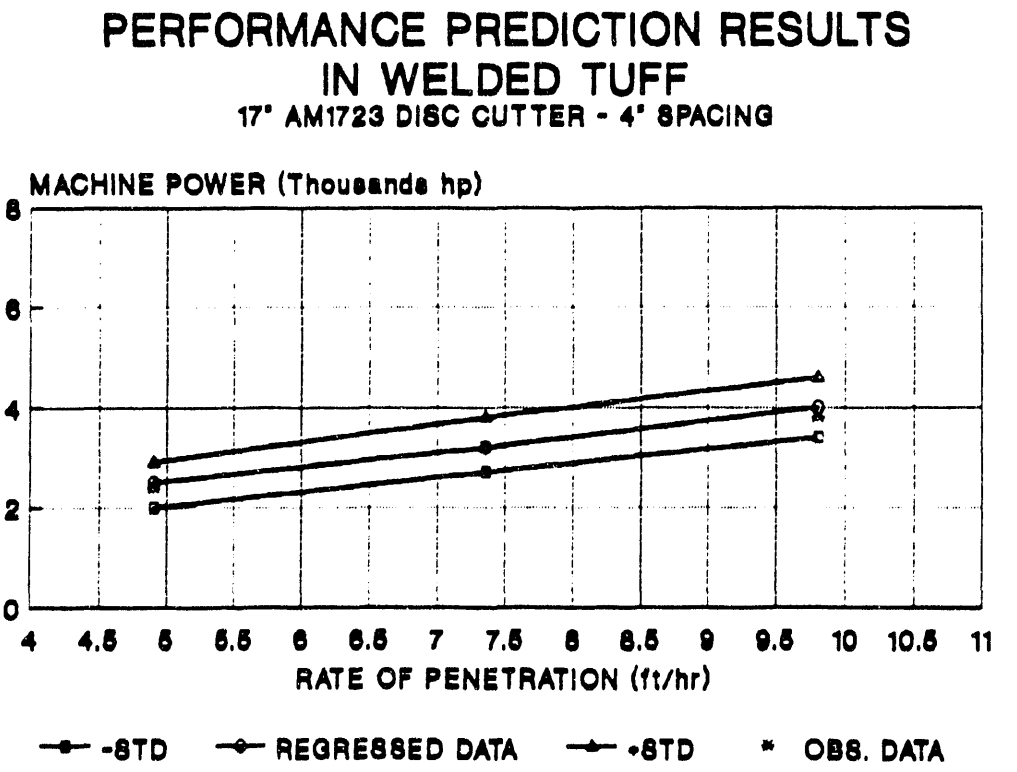

Figure 4-16. Power Prediction at 4-in. Spacing for the AM1723 Disc Cutter

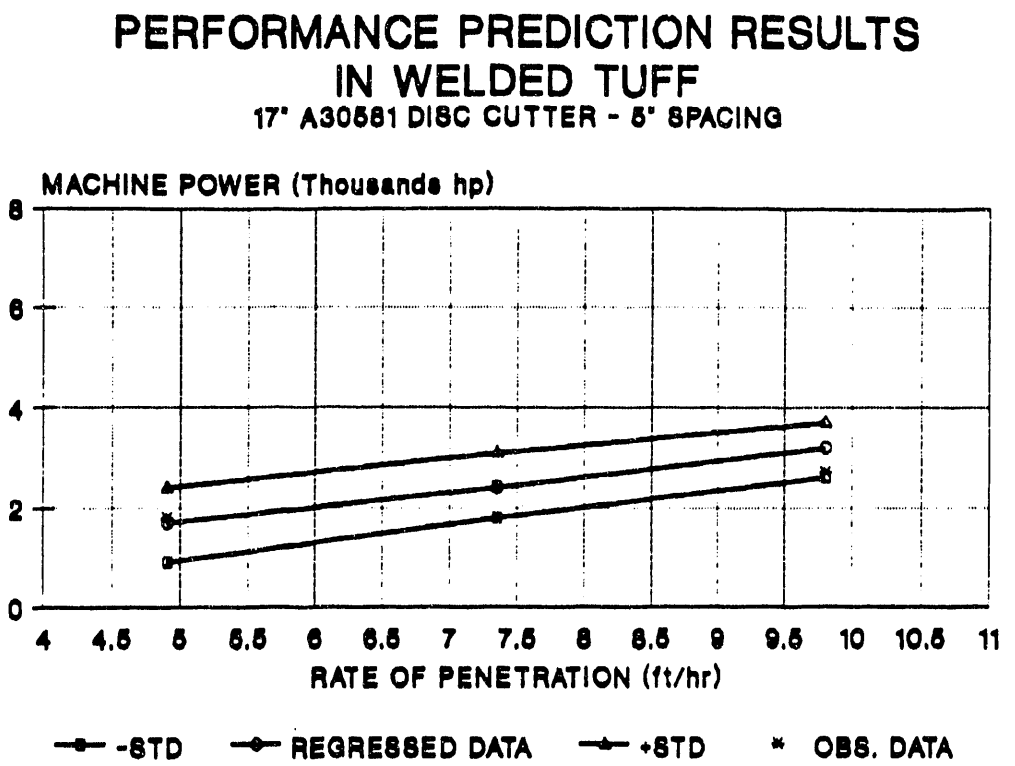

Figure 4-17. Power Prediction at 5-in. Spacing for the A30581 Disc Cutter

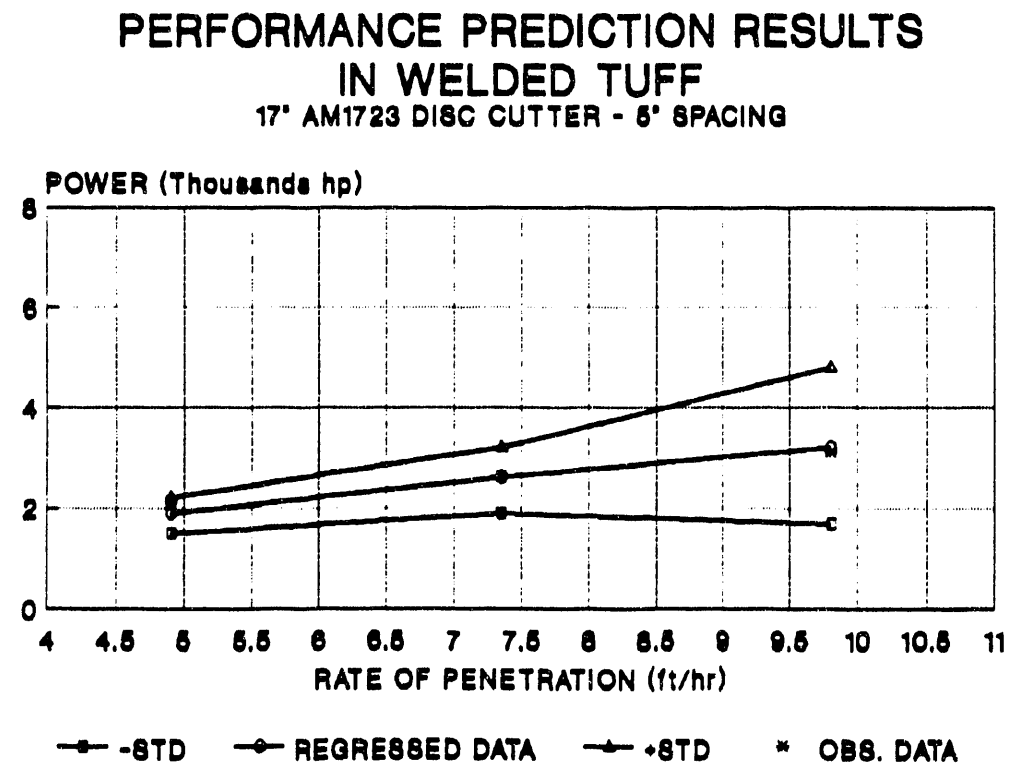

Figure 4-18. Power Prediction at 5-in. Spacing for the AM1723 Disc Cutter

In both tables, the upper data set, labeled "Measured Data," gives the performance predictions based on the observed LCM data. In this set the predictions are calculated by the methodology in Section 4.1 from the observed average forces. These are the same measured force data as shown in Table 3-1, except the predictions are added.

The lower data set, labeled "Regressed Data," is the performance predictions based on the regressed cutter forces. The cutter forces were regressed linearly as a function of spacing and penetration. Because the performance predictions are calculated from the force data, the performance predictions are also a function of spacing and penetration. The regression analysis smooths both the forces and the performance predictions. Further, in the regressed data set, the penetrations are reduced to account for cutter wear according to Equation 10 and discussed in detail in Section 4.1.7. Recall that this reduces the penetration rate by the same factor.

In both data sets, the cutter forces and performance data for the 0.5-in. penetration are shown. This penetration was not required by the test program and consisted of fewer test cuts than the rest of the tests. Consequently, the 0.5-in. penetration data will not generally be discussed.

The performance predictions based on the regression analysis are plotted in Figures 4-1 through 4-18. The figures also show the plus and minus standard deviations. In addition, the actual test data averages are plotted.

4.3.1 Thrust

For both disc types, total machine thrust increases with penetration and decreases with spacing. Thrust is plotted as a function of penetration rate in Figures 4-1 through 4-6. For the A30581 sharp cutter, the thrust range to attain a penetration rate of 4.9 to 9.8 ft/hr is 1.39 to 2.38 million pounds, for the blunt AM1723, 1.41 to 2.53. Both cutters have the lowest thrust at 5-in. spacing and 0.2-in. penetration, and the highest at 3-in. spacing and 0.4-in. penetration.

From Equation 4, thrust is a function of normal force and the number of cutters. It has already been shown that spacing does not have a strong effect on normal force. As spacing increases, normal forces increase slightly (see Section 3.1.1). An increase in spacing decreases the number of cutters on the cutterhead (Equation 2), thereby decreasing machine thrust.

Similarly, an increase in penetration increases normal force and, hence, the machine thrust.

4.3.2 Torque

For both disc types, machine torque increases with penetration and decreases with spacing. Torque is plotted as a function of penetration rate in Figures 4-7 through 4-12. For the A30581 sharp cutter, the torque range to attain a penetration rate from 4.9 to 9.8 ft/hr is 1.24 to 3.03 million foot pounds, for the blunt AM1723, 1.41 to 3.17. As with thrust, torque maximum occurs at a spacing of 3 in. and a penetration of 0.4 in. and the minimum occurs at a spacing of 5 in. and a penetration of 0.2 in.

From Equation 5, torque is a function of rolling force and the number of cutters. Rolling force does not significantly increase with increases in spacing (Section 3.1.1). When spacing increases, the number of cutters goes down, thereby decreasing torque requirements.

Similarly, an increase in penetration increases rolling force and, hence, the machine torque.

4.3.3 Power

For both disc types, machine power requirements increase with penetration and decrease with spacing. Power is plotted as a function of penetration rate in Figures 4-13 through 4-18. For the sharp A30581 cutter, the power range to attain penetration rates of 4.9 to 9.8 ft/hr is 1700 to 4000 hp, for the blunt AM1723 cutter, 1900 to 5200. Following the torque requirements, the maximum occurs at a spacing of 3 in. and penetration of 0.4 in., and the minimum at a spacing of 5.0 in. and a penetration of 0.2 in.

From Equation 6, power is a function of torque and rotation rate. Rotation rate is held constant at 7 rpm. This makes power a function of torque, yielding the same relationship to spacing and penetration that torque has.

4.3.4 Penetration Rate

Machine penetration rate (the instantaneous rate of machine penetration into the rock face) is a function of the penetration of the cutter into the rock and the cutterhead rotation rate. The more penetration, the more advance per period of time. The rotation rate is held constant at 7 rpm.

Three penetrations were tested in the LCM, 0.2, 0.3, and 0.4 in. By Equations 7 and 10, these penetrations translate to advance rates of 4.9, 7.4, and 9.8 ft/hr. These predicted advance rates were reduced by 30 percent to account for cutter dulling (Section 4.1.6).

4.3.5 Tunnel Boring Machine Design and Performance

In this section, three performance predictions are presented, all based on the measured LCM forces in the welded tuff. One will compare the predictions by Ozdemir et al. (1992) to new predictions for the same TBM configurations. The second will predict the performance of the best performing TBM as determined by the LCM test program, which uses 5-in. cutter spacing. The third will predict the performance of a TBM using a 4-in. cutter spacing.

Ozdemir et al. (1992) predicted the performance of two TBM configurations, a standard and a high power machine. The standard TBM is a typical machine that might commonly be found in a project similar to Yucca Mountain. It is capable of generating 2400 hp and is fitted with standard 17-in. disc cutters. The high power TBM incorporates the maximum power that can be physically packed into a 25-ft-diameter machine, 3150 hp. The standard TBM has 17-in. cutters and operates at a 6.36 rpm rotation rate. The high power TBM has 19-in.-diameter disc cutters, the largest cutters commercially available at present, and operates at 7 rpm.

Table 4-3 shows the results of the standard TBM performance predictions based on the LCM tests together with the predictions developed by Ozdemir et al. (1992) from the physical and geologic properties of the welded tuff. Both sets of predictions correspond to a maximum machine power of 2400 hp, which a standard TBM would be designed to produce with current technology. Cutter spacing, number of cutters, and machine power were not changed from those reported by Ozdemir et al. (1992). These operating parameters for the TBM were fixed and new requirements for machine thrust, torque, and a new attainable rate of penetration based on the LCM results were calculated.

Predictions listed in Table 4-3 indicate that more torque and consequently more power is needed to excavate the welded tuff than was indicated by the performance predictions of Ozdemir et al. (1992). The increased power requirements are a direct result of the higher-than-expected rolling forces measured in actual cutting of the welded tuff on the LCM. The higher torque requirements also mean that the attainable rate of penetration is reduced for the same machine power. This is an important finding from the LCM test program. In developing the earlier performance predictions based on physical property data, the welded tuff was assumed to behave in a manner similar to rock formations of similar strength and properties in order to arrive at an estimate of rolling force requirements; however, the LCM tests have clearly shown that welded tuff produces more rolling friction on the cutter, resulting in higher rolling force to maintain a given depth of cut. This is believed to result from the particular chipping response of the welded tuff under the action of a mechanical tool penetrating it. Welded tuff does not fracture efficiently until a certain cutter penetration is reached. Prior to that critical penetration, extensive crushing of the material occurs beneath the cutter tip, producing a crushed zone larger than in rocks of similar strength. This in turn increases cutter rolling friction, resulting in high rolling forces and therefore, increased machine torque requirements. The extensive crushed zone was observed during the LCM tests and are quantified in the sieve analysis.

The TBM thrust requirements based on the LCM tests are lower than previously estimated (Ozdemir et al., 1992). Thus, the TBM will be torque- and power-limited before its thrust capacity is reached. This is a finding of major importance with respect to TBM performance evaluation.

Table 4-4 (page 4-6) presents the same performance comparison for the high-powered TBM as was presented in Table 4-3 for the standard TBM. The high-power machine carries the maximum power that can be installed on a 25-ft-diameter machine, 7 motors at 450 hp each for a total of 3150 hp. It has 19-in. cutters, and operates at a rotation rate of 7 rpm.

As indicated in Table 4-4, the high power machine also becomes power-limited, resulting in a decreased penetration rate. While the high power TBM carries more power than the standard TBM, it still reaches its power limit before reaching its thrust limit.

Because of reduced penetration rate, the predictions based on the LCM tests give higher cutter costs than previously estimated. As noted earlier, TBM

cutter costs decline as the penetration rate increases due to the production of more material for a given rolling distance. Also, the high power TBM has lower cutter costs than the standard TBM because it uses larger diameter cutters in addition to attaining higher penetration rates.

The results from the LCM tests indicate that a TBM operating at 5-in. spacing yields the most efficient excavation of all the spacings tested for the welded tuffs at Yucca Mountain. A cutter spacing of 5 in. provides the lowest specific energy of all the spacings tested. Two 5-in. spacing designs are presented in Table 4-5, one for a standard and one for a high-power TBM. The design configurations are based on the LCM test data for the sharp A30581 cutter. Since the TBMs are operating at the lowest experimentally determined specific energy, they provide the highest attainable rate of penetration for a given machine power.

Both 5-in. spacing machines, standard and high power, operate at a maximum allowable rotation rate of 7 rpm (see Section 4.1). Both configurations require less thrust than the TBMs listed in Tables 4-3 and 4-4, since they have fewer cutters due to increased cutter spacing.

As expected, a TBM fitted with 19-in. cutters spaced at 5 in. provides the highest rate of penetration because the laboratory tests showed this spacing to be the most efficient of all spacing tested, meaning the lowest specific energy of cutting. The welded tuff exhibits high brittleness, and as a result, exhibits good chip-formation characteristics when cut at deep penetrations combined with wide spacings. However, if less brittle rock is encountered during repository excavation, the performance of a TBM with a 5-in. cutter spacing may be adversely affected as the rock may not fail during each cutterhead revolution. For this reason, a 4-in. spacing machine may be preferable to allow efficient excavation in harder and less brittle rocks than the welded tuff tested in the laboratory. Therefore, performance estimates were also developed for a standard and high-power TBM using a 4-in. spacing in welded tuff. The results are shown in Table 4-6.

A TBM with 4-in. spacing sacrifices approximately 10 percent of the advance rate of the 5-in. spacing machine. This is not a large difference to ensure that the TBMs will be capable of efficiently excavating rocks harder or less brittle than the welded tuff tested in the laboratory. This type of compromise is common industry practice. Even within the same formation, harder rock than expected can be encountered, particularly if the formation is extensive, such as TSw2.

4.3.6 Machine Utilization Factor

Estimating the daily advance rate requires estimation of an average utilization factor for the TBM. As discussed by Ozdemir et al. (1992), the rate of advance is simply the product of the penetration rate and the utilization factor. The machine utilization factor is influenced by the following factors:

- Tunnel grade;
- Haulage method (rail, rubber-tired, or conveyor);
- Water inflow rate;

Table 4-5

Performance Predictions of Two TBM Configurations
Operating at the Optimal Cutter Spacing of 5 Inches

Parameter	Standard TBM	High-Power TBM
Cutterhead diameter (ft)	25	25
Rotational speed (rpm)	7.0	7.0
Cutters (# @ diameter [in.])	41 @ 17	41 @ 19
Cutter spacing (in.)	5	5
Maximum cutter load (lbf)	50,000	60,000
Power (hp)	2,400	3,150
Maximum operating torque (ft-lbf)	1,850,000	2,360,000
Operating thrust (lbf)	1,620,000	1,850,000
Penetration per revolution (in.)	0.209	0.278
Penetration rate (ft/hr)	7.32	9.73
Cutter life (hr)	71	75
Tunnel length per cutter (ft)	655	690
Approximate cutter cost ($/yd^3)	4.75	4.45

Table 4-6

Performance Predictions of Two TBM Configurations
Operating at 4-Inch Cutter Spacing

Parameter	Standard TBM	High-Power TBM
Cutterhead diameter (ft)	25	25
Rotational speed (rpm)	7.0	7.0
Cutters (# @ diameter [in.])	41 @ 17	41 @ 19
Cutter spacing (in.)	4	4
Maximum cutter load (lbf)	50,000	60,000
Power (hp)	2,400	3,150
Maximum operating torque (ft-lbf)	1,950,000	2,360,000
Operating thrust (lbf)	1,720,000	1,800,000
Penetration per revolution (in.)	0.19	0.25
Penetration rate (ft/hr)	6.65	8.75
Cutter life (hr)	66	71
Tunnel length per cutter (ft)	575	620
Approximate cutter cost ($/yd^3)	5.30	4.95

- Rock quality;
- Tunnel curves;
- Crew training and motivation; and
- Other--testing, characterization, wall mapping, etc.

Estimating the overall advance rate is a judgmental process that is best achieved by breaking the project down into several tunneling scenarios based on the factors listed above. A summary discussion of how each factor can affect the TBM utilization follows.

4.3.6.1 Slope and Haulage System--The slope (grade) of the tunnel being driven affects TBM utilization and therefore the advance rate. A slight upgrade is the most favorable because inflowing water drains by gravity, and haulage vehicles travel downhill when loaded. Slopes up to about +3° and down to -1° can be handled effectively by rail haulage systems. Thus, all excavations with design grades outside these limits are forced to use some haulage/supply system than rail, such as cog or hoist railways, conveyor belts, or trackless haulage (rubber-tired loaders and trucks). Slurry or pneumatic transport of muck also is possible, but neither has been proven cost effective in a construction job.

Conveyor haulage systems are rapidly gaining popularity as they are now achieving utilization factors equal to those given by rail haulage. Before recent increases in their reliability, conveyor systems working with TBMs reached utilizations of slightly more than 30 percent. As improvements continue, conveyors probably will become the primary means of material haulage in mechanically bored tunnels. The fundamental advantage of conveyors is their truly continuous nature, which is very conducive to full automation.

4.3.6.2 Water Inflow--Generally, water inflows must exceed 1000 gpm (3800 l/min) to cause significant delays during tunnel excavation with TBMs. Flows of this magnitude are not expected to be encountered during construction of the ESF openings.

4.3.6.3 Rock Quality--The highest rates of TBM advance are associated with rock quality designation (RQD) values between 50 percent and 75 percent, which is the common range of the tuffs at the Yucca Mountain site. Very massive formations tend to reduce the penetration rate and increase the frequency of required cutter changes. At the other end of the spectrum, RQD below about 25 percent indicates poor ground conditions that can frequently halt the TBM during support installation or other ground treatment.

Present TBM technology has advanced to the point that the machines can be designed to accommodate bad ground conditions through the use of different types of shields combined with standard methods of ground support (concrete liner segments or ring beams, rock bolts, wire mesh, and shotcrete). Installation of rock support, however, reduces the utilization percentage of the excavation machine.

4.3.6.4 Curves--The excavation of curved tunnels adversely affects TBM advance rate because the machine thrust and penetration rate must be reduced to minimize the uneven loading of the cutters and the main bearing. Utilization also drops due to increased necessity of surveying and repositioning of the surveyor's laser reference. Backup systems often display difficulties in negotiating curves, as well. Towed sleds tend to ride up the inside of the curve while rail-mounted backup units derail more often. The muck transfer and loading conveyors and the tunnel service lines must be adjusted continually to account for the positioning of each segment of the TBM support deck. These details all contribute to machine delays and subsequently to reduced utilization.

4.3.6.5 Crew Training and Motivation--Each TBM project undergoes a learning period during which system bugs are resolved and the crew develops a work rhythm. All TBM manufacturers provide experienced help for this startup phase in order to minimize delays, but machine utilization remains lower during this period than any other.

4.3.6.6 Access for Site Characterization--The high level of characterization required during excavation of the ESF openings could significantly reduce machine utilization. The amount of reduction will depend on the ease of access to the face and the area directly adjacent to and behind the machine, which in turn depends on the machine design and the tests to be conducted there.

Table 4-7 lists the suggested haulage systems in addition to the expected utilization factors and advance rates for the TBM using a 5-in. cutter spacing. As discussed earlier, the laboratory tests showed the 5-in. spacing to be the most efficient of those tested for the Yucca Mountain welded tuffs. The data shown in Table 4-7 represent good commercial practice with a new machine/backup system under steady state conditions. No significant delays due to rock support requirements were included. A widely spaced pattern of rock bolts was assumed to be adequate in the immediate vicinity of the TBM; more elaborate supports could be installed by the backup system with little effect on TBM performance.

4.4 Roadheader Performance Predictions

Roadheader performance in the repository horizon welded tuffs was predicted based on the specific energy requirements developed from the LCM test data presented in Table 3-2. The performance results are shown in Figures 4-19 and 4-20 for two different sized openings, 22 ft by 15.5 ft and 15 ft by 21.5 ft, respectively. The calculated penetration rate in TSw2 for a specific energy value of 7 hp-hr/ton is for a roadheader operating at a spacing of 2.5 in. The predictions shown in the figures include four different levels of efficiency factors (e) that were discussed in Sections 3.4.4 and 4.2. Machine mechanical efficiency was set at 75 percent (Equation 11).

Table 4-7

Advance Rates of Two TBM Configurations in the Potential Repository Horizon (TSw2) Based on LCM Results (Each scenario changes one condition likely to be encountered during construction.)

STANDARD TBM:

Scenario Number	Slope Percent	Curve Radius (ft)	Backup System	Penetration Rate (ft/hr)	Utilization Percent	Advance Rate (ft/day)
1	+1	none	rail	7.32	55	97
2	+1	none	conveyor	7.32	50	88
3	-9	none	conveyor	6.06	45	65
4	-14	none	conveyor	5.40	40	52
5	-21	none	conveyor	5.10	35	43
6	+1	600	rail	4.52	35	37
7	-15	600	conveyor	4.14	30	29

HIGH-POWER TBM:

Scenario Number	Slope Percent	Curve Radius (ft)	Backup System	Penetration Rate (ft/hr)	Utilization Percent	Advance Rate (ft/day)
1	+1	none	rail	9.73	55	128
2	+1	none	conveyor	9.73	50	116
3	-9	none	conveyor	8.30	45	89
4	-14	none	conveyor	7.75	40	74
5	-21	none	conveyor	7.51	35	63
6	+1	600	rail	5.53	35	47
7	-15	600	conveyor	5.53	30	40

For the repository horizon welded tuffs, an efficiency factor (e) of 0.5 is believed most appropriate. Using this factor for a 400-hp roadheader, the penetration rate for a 100-ton machine is 2.07 ft/hr for a 22 ft by 12.5 ft opening. For a 15 ft by 21.5 ft opening, the predicted rate of penetration for the same weight and power roadheader is 1.77 ft/hr (Figures 4-19 and 4-20).

Like the TBM, the roadheader should be designed to operate at high penetrations because specific energy decreases as penetration increases.

The effect of spacing must be taken into account when candidate roadheaders are analyzed. The LCM test results showed that spacing has a small effect on specific energy. Therefore, increasing cutter spacing will not decrease specific energy requirements or increase the penetration rate. An increase in spacing reduces torque requirements, but increases cutter force loading.

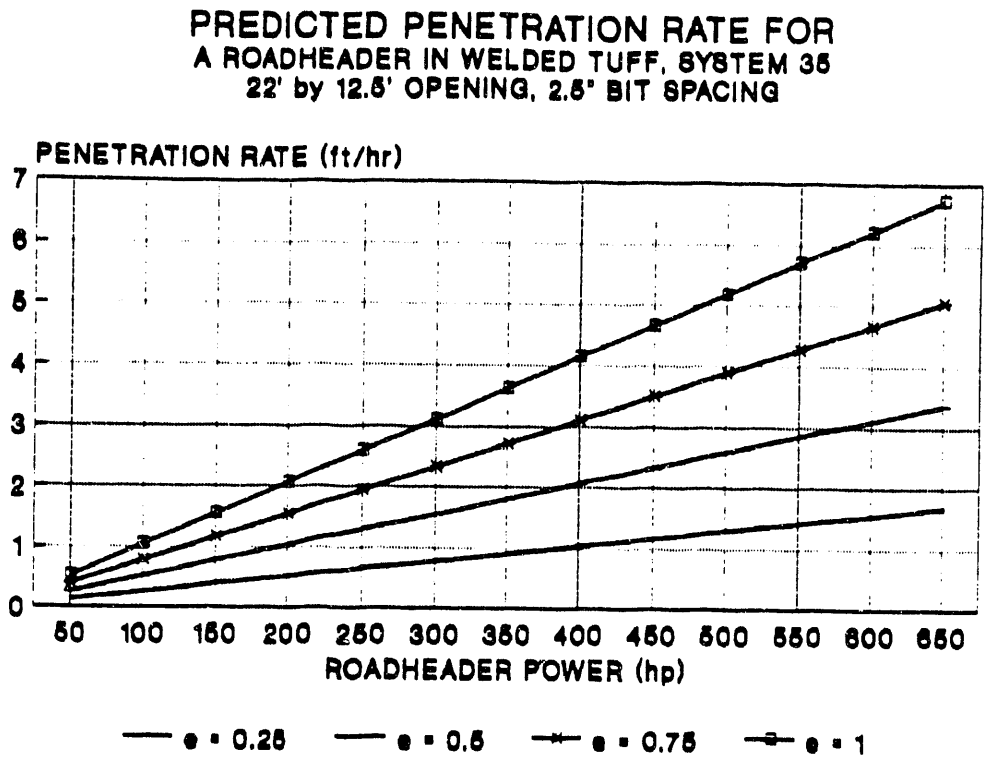

Figure 4-19. Roadheader Performance in a 22 ft by 12.5 ft Opening

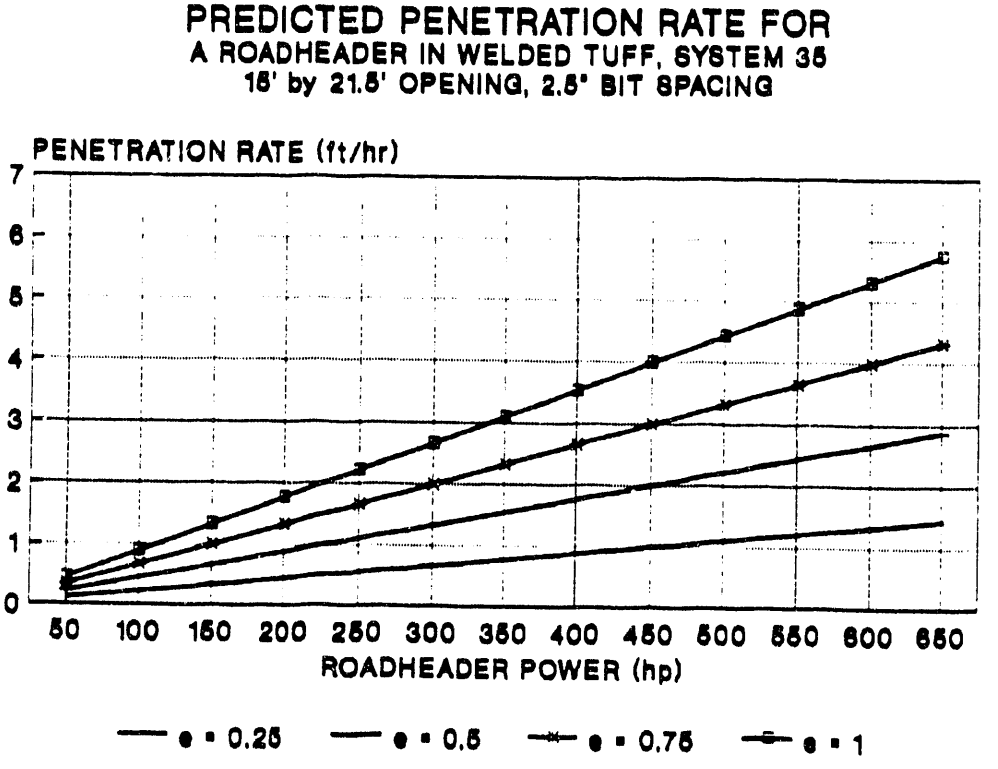

Figure 4-20. Roadheader Performance in a 15 ft by 21.5 ft Opening

Lowering torque requirements for the cutterhead is generally a design goal for roadheaders. Consequently, larger spacings are usually preferred in roadheader design if the allowable cutter forces are not exceeded. Recall that larger spacings should also reduce fines generation during excavation. Given these factors, it appears that the larger spacings should be used.

Because of high cutter costs, roadheaders should not be considered production machines for welded tuff. That is, they do not provide favorable economics for construction of long drifts or tunnels in the repository horizon. However, they can be effective tools for the excavation of small or complex openings by providing a high degree of system flexibility and versatility. They could also find use in constructing non-circular tunnels, modifying circular to noncircular, or driving openings in the nonwelded tuff members, such as the Calico Hills.

Roadheader power in the 100-ton class machines is limited to approximately 450 hp, since larger power units are difficult to mount on the machine and have problems transmitting power and torque to the rock. A few higher power machines are available, up to 650 hp, but these are very large specialized units. In order to achieve reasonable production rates, a high-powered 100-ton machine is recommended.

4.5 Other Excavators

The performance of several other excavators where updated based on the LCM results. Like the TBM and roadheader, thrust requirements were lower and power requirements where higher than predicted by Ozdemir et al. (1992).

4.5.1 The Mobile Miner

The Mobile Miner performance predictions based on the LCM tests for the two different size openings are shown in Table 4-8. As with the TBM results, the machine performance has been downgraded from previous estimates due to higher than anticipated torque and power requirements for mechanical excavation of welded tuff. Thus, the Mobile Miner also becomes power-limited before its thrust capacity is reached.

As expected, the attainable penetrations with the Mobile Miner are much less than for either TBM configuration. The cutter costs for the Mobile Miner are higher due to lower system rigidity and the cyclic contact of the cutters with the rock.

Table 4-9 shows the performance predictions based on the LCM results combined with estimated utilization factors. The utilization percentage and subsequent advance rates for the Mobile Miner depend on the same factors as those discussed in the previous section for TBMs, with some modifications. Again, a considerable degree of judgment and experience is required to estimate a realistic utilization percentage. Note that the utilizations are lower than for the TBMs.

The Mobile Miner is not intended to compete with TBMs in advance rate or production rate. It is inherently incapable of TBM rates by virtue of its

mobility, which requires less mass and a less rigid structure. Fewer cutters contact the rock than for a TBM in a similarly sized opening (e.g., in the smaller opening, three versus 47 cutters). Unlike the full-face TBM, the Mobile Miner attacks only a small portion of the tunnel face at any given time. However, the Mobile Miner is capable of excavating openings with flat floors, making small radius turns, and easily tramming about the excavation. It also allows ready access to the face for inspection, support installation, and dewatering.

Table 4-8

Performance Prediction of a Mobile Miner in Two Opening Shapes in the Potential Repository Horizon (TSw2) Based on LCM Results

Parameter	14 ft x 22 ft Opening	16 ft x 30.5 ft Opening
Cutterhead diameter (ft)	14	16
Width of cut (ft)	22	30.5
Sweep radius (ft)	19	22.5
Sweep angle (degrees)	68.5	82
Rotational speed (rpm)	14	11
Cutters (total/center/gage)	15 /7 /8	15 /7 /8
Power (hp)	700	900
Maximum operating torque (ft-lbf)	262,000	429,700
Penetration per sweep (in.)	0.34	0.37
Sweep time (sec)	25.5	35
Plunge time (sec)	3	3
Penetration rate (ft/hr)	3.67	2.90
Cutter life (hr)	72	74
Tunnel length per cutter (ft)	251	210
Approximate cutter cost ($/yd^3)	8.30	7.45

4.5.2 Blind Shaft Borer

For the full-face BSB, the preliminary performance predictions for shaft excavation in welded tuff were governed primarily by the backup systems, including muck removal and shaft lining. The instantaneous rate of penetration was fixed at a maximum of 6 ft/hr for a daily shaft lining rate of 40 ft. This was based on the current capabilities of shaft lining systems which generally are limited to installation of two 20-ft liner sections per day. Because of liner speed limitations, the machine rate of penetration was kept lower than what the system was capable of achieving from a mechanical feasibility standpoint. Even with the higher torque requirements for cutting the welded tuff, it was determined that the BSB still had sufficient power to maintain a penetration rate of 6 ft/hr. Therefore, no modifications were made to the earlier performance predictions (Ozdemir et al., 1992) as shown in Table 4-10.

Table 4-9

Advance Rates of a Mobile Miner in Two Opening Sizes in the Potential Repository Horizon (TSw2) Based on LCM Results (Each scenario changes one condition likely to be encountered during construction.)

14 ft by 22 ft OPENING:

Scenario Number	Slope Percent	Curve Radius (ft)	Backup System	Penetration Rate (ft/hr)	Utilization Percent	Advance Rate (ft/day)
1	+1	none	50+	3.67	40	35
2	+1	none	25 to 50	3.67	30	27
3	-9	none	50+	3.67	35	31
4	-18	none	50+	3.67	30	27
5	-15	none	25 to 50	3.67	24	21
6	+1	100	50+	3.14	30	23
7	-15	100	50+	3.14	27	20

16 ft by 30.5 ft OPENING:

Scenario Number	Slope Percent	Curve Radius (ft)	Backup System	Penetration Rate (ft/hr)	Utilization Percent	Advance Rate (ft/day)
1	+1	none	50+	2.9	45	31
2	+1	none	25 to 50	2.9	35	25
3	-9	none	50+	2.9	40	29
4	-18	none	50+	2.9	37	26
5	-15	none	25 to 50	2.9	30	21
6	+1	100	50+	2.4	35	20
7	-15	100	50+	2.4	33	19

4.5.3 Vertical-Wheel Shaft Boring Machine

The preliminary performance estimates for the SBM resulted in a penetration rate of about 5 ft/hr for an 800 hp machine. Since the LCM tests showed that the welded tuff requires higher torque than originally estimated, the SBM performance was reduced to reflect this limitation. The new estimates are listed in Table 4-11.

Table 4-10

Performance Prediction of Two BSB Speeds in the Potential Repository Horizon (TSw2) Based on LCM Results

Parameter	High Speed	Low Speed
Cutterhead diameter (ft)	18	18
Rotational speed (rpm)	8.2	6.15
Cutters (# @ diameter (in.))	35 @ 17	35 @ 17
Maximum cutter load (lbf)	50,000	50,000
Power (hp)	1125	1125
Maximum operating torque (ft-lbf)	720,500	960,700
Operating thrust (lbf)	1,750,000	1,750,000
Penetration/revolution (in.)	0.15	0.20
Penetration rate (ft/hr)	6	6
Cutter life (hr)	86	116
Shaft length per cutter (ft)	515	698
Approximate cutter cost ($/yd^3)	7.51	5.54

Table 4-11

Performance Prediction of a Vertical Wheel SBM in the Potential Repository Horizon (TSw2) Based on LCM Results

Parameter	
Cutterwheel diameter	18 ft
Rotational speed	9 rpm
Traverse speed	0.95 rpm (around shaft)
Cutters	16 @ 17-in. diameter
Cutter spacing	4.0 in. (@ perimeter)
Maximum cutter load	50,000 lbf
Power	800 hp
Maximum operating torque	396.8 x 10^3 ft-lbf
Operating thrust	348 x 10^3 lbf
Penetration per traverse	1.05 in.
Penetration rate	4.6 ft/hr
Cutter life	27 hr
Shaft length per cutter	114 ft
Approximate cutter cost	5.10 $/yd^3

The SBM is a partial-face excavator, meaning that it cuts only a portion of the shaft bottom at a time. As a result, it is not capable of matching the production capacity offered by the BSB. From the perspective of repository site characterization, the SBM has a unique advantage over the BSB in that it provides ready personnel access to the shaft bottom. Further, the SBM offers more options for implementation of various muck pickup and removal techniques. For these reasons, it may prove to be a more effective shaft excavator for the potential repository.

4.5.4 Raise Drills

The new performance estimate for raise drills based on LCM tests are shown in Table 4-12. The penetration rates were reduced from the previous estimates to account for the higher torque requirements for mechanical excavation of welded tuff.

4.5.5 V-Mole

The V-Mole performance based on the results of the LCM tests are listed in Table 4-13 for the repository horizon welded tuffs. Again, the new rate of penetration is lower than previously estimated due to the greater-than-expected rolling friction imposed by the welded tuff on the cutters.

Table 4-12

Performance Prediction of Two Sizes of Raise Drills in the Potential Repository Horizon (TSw2) Based on LCM Results

Parameter	Raise Diameter	
	18 ft	6 ft
Pilot string diameter (in.)	12.875	10
Pilot bit diameter (in.)	13.75	11
Reaming head diameter (ft)	18	6
Rotational speed (rpm)	6	10
Cutters with tungsten-carbide inserts (# cutters @ # discs/cutter)	26 @ 4	10 @ 4
Cutter spacing (in.)	2.0	2.0
Maximum cutter load (lbf)	50,000	65,800
Power (hp)	400	300
Maximum operating torque (ft-lbf)	258,500	44,100
Operating thrust (lbf)	1,307,000	492,300
Penetration/revolution (in.)	0.07	0.08
Penetration rate (ft/hr)	2.00	7.32
Cutter life (hr)	540	465
Shaft length per cutter (ft)	1260	3670
Approximate cutter cost ($/yd^3)	18.75	17.80

Table 4-13

Revised Performance Prediction of Two V-Mole Configurations in the Potential Repository Horizon (TSw2)

Parameter	V-Mole	
	Standard	Upgraded
Cutterhead diameter (ft)	18	18
Rotational speed (rpm)	6	8
Cutters (# @ diameter (in.))	34 @ 14	23 @ 17
Maximum cutter load (lbf)	35,000	50,000
Power (hp)	900	1200
Maximum operating torque (ft-lbf)	551,500	669,600
Operating thrust (lbf)	1,190,000	1,150,000
Penetration/revolution (in.)	0.15	0.19
Penetration rate (ft/hr)	4.70	7.73
Cutter life (hr)	71	59
Tunnel length per cutter (ft)	348	490
Approximate cutter cost ($/yd^3)	14.20	6.30

5.0 CONCLUSIONS

Based on the results of this study, the following conclusions can be drawn regarding the predicted performance of various mechanical excavators for the construction of the ESF and the potential repository at Yucca Mountain.

- The LCM tests have shown that an industry standard TBM will effectively excavate the welded tuffs at the potential repository horizon at highly favorable advance rates and cutter costs. The cutting tests have also shown the welded tuffs to be highly suitable for excavation by disc cutters if the cutter penetration is sufficiently large to take advantage of the highly brittle behavior that welded tuff exhibits.

- Excavation of the welded tuffs such as TSw2 by a roadheader is technically feasible, but not economically competitive with respect to other types of mechanical excavators. The relatively high strength and abrasivity of the welded tuffs require a roadheader design that stretches the current limits of roadheader technology. The machine will need the most robust drag cutters available combined with a large, massive, and stiff power unit and actuating frame. Roadheader cutter costs are expected to be substantially higher than TBM cutter costs.

- The LCM tests have shown that the welded tuff requires more machine torque for excavation than previously estimated from the physical and geologic properties of the rock. The higher torque requirements stem from increased rolling or drag friction experienced by the disc and point-attack cutters during cutting. Typical of most brittle rocks, welded tuff requires deep penetration for efficient excavation. Chipping does not occur until the cutter penetration is sufficient to develop high stresses in the rock. This also creates additional rock crushing directly beneath the cutter tip, resulting in a larger than normal crushed zone and, consequently, increased friction on the cutter. The primary implication of this finding is that any mechanical excavator designed to excavate the welded tuff must incorporate sufficient torque and power capacity to achieve efficient operation (high rates of production at relatively low cutter costs).

- The specific energy as a function of spacing and penetration for both cutter types, disc and point-attack, were similar although at different orders of magnitude. As expected, the specific energy of cutting for both cutters was found to decrease with increasing spacing and penetration.

- The LCM tests show the 5-in. cutter spacing to be the most efficient of all the spacings tested for a disc cutter in welded tuff. The most efficient spacing for a point-attack cutter was found to be 2.5 in. These were the widest spacings used in the test program.

- The preliminary performance estimates of the various mechanical excavators evaluated in this study were adjusted to reflect the higher torque and power requirements of welded tuff. As a result, the previous predictions by Ozdemir et al. (1992) were reduced and the cutter costs increased based on these findings. The new performance predictions for mechanical excavation of the repository horizon welded tuff are as follows:

  - A standard TBM with a 3-in. cutter spacing is expected to reach an instantaneous rate of penetration of 6.7 ft/hr at a cutter cost of $\$5.75/yd^3$.

  - A high power TBM with a 3.2-in. cutter spacing is expected to reach an instantaneous rate of penetration of 9.0 ft/hr at a cutter cost of $\$4.65/yd^3$.

  - A standard TBM with a 4-in. cutter spacing is expected to reach an instantaneous rate of penetration of 6.7 ft/hr at a cutter cost of $\$5.30/yd^3$.

  - A high power TBM with a 4-in. cutter spacing is expected to reach an instantaneous rate of penetration of 8.75 ft/hr at a cutter cost of $\$4.95/yd^3$.

  - A standard TBM with a 5-in. cutter spacing is expected to reach an instantaneous rate of penetration of 7.3 ft/hr at a cutter cost of $\$4.75/yd^3$.

  - A high power TBM with a 5-in. cutter spacing is expected to reach an instantaneous rate of penetration of 9.7 ft/hr at a cutter cost of $\$4.45/yd^3$.

  - A Mobile Miner excavating a 14 ft by 22 ft opening is expected to reach an instantaneous rate of penetration of 3.7 ft/hr at a cutter cost of $\$8.30/yd^3$.

  - A Mobile Miner excavating a 16 ft by 30.5 ft opening is expected to reach an instantaneous rate of penetration of 2.9 ft/hr at a cutter cost of $\$7.45/yd^3$.

  - A low speed BSB is expected to reach an instantaneous rate of penetration of 6.0 ft/hr at a cutter cost of $\$5.75/yd^3$, a high speed at 6.0 ft/hr and $\$5.54/yd^3$. These values are unchanged from Ozdemir et al. (1992).

  - A vertical wheel BSB excavating an 18-ft shaft is expected to reach an instantaneous rate of penetration of 4.6 ft/hr at a cutter cost of $\$5.10/yd^3$.

  - A raise drill excavating an 18-ft shaft is expected to reach an instantaneous rate of penetration of 2.0 ft/hr at a cutter cost of $\$18.75/yd^3$.

- A raise drill excavating a 6-ft shaft is expected to reach an instantaneous rate of penetration of 7.3 ft/hr at a cutter cost of $17.80/yd^3$.

- A standard V-Mole excavating an 18-ft shaft is expected to reach an instantaneous rate of penetration of 4.7 ft/hr at a cutter cost of $14.20/yd^3$.

- An upgraded V-Mole excavating an 18-ft shaft is expected to reach an instantaneous rate of penetration of 7.7 ft/hr at a cutter cost of $6.30/yd^3$.

6.0 RECOMMENDATIONS

Based on the conclusions of this study, the following areas are recommended for additional investigations of the applicability of mechanical excavators for the ESF and the potential repository construction at Yucca Mountain.

- An additional series of linear cutter tests should be run to evaluate the effects of wear on disc performance in welded tuff. In this study and report, an assumption was made that excavator performance would decline by approximately 30 percent due to cutter wear. As this study has shown the uniqueness of welded tuffs in their response to mechanical cutting, it is possible that cutter wear may have a greater adverse effect on machine performance than was presumed. The effect of cutter wear can be fully investigated through a series of LCM tests using disc cutters at various stages of dullness.

- The cuttability of welded tuff at larger cutter spacings than those tested in this program should be evaluated. The specific energy reached a minimum at the widest spacings tested in the program, and the effect of wider spacings is currently unknown. These additional tests can also provide a more accurate definition of the optimum cutting conditions for welded tuff.

- Various cut sequencing patterns should be studied to develop guidelines as to the optimum cutter layout on the excavators considered in this study. This could also include tests to simulate and evaluate gage cutter placement patterns.

- LCM tests should be run with different angles of attack for the point-attack cutters. This information can then be used to determine the optimum angles of attack to minimize the specific energy of cutting and the wear on the point-attack cutter.

- Since this test program was initiated, some technological advancements have been made in point-attack cutters and drag bits, including more efficient bit designs and diamond coated tungsten carbide bit tips. The new materials are designed to improve cutter life and reduce excavation costs in abrasive rocks. A series of LCM tests should be conducted to evaluate the applicability of these cutters in welded tuff. As discussed in this report, the lack of point-attack cutter technology appears to be the main impediment to the economic use of roadheaders in welded tuff.

- The cutting tests report herein only included the mechanical excavatibility of welded tuff. The current ESF plans call for a significant amount of excavation to take place in the Calico Hills nonwelded tuff formation. In order to develop data to allow optimal excavator design and to reduce construction costs, LCM tests should

be performed using both disc and point-attack cutters on the Calico Hills material. In particular, attention should be given to assessing the potential plastic behavior and mechanical cuttability of the nonwelded tuffs. Further, the machine backup and ground support requirements should be studied.

- Although LCM testing has been shown to provide reliable data simulating the field performance of mechanical excavators, it still lacks the capability to duplicate fully the multiple operation and interaction of field cutters. This stems from the fact that only one cutter at a time can be tested in the linear cutting machine. Moreover, the LCM cannot simulate the particular layout and operation of gage cutters, an issue of major importance for TBMs designed to negotiate tight turns. Also the LCM is limited in its capability to investigate high cutter velocity performance and cutter wear. All these issues can, however, be studied on the Earth Mechanics Institute laboratory tunnel boring machine (LTBM). It is designed to simulate the actual operation of field raise, shaft, and tunnel boring equipment. The LTBM tests also allow preliminary studies to be conducted concerning the geologic mappability of the bored openings. Further, the excavation walls can be cored to assess the extent of wall damage caused by mechanical excavators. The tests can include wet cutting to determine the water penetration depth into the formation. In summary, the LTBM tests can yield a vast amount of information on nearly all aspects of mechanical excavator use in welded tuff or other lithologies at Yucca Mountain. Therefore, it is strongly recommended that these tests should be conducted. These tests will also allow the final refinement of the machine performance estimates developed in the LCM tests.

7.0 REFERENCES

Ortiz, T. S., R. L. Williams, F. B. Nimick, B. C. Whittet, and D. L. South, 1985. A Three-Dimensional Model and Reference Thermal/Mechanical and Hydrological Stratigraphy at Yucca Mountain, Southern Nevada, SAND84-1076, Sandia National Laboratories, Albuquerque, New Mexico. (NNA.890315.0013)

Ozdemir, L., R. Miller, and F. Wang, 1977. Mechanical Tunnel Boring Prediction and Machine Design, Annual Report to the National Science Foundation, NSF/RA-770199, Earth Mechanics Institute, Colorado School of Mines, Colorado. (NNA.910620.0119)

Ozdemir, L., L. Gertsch, D. Neil, and J. Friant, 1992. Performance Predictions for Mechanical Excavators in Yucca Mountain Tuffs, SAND91-7035, Sandia National Laboratories, Albuquerque, New Mexico. (NNA.920819.0246)

APPENDIX A

INFORMATION FROM THE REFERENCE INFORMATION BASE USED IN THIS REPORT

APPENDIX A

Information From the Reference Information Base Used in this Report

This report contains no information from the Reference Information Base.

Candidate Information for the Reference Information Base

This report contains the following candidate information for the Reference Information Base:

1. Performance predictions for tunnel boring machines (see Tables 4-3 through 4-7).

2. Performance predictions for roadheaders (see Figures 4-19 and 4-20).

3. Performance predictions for a Mobile Miner (see Tables 4-8 and 4-9).

4. Performance predictions for blind shaft borers (see Table 4-10).

5. Performance predictions for vertical wheel shaft borers (see Table 4-11).

6. Performance predictions for raise drills (see Table 4-12).

7. Performance predictions for V-moles (see Table 4-13).

Candidate Information for the Site & Engineering Properties Data Base

This report contains the following candidate information for the Site and Engineering Properties Data Base:

1. Performance predictions for tunnel boring machines (see Tables 4-3 through 4-7).

2. Performance predictions for roadheaders (see Figures 4-19 and 4-20).

3. Performance predictions for a Mobile Miner (see Tables 4-8 and 4-9).

4. Performance predictions for blind shaft borers (see Table 4-10).

5. Performance predictions for vertical wheel shaft borers (see Table 4-11).

6. Performance predictions for raise drills (see Table 4-12).

7. Performance predictions for V-Moles (see Table 4-13).

APPENDIX B

DESCRIPTION OF LINEAR CUTTING MACHINE

APPENDIX B

B.1 Equipment

The linear cutting machine consists of the following components: the test frame, the hydraulic components, the cutter and saddle assembly, the rock sample box, and the electronic instrumentation.

B.1.1 Test Frame

The test frame consists of a large rigid frame that holds the cutter and saddle assembly firmly to the rock surface. Under the frame are two round hardened steel rails that support and guide the movable sled where the rock sample and its confinement box a replaced. The frame and rails are connected beneath the floor by a large frame imbedded in reinforced concrete. Hydraulic actuating and positioning cylinders are attached to the frame and the sled to allow precision positioning of the sample in relation to the cutter.

B.1.2 Hydraulic Components

The desired cutter penetration is controlled by a hydraulic cylinder that lowers the cutter and saddle assembly. Metal spacers are inserted between the saddle and the main supporting frame, after which the hydraulic cylinder is reversed to hold the system firmly together.

Spacing is set with hydraulic rams on the rock box. After each cut, the rock box is moved sideways, with the amount of translation corresponding to the desired spacing between cuts.

The rock is cut by moving it under the cutter, which is stationary, with a servo-controlled horizontal hydraulic actuator capable of 32,000 lbf (142 kN) stall force. The LVDT used to control data acquisition also monitors the movement of the actuator. The electronic controller maintains constant cutting speed by comparing the output of the LVDT to that of a ramp function generator.

The cutting velocity is held constant at 10 in./sec (25 cm/sec). This choice is based on past experimental studies performed at EMI, which show that cutter performance is not affected by the cutting velocity over wide velocity ranges (Ozdemir et al., 1977).

B.1.3 Cutter and Saddle Assembly

The cutter and saddle assembly consists of a replaceable disc cutter ring, a bearing/hub assembly, and a quick-change bearing saddle. To replace a cutter, the ring and bearing/hub assembly are removed from the quick-change saddle. The cutter ring is removed from the bearing/hub assembly, a new ring is pressed on the hub, and ring and hub are bolted back onto the quick-change saddle.

B.1.4 Rock Sample Box

The steel rock box with rock sample fits on the movable sled in the test frame. The box is capable of holding a rock up to 38 by 36 by 20 in. (97 by 91 by 51 cm). The rock is held in the sample box by casting a concrete jacket between the rock and box. The steel sample boxes are constructed with a tapered cross-section to ensure maximum confinement throughout the testing sequence. The taper increases confinement as the cutter bears down on the rock surface, forcing rock and concrete into the taper. The confinement is necessary to prevent splitting or cracking of the sample and to limit rock movement during cutting. Lateral movement of the rock and box is limited by the lateral positioning ram between the box and the sled.

B.1.5 Electronic Instrumentation

The electronic instrumentation consists of a load cell, signal conditioners, analog-to-digital converters, digital-to-analog converters, and a computer system.

The load cell, designed and fabricated at the Earth Mechanics Institute, is placed between the linear cutter frame and the cutter saddle. The load cell was machined from a single block of high strength aluminum, creating a unit where each of the four posts is integral with the top and bottom plates. This cell is more accurate than non-integrated designs, which tend to lose calibration over time. Each post carries an array of eight balanced strain gages in full bridge circuits to measure the load at that post. Signal output from the load cell, then, consists of four channels, one from each post. The four outputs are reduced into normal, rolling and side components by the data acquisition/reduction software.

Strain gage bridge circuit power is supplied by four strain gage conditioners/amplifiers consisting of self-balancing, isolated power units with built-in amplifier circuits (Measurements Group, Model 2100). The strain gage conditioners/amplifiers supply power to the bridge circuits and amplify the return load signal to levels appropriate for the data acquisition system (plus or minus approximately two volts). The load cell and signal conditioner system provides a full range of bridge sensitivities.

From the signal conditioner, the load signals are passed directly to an analog-to-digital converter (ADC, Data Translation Model DT2762). The ADC samples the conditioned load signals, and the linear variable distance transducer (LVDT), at a rate of 1000 data points per second. It then passes these data to the computer.

B.1.6 Calibration

The force measuring system on the linear cutter is calibrated with a precision pressure gage mounted on a hydraulic cylinder. The cylinder is oriented on the cutter such that the load cell is loaded at an angle representative of actual cutting. This angle is measured and recorded so

that the three-dimensional applied force can be resolved into its three mutually orthogonal components--the normal, rolling, and side forces. The load cell outputs corresponding to the three mutually perpendicular force components are recorded and compared to the applied loads. The load cell outputs are linear, allowing least squares linear regression of the voltages to pounds-force. Each calibration consists of seven different total loads from zero to 36,000 lbf (160 kN). After a minimum of three calibration tests, the calibration factors are calculated and entered into the data acquisition/reduction program. The calibration procedure incorporates the entire testing and data acquisition/analysis system so further data reduction steps are not needed.

B.1.7 Rock Sample Preparation and Conditioning

Samples are cast in high strength concrete within steel rock boxes and allowed to cure. The rock boxes then are positioned on the machine sled and attached to the lateral indexing hydraulic cylinders. Prior to data acquisition, the rock surface is conditioned to steady-state cutting condition by making several passes with the cutter. The conditioning passes are at the same spacing and penetration as the test passes. The penetration in each sample starts low and increases as testing progresses. The spacings are not be changed on any given sample, as the effects of previous cutting at a different spacing are difficult to eliminate.

B.1.8 Data Acquisition and Analysis

Cutter loads are resolved into three mutually perpendicular components using a four-post load cell, a set of signal conditioners, an analog-to-digital converter, and a computer for data acquisition and analysis. The raw force data from the load cell are analyzed by first calculating the raw load on each post of the four-post load cell. From the individual forces on the posts, the computer then calculates the normal, rolling, and side forces on the cutter. From these, the software calculates the normal, rolling (drag), and side force for each cut. The values for each cut are then averaged for all the cuts in the test. Finally, several parameters are calculated from the various test averages: minima, maxima, standard deviations, cutting coefficients, specific energies, and peak-to-mean force ratios.

A test report is generated by the software. The average forces are the sum of the average force for each cut divided by the number of cuts. Similarly, the average peak forces are the sum of the peak forces for each cut divided by the number of cuts. Minima, maxima, and standard deviations are calculated from the averages of each cut. The specific energy, defined as the energy required to remove a unit volume of rock, is simply the average rolling (drag) force divided by the spacing and multiplied by the penetration. The cutting coefficient, indicating the torque verses thrust requirements, is the average rolling (drag) force divided by the average normal force. The peak-to-mean force ratios are the average peak force divided by the average mean force for each force component. The forces for each cut are shown opposite the cut numbers, and the force summaries for the entire test are shown below the cut numbers. The calculated values appear at the bottom of the table.

APPENDIX C

SIEVE ANALYSIS RESULTS

Table C-1

Sieve Analysis Results for A30581
17-Inch CCS Disk Cutter

Sieve Size		Percent		Percent		Percent	
		Fraction	Cumulative	Fraction	Cumulative	Fraction	Cumulative
Inch	mm	YMP08 S-3	P-0.2	YMP09 S-3	P-0.3	YMP10 S-3	P-0.4
1.000	25.4	48.86	48.86	42.23	42.23	37.95	37.95
0.750	19.1	14.05	62.91	12.14	54.37	10.71	48.66
0.500	12.7	7.80	70.71	4.54	58.91	12.01	60.67
0.371	9.423	4.77	75.48	6.84	65.75	7.32	67.99
0.091	2.362	13.44	88.92	18.02	83.77	18.61	86.60
0.023	0.589	6.05	94.97	8.62	92.39	7.65	94.25
0	0	5.03	100.00	7.61	100.00	5.75	100.00
		YMP12 S-4	P-0.2	YMP13 S-4	P-0.3	YMP14 S-4	P-0.4
1.000	25.4	47.19	47.19	62.06	62.06	55.88	55.88
0.750	19.1	11.20	58.39	2.95	65.01	6.67	62.54
0.500	12.7	9.66	68.05	6.46	71.47	7.37	69.92
0.371	9.423	6.44	74.49	5.68	77.14	5.78	75.70
0.091	2.362	13.93	88.42	11.98	89.13	13.33	89.03
0.023	0.589	6.09	94.51	5.69	94.82	5.59	94.62
0	0	5.49	100.00	5.18	100.00	5.38	100.00
		YMP16 S-5	P-0.2	YMP17 S-5	P-0.3	YMP18 S-5	P-0.4
1.000	25.4	70.91	70.91	58.46	58.46	72.02	72.02
0.750	19.1	4.11	75.02	5.86	64.33	4.64	76.66
0.500	12.7	6.97	81.99	7.21	71.53	5.73	82.39
0.371	9.423	3.36	85.36	6.06	77.59	3.78	86.17
0.091	2.362	8.44	93.80	11.64	89.24	8.17	94.34
0.023	0.589	3.37	97.17	5.47	94.70	3.21	97.55
0	0	2.83	100.00	5.30	100.00	2.45	100.00

Table C-2

Sieve Analysis Results for AM1723
17-Inch CCS Disk Cutter

Sieve Size		Percent		Percent		Percent	
		Fraction	Cumulative	Fraction	Cumulative	Fraction	Cumulative
Inch	mm	YMP33 S-3	P-0.2	YMP34 S-3	P-0.3	YMP35 S-3	P-0.4
1.000	25.4	50.28	50.28	35.43	35.43	44.12	44.12
0.750	19.1	7.97	58.25	9.92	45.35	9.91	54.02
0.500	12.7	5.57	63.83	10.54	55.90	10.56	64.59
0.371	9.423	5.35	69.18	6.62	62.52	5.50	70.09
0.091	2.362	15.21	84.39	19.58	82.10	16.28	86.37
0.023	0.589	7.81	92.20	9.14	91.25	6.88	93.25
0	0	7.80	100.00	8.75	100.00	6.75	100.00
		YMP28 S-4	P-0.2	YMP29 S-4	P-0.3	YMP42 S-4	P-0.4
1.000	25.4	50.53	50.53	57.12	57.12	67.96	67.96
0.750	19.1	7.00	57.53	6.90	64.02	4.53	72.49
0.500	12.7	9.61	67.14	9.02	73.04	4.21	76.70
0.371	9.423	5.79	72.92	5.33	78.37	3.17	79.87
0.091	2.362	13.85	86.77	10.64	89.01	10.41	90.27
0.023	0.589	6.93	93.70	5.35	94.36	4.90	95.17
0	0	6.30	100.00	5.64	100.00	4.83	100.00
		YMP30 S-5	P-0.2	YMP31 S-5	P-0.3	YMP32 S-5	P-0.4
1.000	25.4	52.68	52.68	53.93	53.93	67.46	67.46
0.750	19.1	5.90	58.58	8.99	62.92	5.13	72.59
0.500	12.7	9.06	67.64	9.08	71.99	6.38	78.97
0.371	9.423	5.21	72.85	5.13	77.12	3.70	82.67
0.091	2.362	14.03	86.88	12.23	89.35	8.48	91.16
0.023	0.589	6.82	93.70	5.57	94.93	4.37	95.53
0	0	6.30	100.00	5.07	100.00	4.47	100.00

Table C-3

Sieve Analysis Results for 84HCT
Point-Attack Cutter

Sieve Size		Percent		Percent		Percent	
		Fraction	Cumulative	Fraction	Cumulative	Fraction	Cumulative
Inch	mm	YMP19 S=1.5	P=0.2	YMP20 S=1.5	P=0.3	YMP21 S=1.5	P=0.4
1.000	25.4	11.61	11.61	32.93	32.93	10.92	10.92
0.750	19.1	15.23	26.84	12.44	45.37	27.32	38.24
0.500	12.7	21.87	48.71	16.39	61.76	14.24	52.48
0.371	9.423	9.57	58.28	8.37	70.13	9.85	62.34
0.091	2.362	23.68	81.95	18.48	88.61	22.98	85.32
0.023	0.589	9.02	90.97	5.99	94.60	7.56	92.88
0	0	9.03	100.00	5.40	100.00	7.12	100.00
		YMP25 S=2	P=0.2	YMP26 S=2	P=0.3	YMP27 S=2	P=0.4
1.000	25.4	41.91	41.91	36.90	36.90	37.76	37.76
0.750	19.1	7.48	49.39	13.96	50.85	10.28	48.04
0.500	12.7	11.03	60.42	10.86	61.72	13.34	61.38
0.371	9.423	8.06	68.48	6.76	68.47	9.21	70.59
0.091	2.362	18.65	87.13	17.74	86.21	18.47	89.05
0.023	0.589	6.62	93.74	6.84	93.05	5.97	95.03
0	0	6.26	100.00	6.95	100.00	4.97	100.00
		YMP22 S=2.5	P=0.2	YMP23 S=2.5	P=0.3	YMP24 S=2.5	P=0.4
1.000	25.4	52.94	52.94	42.42	42.42	50.26	50.26
0.750	19.1	7.45	60.39	14.25	56.67	8.53	58.79
0.500	12.7	8.90	69.29	11.56	68.23	9.66	68.45
0.371	9.423	6.27	75.56	6.26	74.49	6.68	75.13
0.091	2.362	12.44	88.00	13.67	88.16	15.38	90.51
0.023	0.589	5.78	93.78	6.17	94.33	5.13	95.64
0	0	6.22	100.00	5.67	100.00	4.36	100.00

Table C-4

Sieve Analysis Results for System 35
Point-Attack Cutter

Sieve Size		Percent		Percent		Percent	
		Fraction	Cumulative	Fraction	Cumulative	Fraction	Cumulative
Inch	mm	YMP39 S=1.5	P=0.2	YMP40 S=1.5	P=0.3	YMP41 S=1.5	P=0.4
1.000	25.4	8.23	8.23	23.74	23.74	23.88	23.88
0.750	19.1	23.61	31.85	26.42	50.15	22.28	46.16
0.500	12.7	22.09	53.94	13.98	64.14	20.30	66.46
0.371	9.423	9.39	63.33	8.97	73.10	8.46	74.92
0.091	2.362	22.45	85.79	16.84	89.94	16.22	91.14
0.023	0.589	7.76	93.54	5.38	95.33	4.61	95.75
0	0	6.46	100.00	4.67	100.00	4.25	100.00
		YMP36 S=2	P=0.2	YMP37 S=2	P=0.3	YMP38 S=2	P=0.4
1.000	25.4	37.43	37.43	36.65	36.65	44.42	44.42
0.750	19.1	17.22	54.65	11.33	47.97	14.13	58.55
0.500	12.7	11.17	65.83	14.45	62.42	12.75	71.30
0.371	9.423	7.99	73.82	7.54	69.96	6.32	77.62
0.091	2.362	15.00	88.82	18.64	88.60	14.09	91.71
0.023	0.589	6.19	95.01	6.54	95.14	4.51	96.22
0	0	4.99	100.00	4.86	100.00	3.78	100.00
		YMP43 S=2.5	P=0.2	YMP44 S=2.5	P=0.3	YMP45 S=2.5	P=0.4
1.000	25.4	42.97	42.97	57.97	57.97	57.97	57.97
0.750	19.1	11.53	54.50	4.96	62.93	4.96	62.93
0.500	12.7	9.96	64.46	8.18	71.11	8.18	71.11
0.371	9.423	7.18	71.64	7.10	78.21	7.10	78.21
0.091	2.362	14.34	85.98	13.67	91.88	13.67	91.88
0.023	0.589	7.29	93.27	4.56	96.44	4.56	96.44
0	0	6.73	100.00	3.56	100.00	3.56	100.00

DISTRIBUTION LIST

1 J. W. Bartlett, Director (RW-1)
Office of Civilian Radioactive
Waste Management
U.S. Department of Energy
1000 Independence Avenue, S.W.
Washington, DC 20585

1 F. G. Peters, Deputy Director (RW-2)
Office of Civilian Radioactive
Waste Management
U.S. Department of Energy
1000 Independence Avenue, S.W.
Washington, DC 20585

1 T. H. Isaacs (RW-4)
Office of Strategic Planning
and International Programs
Office of Civilian Radioactive
Waste Management
U.S. Department of Energy
1000 Independence Avenue, S.W.
Washington, DC 20585

1 J. D. Saltzman (RW-5)
Office of External Relations
Office of Civilian Radioactive
Waste Management
U.S. Department of Energy
1000 Independence Avenue, S.W.
Washington, DC 20585

1 Samuel Rousso (RW-10)
Office of Program and Resources
Management
Office of Civilian Radioactive
Waste Management
U.S. Department of Energy
1000 Independence Avenue, S.W.
Washington, DC 20585

1 J. C. Bresee (RW-10)
Office of Civilian Radioactive
Waste Management
U.S. Department of Energy
1000 Independence Avenue, S.W.
Washington, DC 2058

1 C. P. Gertz (RW-20)
Office of Geologic Disposal
Office of Civilian Radioactive
Waste Management
U.S. Department of Energy
1000 Independence Avenue, S.W.
Washington, DC 20585

1 S. J. Brocoum (RW-22)
Analysis and Verification Division
Office of Civilian Radioactive
Waste Management
U.S. Department of Energy
1000 Independence Avenue, S.W.
Washington, DC 20585

1 J. Roberts, Acting Assoc. Dir.
(RW-30)
Office of Systems and Compliance
Office of Civilian Radioactive
Waste Management
U.S. Department of Energy
1000 Independence Avenue, S.W.
Washington, DC 20585

1 J. Roberts (RW-33)
Director, Regulatory Compliance
Division
Office of Civilian Radioactive
Waste Management
U.S. Department of Energy
1000 Independence Avenue, S.W.
Washington, DC 20585

1 G. J. Parker (RW-332)
Office of Civilian Radioactive
Waste Management
U.S. Department of Energy
1000 Independence Avenue, S.W.
Washington, DC 20585

1 R. A. Milner (RW-40)
Office of Storage and Transportation
Office of Civilian Radioactive
Waste Management
U.S. Department of Energy
1000 Independence Avenue, S.W.
Washington, DC 20585

1 S. Rousso, Acting Assoc. Director
(RW-50)
Office of Contract Business
Management
Office of Civilian Radioactive
Waste Management
U.S. Department of Energy
1000 Independence Avenue, S.W.
Washington, DC 20585

1 Trudy Wood (RW-52)
Director, M&O Management Division
Office of Civilian Radioactive
Waste Management
U.S. Department of Energy
1000 Independence Avenue, S.W.
Washington, DC 20585

1 D. U. Deere, Chairman
Nuclear Waste Technical Review Board
1100 Wilson Blvd. #910
Arlington, VA 22209-2297

1 Dr. Clarence R. Allen
Nuclear Waste Technical Review Board
1000 E. California Blvd.
Pasadena, CA 91106

1 Dr. John E. Cantlon
Nuclear Waste Technical Review Board
1795 Bramble Dr.
East Lansing, MI 48823

1 Dr. Melvin W. Carter
Nuclear Waste Technical Review Board
4621 Ellisbury Dr., N.E.
Atlanta, GA 30332

1 Dr. Donald Langmuir
Nuclear Waste Technical Review Board
109 So. Lookout Mountain Cr.
Golden, CO 80401

1 Dr. D. Warner North
Nuclear Waste Technical Review Board
Decision Focus, Inc.
4984 El Camino Real
Los Altos, CA 94062

1 Dr. Dennis L. Price
Nuclear Wast Technical Review Board
1011 Evergreen Way
Blacksburg, VA 24060

1 Dr. Ellis D. Verink
Nuclear Waste Technical Review Board
4401 N.W. 18th Place
Gainesville, FL 32605

5 C. P. Gertz, Project Manager
Yucca Mountain Site Characterization
Project Office
U.S. Department of Energy
P.O. Box 98608--MS 523
Las Vegas, NV 89193-8608

1 C. L. West, Director
Office of External Affairs
DOE Field Office, Nevada
U.S. Department of Energy
P.O. Box 98518
Las Vegas, NV 89193-8518

12 Technical Information Officer
DOE Nevada Field Office
U.S. Department of Energy
P.O. Box 98518
Las Vegas, NV 89193-8518

1 P. K. Fitzsimmons, Technical
Advisor
Office of Assistant Manager for
Environmental Safety and Health
DOE Field Office, Nevada
U.S. Department of Energy
P.O. Box 98518
Las Vegas, NV 89193-8518

1 D. R. Elle, Director
Environmental Protection Division
DOE Nevada Field Office
U.S. Department of Energy
P.O. Box 98518
Las Vegas, NV 89193-8518

1 Repository Licensing & Quality
Assurance
Project Directorate
Division of Waste Management
U.S. Nuclear Regulatory Commission
Washington, DC 20555

1 Senior Project Manager for Yucca
Mountain
Repository Project Branch
Division of Waste Management
U.S. Nuclear Regulatory Commission
Washington, DC 20555

1 NRC Document Control Desk
Division of Waste Management
U.S. Nuclear Regulatory Commission
Washington, DC 20555

1 P. T. Prestholt
NRC Site Representative
301 E. Stewart Ave., Room 203
Las Vegas, NV 89101

1 E. P. Binnall
Field Systems Group Leader
Building 50B/4235
Lawrence Berkeley Laboratory
Berkeley, CA 94720

1 Center for Nuclear Waste
Regulatory Analyses
6220 Culebra Road
Drawer 28510
San Antonio, TX 78284

3 W. L. Clarke
Technical Project Officer for YMP
Attn: YMP/LRC
Lawrence Livermore National
Laboratory
P.O. Box 5514
Livermore, CA 94551

4 J. A. Canepa
Technical Project Officer for YMP
N-5, Mail Stop J521
Los Alamos National Laboratory
P.O. Box 1663
Los Alamos, NM 87545

1 H. N. Kalia
Exploratory Shaft Test Manager
Los Alamos National Laboratory
Mail Stop 527
101 Convention Center Dr., Suite 820
Las Vegas, NV 89109

1 J. F. Divine
Assistant Director for
Engineering Geology
U.S. Geological Survey
106 National Center
12201 Sunrise Valley Dr.
Reston, VA 22092

6 L. R. Hayes
Technical Project Officer
Yucca Mountain Project Branch--MS 425
U.S. Geological Survey
P.O. Box 25046
Denver, CO 80225

1 V. R. Schneider
Asst. Chief Hydrologist--MS 414
Office of Program Coordination
& Technical Support
U.S. Geological Survey
12201 Sunrise Valley Drive
Reston, VA 22092

1 J. S. Stuckless
Geological Division Coordinator
MS 913
Yucca Mountain Project
U.S. Geological Survey
P.O. Box 25046
Denver, CO 80225

1 D. H. Appel, Chief
Hydrologic Investigations Program
MS 421
U.S. Geological Survey
P.O. Box 25046
Denver, CO 80225

1 E. J. Helley
Branch of Western Regional Geology
MS 427
U.S. Geological Survey
345 Middlefield Road
Menlo Park, CA 94025

1 R. W. Craig, Chief
Nevada Operations Office
U.S. Geological Survey
101 Convention Center Drive
Suite 860, MS 509
Las Vegas, NV 89109

1 D. Zesiger
U.S. Geological Survey
101 Convention Center Dr.
Suite 860 - MS 509
Las Vegas, NV 89109

1 R. V. Watkins, Chief
Project Planning and Management
U.S. Geological Survey
P.O. Box 25046
421 Federal Center
Denver, CO 80225

1 A. L. Flint
U.S. Geological Survey
MS 721
P.O. Box 327
Mercury, NV 89023

1 D. A. Beck
U.S. Geological Survey
1500 E. Tropicana, Suite 201
Las Vegas, NV 89119

1 P. A. Glancy
U.S. Geological Survey
Federal Building, Room 224
Carson City, NV 89701

1 Sherman S. C. Wu
Branch of Astrogeology
U.S. Geological Survey
2255 N. Gemini Dr.
Flagstaff, AZ 86001

1 J. H. Sass
Branch of Tectonophysics
U.S. Geological Survey
2255 N. Gemini Dr.
Flagstaff, AZ 86001

1 DeWayne A. Campbell
Technical Project Officer for YMP
U.S. Bureau of Reclamation
Code D-3790
P.O. Box 25007
Denver, CO 80225

1 K. W. Causseaux
NHP Reports Chief
U.S. Geological Survey
421 Federal Center
P.O. Box 25046
Denver, CO 80225

1 W. R. Keefer
U.S. Geological Survey
913 Federal Center
P.O. Box 25046
Denver, CO 80225

1 J. H. Nelson
Technical Project Officer for YMP
Science Applications International Corp.
101 Convention Center Dr.
Suite 407
Las Vegas, NV 89109

2 SAIC-T&MSS Library
Science Applications International Corp.
101 Convention Center Dr.
Suite 407
Las Vegas, NV 89109

2 L. D. Foust
Nevada Site Manager
TRW Environmental Safety Systems
101 Convention Center Drive
Suite 540, MS 423
Las Vegas, NV 89109

1 C. E. Ezra
YMP Support Project Manager
EG&G Energy Measurements, Inc.
MS V-02
P.O. Box 1912
Las Vegas, NV 89125

1 R. E. Jackson, Program Manager
Roy F. Weston, Inc.
955 L'Enfant Plaza, Southwest
Washington, DC 20024

1 Technical Information Center
Roy F. Weston, Inc.
955 L'Enfant Plaza, Southwest
Washington, DC 20024

1 D. Hedges, Vice President,
Quality Assurance
Roy F. Weston, Inc.
4425 Spring Mountain Road, Suite 300
Las Vegas, NV 89102

1 D. L. Fraser, General Manager
Reynolds Electrical & Engineering Co.
Mail Stop 555
P.O. Box 98521
Las Vegas, NV 89193-8521

1 R. F. Pritchett
Technical Project Officer for YMP
Reynolds Electrical & Engineering Co.
MS 408
P.O. Box 98521
Las Vegas, NV 89193-8521

1 B. W. Colston
President/General Manager
Las Vegas Branch
Raytheon Services Nevada
MS 416
P.O. Box 95487
Las Vegas, NV 89193-5487

1 R. L. Bullock
Technical Project Officer for YMP
Raytheon Services Nevada
Suite P250, MS 403
101 Convention Center Dr.
Las Vegas, NV 89109

1 R. E. Lowder
Technical Project Officer for YMP
MAC Technical Services
101 Convention Center Drive
Suite 1100
Las Vegas, NV 89109

1 Paul Eslinger, Manager
PASS Program
Pacific Northwest Laboratories
P.O. Box 999
Richland, WA 99352

1 A. T. Tamura
Science and Technology Division
Office of Scientific and Technical Information
U.S. Department of Energy
P.O. Box 62
Oak Ridge, TN 37831

1 Carlos G. Bell, Jr.
Professor of Civil Engineering
Civil and Mechanical Engineering Department
University of Nevada, Las Vegas
4505 South Maryland Parkway
Las Vegas, NV 89154

1 C. F. Costa, Director
Nuclear Radiation Assessment Division
U.S. Environmental Protection Agency
Environmental Monitoring Systems Laboratory
P.O. Box 93478
Las Vegas, NV 89193-3478

1 ONWI Library
Battelle Columbus Laboratory
Office of Nuclear Waste Isolation
505 King Avenue
Columbus, OH 43201

1 T. Hay, Executive Assistant
Office of the Governor
State of Nevada
Capitol Complex
Carson City, NV 89710

3 R. R. Loux, Jr.
Executive Director
Nuclear Waste Project Office
State of Nevada
Evergreen Center, Suite 252
1802 North Carson Street
Carson City, NV 89710

1 C. H. Johnson
Technical Program Manager
Nuclear Waste Project Office
State of Nevada
Evergreen Center, Suite 252
1802 North Carson Street
Carson City, NV 89710

1 John Fordham
Water Resources Center
Desert Research Institute
P.O. Box 60220
Reno, NV 89506

1 Dr. Martin Mifflin
Water Resources Center
Desert Research Institute
2505 Chandler Avenue, Suite 1
Las Vegas, NV 89120

1 Eric Anderson
Mountain West Research-Southwest Inc.
2901 N. Central Ave. #1000
Phoenix, AZ 85012-2730

1 Department of Comprehensive Planning
Clark County
225 Bridger Avenue, 7th Floor
Las Vegas, NV 89155

1 Planning Department
Nye County
P.O. Box 153
Tonopah, NV 89049

1 Lincoln County Commission
Lincoln County
P.O. Box 90
Pioche, NV 89043

5 Judy Foremaster
City of Caliente
P.O. Box 158
Caliente, NV 89008

1 Economic Development Department
City of Las Vegas
400 East Stewart Avenue
Las Vegas, NV 89101

1 Community Planning & Development
City of North Las Vegas
P.O. Box 4086
North Las Vegas, NV 89030

1 Director of Community Planning
City of Boulder City
P.O. Box 367
Boulder City, NV 89005

1 Commission of the European Communities
200 Rue de la Loi
B-1049 Brussels
BELGIUM

2 M. J. Dorsey, Librarian
YMP Research and Study Center
Reynolds Electrical & Engineering Co., Inc.
MS 407
P.O. Box 98521
Las Vegas, NV 89193-8521

1 Amy Anderson
Argonne National Laboratory
Building 362
9700 So. Cass Ave.
Argonne, IL 60439

1 Steve Bradhurst
P.O. Box 1510
Reno, NV 89505

1 Phillip Niedzeilski-Eichner
13013 Lee Jackson Highway
Fairfax, VA 22033

1 Vernon Poe
P.O. Box 1026
Hawthorne, NV 89415

1 Jason Pitts
Lincoln County Courthouse
Pioche, NV 89043

1 Michael L. Baughman
35 Clark Road
Fiskdale, MA 01518

1 Glenn Van Roekel
Director of Community Development
P.O. Box 158
Caliente, NV 89008

1 Ray Williams, Jr.
P.O. Box 10
Austin, NV 89310

1 Leonard J. Fiorenzi
P.O. Box 257
Eureka, NV 89316

1 Brad Mettam
P.O. Box 539
Goldfield, NV 89013

1 Bjorn Selinder
190 W. First St.
Fallon, NV 89406

1 Charles Thistlethwaite, AICP
Associate Planner
Planning Department
Drawer L
Independence, CA 93526

1 6300 D. E. Miller
1 6302 T. E. Blejwas
1 6304 J. T. Holmes
1 6312 F. W. Bingham
1 6313 L. S. Costin
1 6641 R. P. Sandoval
2 6318 M. Shain for 100/124213/SAND 91-7038/NQ
2 6318 F. Cheek-Martin for DRMS file 51/L02-7/11/90
1 6319 R. R. Richards
20 6341 WMT Library
1 6340 D. A. Dahlgren
1 6641 R. P. Sandoval
5 7141 S. A. Landenberger
8 7145 Document Processing for DOE/OSTI
3 7151 G. C. Claycomb
1 8523-2 Central Technical Files

END

DATE FILMED

12/28/92